Characterisation of apoptosis-stimulating p53 binding protein 2 (ASPP2) as a new substrate for asparaginyl hydroxylation

Inaugural-Dissertation

zur

Erlangung des Doktorgrades

Dr. rer. nat.

der Fakultät für

Biologie

an der

Universität Duisburg-Essen

vorgelegt von

Kirsten Janke

aus Wuppertal

April, 2013

Die der vorliegenden Arbeit zugrunde liegenden Experimente wurden am Institut für Physiologie AG Metzen, Universitätsklinikum Essen, Universität Duisburg-Essen durchgeführt.

1. Gutachter: Prof. Dr. Eric Metzen

2. Gutachter: Prof. Dr. Verena Jendrossek

3. Gutachter: -

Vorsitzender des Prüfungsausschusses: Prof. Dr. Michael Ehrmann

Tag der mündlichen Prüfung: 04.09.2013

Für Stefan

Table of Contents

1 Introduction

1.1 2-Oxoglutarate-dependent dioxygenases

1.1.1 Cellular function

Hydroxylation is a protein modification of vital importance for eukaryotic organisms. For example prolyl and lysyl hydroxylation are essential for the stabilisation of collagen triple helices and thereby mediate the stability of connective tissue, which mainly consists of collagen (Uitto and Lichtenstein, 1976). Recently, hydroxylation has been shown to provide a mechanism for histone demethylation where hydroxylation of the methyl group was found to remove the histone modification in the course of the reaction (Loenarz and Schofield, 2011). Hydroxylated amino acids can also mark proteins for ubiquitination and thus modulate protein stability as exemplified by prolyl hydroxylation of hypoxia-inducible factor (HIF) (Masson and Ratcliffe, 2003). Until recently, posttranslational hydroxylation of cellular proteins was thought to be uncommon, but over the last decade advances in mass spectrometry and proteomic analyses facilitated the detection of this protein modification and led to the discovery of a number of new hydroxylase substrates with partly unknown function to date (Loenarz and Schofield, 2011).

1.1.2 Hydroxylation mechanism

All the hydroxylation reactions outlined above are catalyzed by Fe(II)- and 2-oxoglutarate-dependent dioxygenases which are involved in a variety of essential cellular functions (Loenarz and Schofield, 2011). The mechanism of the reaction catalyzed by these enzymes is highly conserved. First, the co-substrate 2-oxoglutarate (2-OG) binds to the active site of the enzyme, occupying two coordination sites of the Fe(II) which is attached to the enzyme via a facial triad and coordinated by three water molecules in the absence of substrates. Subsequently, binding of the primary substrate displaces the residual water molecule usually coordinating the iron which leaves one coordination site for oxygen to bind leading to the oxidative decarboxylation of 2-OG (Fig. 1 A) (Schofield and Ratcliffe, 2004). This reaction generates carbon dioxide, succinate and a strongly reactive Fe(IV)=O ferryl species that finally oxidizes the primary substrate via intermediate formation of a substrate radical and a Fe(III)-OH species (Dann and Bruick, 2005; Gorres and Raines, 2010).

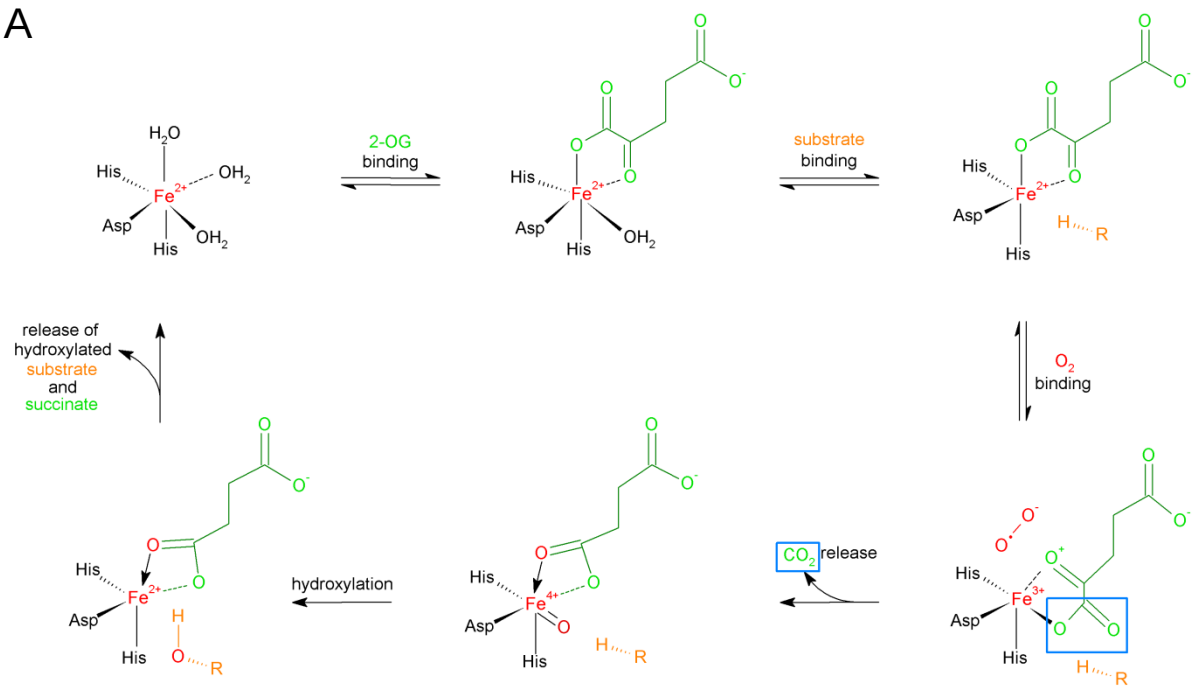

Fig. 1: Hydroxylation by Fe(II)- and 2-oxoglutarate-dependent dioxygenases. (**A**) Mechanism of the hydroxylation reaction catalysed by Fe(II)- and 2-oxoglutarate-dependent dioxygenases (modified from Schofield and Ratcliffe, 2004). Binding of 2-oxoglutarate (2-OG) to the active site of the enzyme displaces two out of three water molecules that coordinate the Fe(II) which is attached to the enzyme via a facial triad (H199, D201, and H279 for factor-inhibiting hypoxia-inducible factor 1 (FIH-1)). Subsequent binding of the substrate replaces the residual water molecule which results in a vacant coordination site for oxygen inducing the oxidative decarboxylation of 2-OG. The decarboxylation step produces a strongly reactive Fe(IV)=O ferryl species which oxidises the substrate releasing succinate and the hydroxylated peptide substrate. (**B**) Chemical structure of 2-OG and derivatives used as inhibitors of Fe(II)- and 2-oxoglutarate-dependent dioxygenase activity.

Hydroxylation by Fe(II)- and 2-oxoglutarate-dependent dioxygenases can be inhibited by addition of an alternative compound, N-oxalylglycine (NOG), which competes with 2-OG for binding to the enzyme. Binding of NOG to the active site of the enzyme still allows the primary substrate to attach to the enzyme but decarboxylation is prevented by an amide group leading to a trapped enzyme substrate complex. The same mechanism applies to the cell-penetrating form of NOG, dimethyloxalylglycine (DMOG), which can be applied to living cells (Fig. 1 B) (Epstein *et al.*, 2001; Jaakkola *et al.*, 2001).

1.1.3 Hypoxia-inducible factor (HIF) hydroxylation

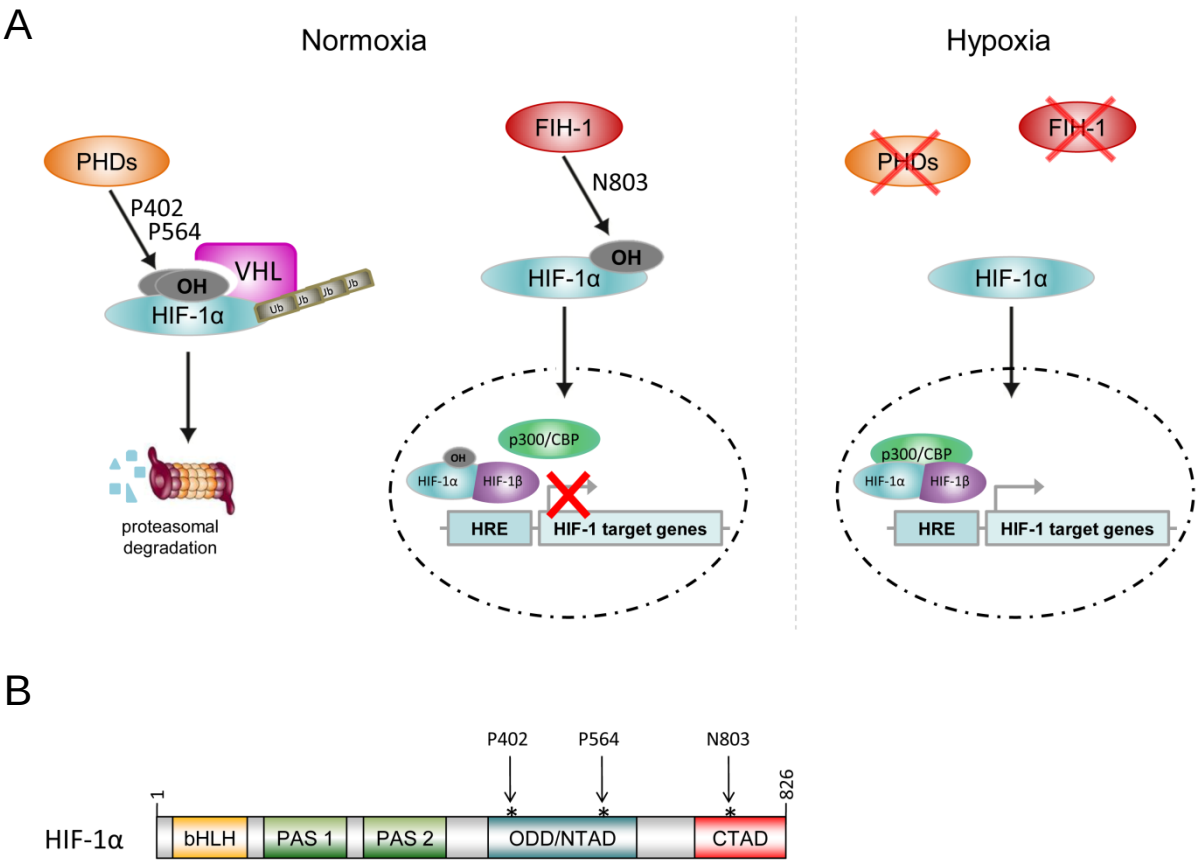

Fig. 2: Regulation of HIF-1 by Fe(II)- and 2-oxoglutarate-dependent dioxygenases. (**A**) Regulation of HIF-1 activity by posttranslational hydroxylation under normoxic and hypoxic conditions. Prolyl hydroxylation of HIF-1α at P402 and P564 by prolyl hydroxylase domain containing enzymes (PHDs) triggers interaction with a von Hippel-Lindau (VHL) dependent E3 ubiquitin ligase mediating HIF-α ubiquitination and proteasomal degradation. Asparaginyl hydroxylation at N803 by FIH-1 prevents the interaction of HIF-1 with transcriptional co-activators, e.g. p300/CREB binding protein (CBP), and thereby represses HIF-1 target gene transcription. Under hypoxic conditions enzyme activity of PHDs and FIH-1 is suppressed which leads to the activation of the transcription factor. (**B**) Domain structure of HIF-1α. Hydroxylation sites are indicated by asterisks. Ub, ubiquitin; bHLH, basic-helix-loop-helix domain; PAS, Per-Arnt-Sim domain; ODD, oxygen-dependent degradation domain; NTAD, N-terminal transactivation domain; CTAD, C-terminal transactivation domain; HRE, hypoxia-reponsive element.

As outlined above, hydroxylation reactions mediated by Fe(II)- and 2-oxoglutarate-dependent dioxygenases are involved in a variety of essential cellular functions. The regulation of HIF by these enzymes is mediated by modulation of protein interactions on the molecular level (Fig. 2 A). On one hand, HIF-α prolyl hydroxylation by prolyl hydroxylase domain containing enzymes (PHDs) triggers interaction with the substrate recognition subunit of the E3 ubiquitin ligase responsible for HIF-α degradation, the von Hippel-Lindau (VHL) protein. PHD activity thereby induces the proteasomal degradation of HIF-α (Kaelin and Ratcliffe, 2008).

On the other hand, HIF asparaginyl hydroxylation by Factor Inhibiting HIF-1 (FIH-1) impairs the interaction with the transcriptional co-activator p300/CREB binding protein (CBP) and thereby decreases transcriptional activity (Lisy and Peet, 2008). Both regulatory processes function independently because prolyl and asparaginyl hydroxylation occur at amino acid residues in different regulatory domains of HIF-α. PHDs hydroxylate two proline residues in the oxygen-dependent degradation domain (ODD) while FIH-1 targets one asparagine in the C-terminal transactivation domain (CTAD) (Fig. 2 B). Therefore, two oxygen-dependent mechanisms ensure the control of HIF activity, on one hand, HIF stability is regulated by PHDs, on the other FIH-1-dependent hydroxylation limits transcriptional activity independent of the degradation machinery (Kaelin and Ratcliffe, 2008; Semenza, 2012).

The corresponding regulatory domains, CTAD and ODD, were reported very early for the transcription factor (Pugh *et al.*, 1997) while the mechanism of HIF hydroxylation and the corresponding enzymes, FIH-1 and PHDs, was illuminated later (Epstein *et al.*, 2001; Mahon *et al.*, 2001; Hewitson *et al.*, 2002; Lando *et al.*, 2002a). Remarkably, the effect of asparaginyl hydroxylation on HIF activity seems to depend on the specific target gene. While carbonic anhydrase 9 (Ca-9) and glucose transporter 1 (Glut-1) expression can be inhibited by FIH-1 activity, expression levels of phosphoglycerate kinase 1 (PGK1) and Bcl-2/adenovirus E1B 19kDa interacting protein 3 (Bnip3) do not differ in the presence or absence of the enzyme. HIF-dependent transactivation of the latter genes is exclusively regulated by the stability of the transcription factor and thus by HIF prolyl hydroxylation (Dayan *et al.*, 2006).

Although FIH-1 and PHDs both belong to the family of Fe(II)- and 2-oxoglutarate-dependent dioxygenases, and share the same set of co-factors required for the hydroxylation reaction, there are also substantial differences between the enzymes. FIH-1 has a higher affinity for molecular oxygen in comparison to PHDs suggesting that mild hypoxic conditions still allow FIH-1-dependent hydroxylation while PHDs are already inactive (Koivunen *et al.*, 2004). This might be of interest because not all HIF target genes were found to be equally sensitive to hydroxylation of the CTAD. Additionally the substrate specificity of PHDs appears to be more restricted as compared to FIH-1 because very few alternative PHD substrates could be identified so far (Cummins *et al.*, 2006; Koditz *et al.*, 2007) while several FIH-1 substrates apart from HIF have been reported (Cockman *et al.*, 2009b; Coleman and Ratcliffe, 2009). In contrast to the transcription factor all these substrates are hydroxylated by FIH-1 in a conserved protein interaction motif termed ankyrin repeat domain (ARD).

1.1.4 Ankyrin repeat domain (ARD) hydroxylation

1.1.4.1 ARD structure

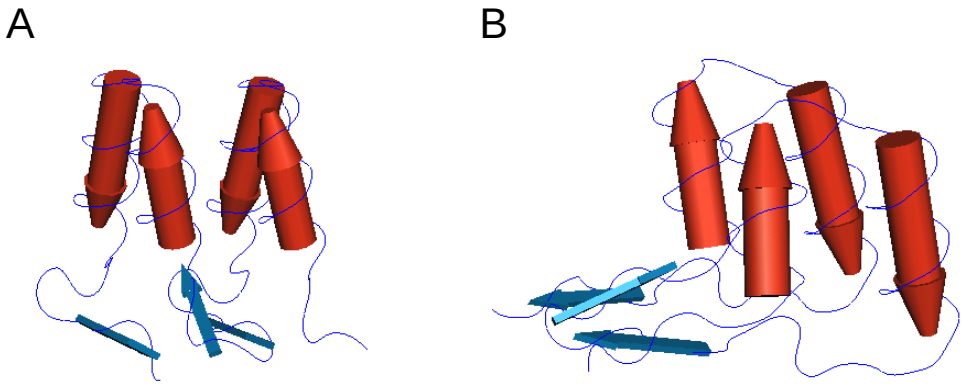

Fig. 3: Ankyrin repeat domain structure of ASPP2. Front (**A**) and side view (**B**) schematic representations of the solution structure of the ankyrin repeat domain (ARD) of apoptosis-stimulating p53 binding protein 2 (ASPP2) (PDI entry 4A63_B) (Canning *et al.*, 2012). The antiparallel α-helices (cylinders) of multiple repeats show the typical stacked conformation of the ARD structure. The loop region projects outward in a 90° angle and forms β-sheet structures which are indicated by arrows. The scheme was generated using the Cn3D 4.3 macromolecular structure viewer (NCBI).

The ARD consists of a motif of approximately 33 amino acids in length, the single ankyrin repeat, which recurs from one to 34 times within the domain. Each single ankyrin repeat adopts a helix-turn-helix conformation with two antiparallel α-helices and a connecting loop pointing outward in a hairpin-like 90° angle to enable formation of β-sheet structures comprising the loops of multiple repeats (Fig. 3) (Mosavi *et al.*, 2004; Li *et al.*, 2006). The α-helices of multiple repeats are stacked together in a helix bundle which is stabilised by hydrophobic interactions and hydrogen bonds. In contrast to the helix bundle, the β-sheet formed by the hairpin-like loop regions of multiple repeats adopts a very flexible conformation. Therefore, it is not surprising that protein interaction interfaces composed of ARDs often comprise the β-sheet structures of the stacked repeats (Mosavi *et al.*, 2004; Li *et al.*, 2006). This composition allows a variety of possible conformations and thereby many interaction partners despite the high conservation of the ankyrin repeat primary sequence but also specificity of protein interactions for different ARD-containing proteins (Mosavi *et al.*, 2004). Regarding the secondary structure, ARDs exhibit less long-range contacts of the polypeptide chain as compared to globular domains, and the stacking of the single repeats determines the secondary structure as well as intra- and inter-repeat short-range contacts.

1.1.4.2 ARD hydroxylation catalysed by FIH-1

Fig. 4: Ankyrin repeat domain consensus sequence (modified from Schmierer *et al.*, 2010). 33 amino acid consensus sequence of the human ankyrin repeat with the hydroxylation site for FIH-1 indicated in red. Secondary structure elements are shown below the sequence.

Although this suggests an intrinsic stability of each single repeat and thus a sequential folding mechanism with multiple transition states, the equilibrium folding and unfolding of ARD-containing proteins is quite similar to that of proteins adopting predominantly globular structures with a two-state transition. This implies that coupling mechanisms between the neighbouring repeats may play a role in ARD folding kinetics which is particularly interesting as some ARD-containing proteins e.g. nuclear factor-κ-B (NF-κB) inhibitor alpha (IκBα) seem not to fold until binding of the interaction partner. Thus the ARD structure notably contributes to binding kinetics of protein interactions with ARD-containing proteins. This is of particular importance for cellular signal transduction because ARD-containing proteins are involved in almost every cellular signalling pathway and 6% of eukaryotic protein sequences contain ankyrin repeats (Mosavi *et al.*, 2004; Barrick *et al.*, 2008).

Hydroxylation of ARDs by FIH-1 as reported for several proteins (Table 1) may influence the stability of the ARD or modify the protein interactions mediated by the domain as the hydroxylation site for FIH-1 is localised in the loop between the single repeats which is often part of interaction interfaces (Fig. 4). Although the ARD is highly conserved, certainly not all ARDs are targeted by FIH-1.

Nonetheless, not only asparaginyl but also aspartyl and histidinyl hydroxylation by FIH-1 has been demonstrated in several ARD proteins as summarised in Table 1. A fraction of these substrates were identified by *in vitro* quantification of enzyme activity on short peptides or protein fragments containing the hydroxylation site using 2-OG decarboxylation assays or mass spectrometry analysis. However, for some of the substrates hydroxylation of overexpressed or even the endogenous protein by FIH-1 has been demonstrated by mass spectrometry in cells (Table 1).

Table 1: ARD-containing FIH-1 substrates verified experimentally *in vitro* and in cells.

Substrate	Hydroxylation site(s)	*In vitro*	In cells	Reference(s)
p19-INK4d	N101	peptide	---	(Cockman *et al.*, 2006)
ILK-1	N94	peptide	---	(Cockman *et al.*, 2006)
FEM1β	N526	peptide	---	(Cockman *et al.*, 2006)
FGIF	N168	peptide	---	(Cockman *et al.*, 2006)
GABP-β1	N98	peptide	---	(Cockman *et al.*, 2006)
Gankyrin	N100	peptide	---	(Cockman *et al.*, 2006)
Myotrophin	N62	peptide	---	(Cockman *et al.*, 2006)
Tankyrase-1	N864 H396, H711	peptide	---	(Cockman *et al.*, 2006; Yang *et al.*, 2011a)
IκBα	N210, N244	full-length protein	endogenous	(Cockman *et al.*, 2006)
p105	N678	protein fragment	exogenous full length	(Cockman *et al.*, 2006)
ASB4	N246	---	exogenous full length	(Ferguson *et al.*, 2007)
RNaseL	N233	---	exogenous full length	(Cockman *et al.*, 2009a)
Tankyrase-2	N203, N271, N427, N518, N586, N671, N706, N739 H238, H553	---	exogenous full length	(Cockman *et al.*, 2009a; Yang *et al.*, 2011a)
Rabankyrin-5	N316, N649, N752, N797	---	exogenous full length	(Cockman *et al.*, 2009a; Singleton *et al.*, 2011)
MYPT1	N67, N100, N226	---	endogenous	(Webb *et al.*, 2009)
hNotch1	N1956	protein fragment	endogenous	(Coleman *et al.*, 2007)
mNotch1	N1945, N2012	protein fragment	exogenous fragment	(Wilkins *et al.*, 2009)
mNotch2	N1902, N1969	protein fragment	---	(Wilkins *et al.*, 2009)
mNotch3	N1867, N1934	protein fragment	---	(Wilkins *et al.*, 2009)
AnkyrinR	N105, N138, N233, N464, N629, N728	protein fragment	endogenous	(Yang *et al.*, 2011b)
GTAR	D1380	peptide	---	(Yang *et al.*, 2011b)
hMASK	D1352	peptide	---	(Yang *et al.*, 2011b)
GABP-β2	H131	peptide	---	(Yang *et al.*, 2011a)
TRPV4	H265	peptide	---	(Yang *et al.*, 2011a)

The function of ARD hydroxylation by FIH-1 could not be revealed yet, although very crucial cellular signalling components like IκBα, Notch1 and p105 are among the ARD-containing substrates of FIH-1 (Cockman *et al.*, 2006; Coleman *et al.*, 2007). Structural studies on recombinant ARD consensus proteins containing three repeats demonstrated that the thermal stability of the ARD fold of these artificial proteins was increased upon hydroxylation by FIH-1 (Hardy *et al.*, 2009; Kelly *et al.*, 2009). Recently, a similar effect on the thermal stability was demonstrated for the repeats 13-24 of AnkyrinR. Binding of this protein fragment to an interaction partner, cytoplasmic domain of band 3 (CDB3), was decreased upon co-expression of FIH-1 (Yang *et al.*, 2011b). This suggests a similar inhibitory effect of FIH-1-dependent hydroxylation on protein interaction as observed for HIF-1α-p300/CBP binding (Lando *et al.*, 2002b). However, further studies are required to demonstrate that these results can be transferred to the endogenous full length protein.

Considering the abundance of ARD-containing proteins in the cell it is also likely that the function of ARD hydroxylation might be the sequestration of the enzyme from HIF regulation. Supporting this hypothesis several studies demonstrate that co-expression of ARD substrates increases HIF reporter gene activity in transfected cells through competition for FIH-1-dependent hydroxylation (Coleman *et al.*, 2007; Zheng *et al.*, 2008; Webb *et al.*, 2009). Furthermore, a predictive kinetic model on hydroxylation of HIF-α in the absence and presence of ARD substrates supports this hypothesis (Schmierer *et al.*, 2010).

Very recently, transgenic mice overexpressing one of the ARD substrates, Gankyrin, specifically in hepatocytes were found to exhibit increased HIF-1 activity leading to increased vascular tumorigenesis due to the disruption of FIH-1-mediated HIF-1 inhibition (Liu *et al.*, 2013). Quantitative mass spectrometry analyses on overexpressed ARD substrates *in vitro* show different levels of hydroxylation ranging from about 20% for Ranbankyrin N316 to about 90% for the murine Notch1 ARD which demonstrates a site-specific regulation by FIH-1 (Singleton *et al.*, 2011). However, to date it is not known how effective the enzyme can hydroxylate endogenous ARD proteins and HIF-α *in vivo*. Thus, it is still unclear whether the abundance of ARD substrates in fact limits the hydroxylation of HIF-α and thereby contributes to HIF regulation.

Nevertheless, the abundance of cellular ARD-containing proteins and the high conservation of the ankyrin repeat sequence and structure suggest that ARD-hydroxylation might be a common protein modification and additional ARD-containing substrates have not been identified for FIH-1 to date. Interestingly, FIH-1-deficient mice do not exhibit aberrant HIF

activity but rather show a dysregulation in the energy metabolism (Zhang *et al.*, 2010). Moreover, FIH-1 suppression in two different cancer cell lines has been shown to induce p53-dependent expression of the cyclin-dependent kinase inhibitor 1 (p21) thereby inhibiting tumor growth in a xenograft model (Pelletier *et al.*, 2011). These HIF-independent functions of FIH-1 underline that the characterisation of new substrates for the enzyme is of major importance. Beside Notch and IκB proteins, there are multiple protein families containing ARDs which are not characterised with respect to their potential to be hydroxylated by FIH-1 to date, among these the family of apoptosis-stimulating p53-binding proteins (ASPPs).

1.2 Apoptosis-stimulating p53-binding proteins (ASPPs)

1.2.1 General characteristics

The ASPP protein family consists of three members, ASPP1, ASPP2 and inhibitory ASPP (iASPP) and was initially found to modulate p53-dependent signalling pathways. The proapoptotic members ASPP1 and ASPP2 were shown to stimulate the proapoptotic function of p53 before iASPP was identified as an oncoprotein inhibiting p53-dependent apoptosis (Samuels-Lev *et al.*, 2001; Bergamaschi *et al.*, 2003). The three family members share a highly conserved C-terminus containing different protein-protein interaction domains, a proline-rich region, an ARD and a Src-homology 3 (SH3) domain. For two ASPPs, truncated forms were described before characterisation of the full length protein (Fig. 5). As a first member of the protein family, ASPP2 was identified.

1.2.2 ASPP1 and ASPP2

1.2.2.1 Structure, function and regulation

Initially, a truncated form of ASPP2, termed p53-binding protein 2 (53BP2), was identified in a yeast two-hybrid screen as a protein interacting with the tumor suppressor p53 (Iwabuchi *et al.*, 1994). 53BP2 comprises the 529 C-terminal amino acids of the full length protein containing the structural motifs important for protein interactions, the proline-rich region, the ARD and the SH3 domain (Fig. 5).

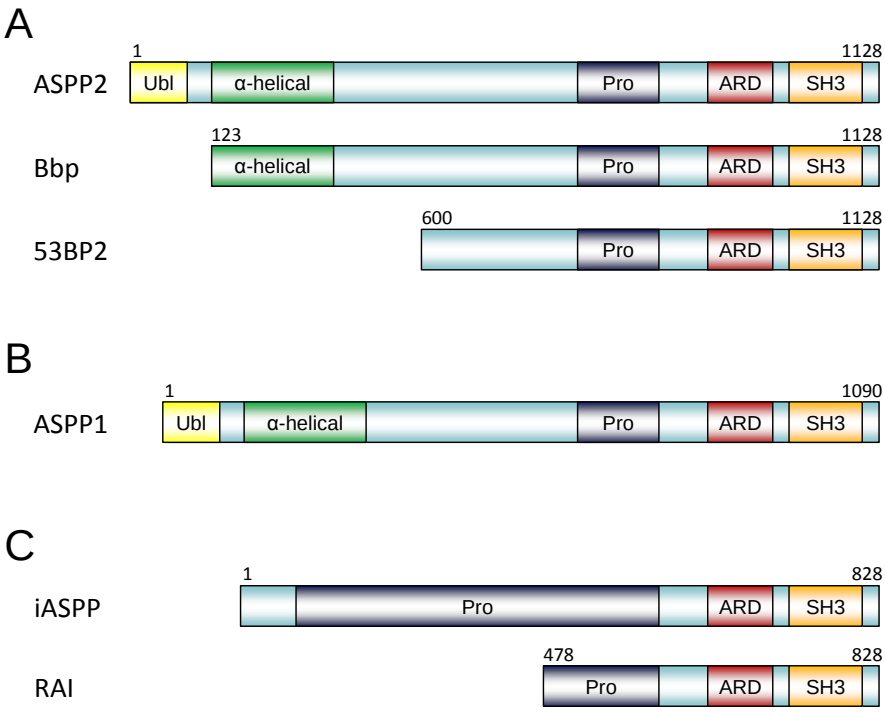

Fig. 5: Domain structure of apoptosis-stimulating p53 binding proteins (ASPPs). (**A**) Structure of the full length protein ASPP2, its splice variant Bcl-2 binding protein (Bbp) and the initially identified protein fragment p53 binding protein 2 (53BP2). (**B**) Structure of ASPP1. (**C**) Structure of full length inhibitory ASPP (iASPP) and the initially identified splice variant RelA-associated inhibitor (RAI). Ubl, ubiquitin-like fold; Pro, proline-rich region; ARD, ankyrin repeat domain; SH3, Src-homology 3 domain.

The ARD-SH3 region not only mediates interaction with p53 but is also involved in binding of numerous other interaction partners of ASPP2 (Table 2). The interaction with B-cell lymphoma 2 (Bcl-2) led to the identification of the splice variant Bcl-2 binding protein (Bbp) comprising the 1005 C-terminal amino acids of ASPP2 in a yeast two-hybrid screen for proteins interacting with Bcl-2 (Naumovski and Cleary, 1996). Finally, the full length protein of 1128 amino acids was characterized together with the family member ASPP1 containing 1090 amino acids (Fig. 5) (Samuels-Lev *et al.*, 2001).

Exogenous expression of ASPP1 and ASPP2 was shown to enhance the transactivation function of p53 on promoters of proapoptotic genes leading to an increased apoptotic response of the cells (Samuels-Lev *et al.*, 2001). Recently, ASPP1 and ASPP2 were shown to induce p53-dependent apoptosis *in vivo* in retinal ganglion cells following optical nerve damage via induction of p53 upregulated modulator of apoptosis (PUMA) and Fas receptor (Wilson *et al.*, 2013). The redundant apoptosis-stimulating function of ASPP1 and ASPP2 not only applies to p53 itself but also to the p53 family members p63 and p73 which were shown to be regulated by ASPPs in a similar fashion concerning the transactivation of proapoptotic genes *in vitro* (Bergamaschi *et al.*, 2004).

Table 2: Protein interactions of ASPP2.

Protein	Function	Interaction site of ASPP2	Functional consequences of interaction	Reference(s)
p53	apoptosis, cell cycle arrest, DNA repair	ARD-SH3	ASPP2: enhanced transactivation of proapoptotic genes C-terminus: dominant negative	(Samuels-Lev *et al.*, 2001)
p63	apoptosis, cell cycle arrest	not mapped	enhanced transactivation of proapoptotic genes	(Bergamaschi *et al.*, 2004)
p73	apoptosis, cell cycle arrest	not mapped	enhanced transactivation of proapoptotic genes	(Bergamaschi *et al.*, 2004)
Bcl-2	apoptosis inhibition	ARD-SH3	---	(Naumovski and Cleary, 1996)
PP1	serine/threonine phosphatase	ARD	promotes dephosphorylation of TAZ by PP1	(Helps *et al.*, 1995; Liu *et al.*, 2010a)
p65 (RelA)	NF-κB subunit	ARD-SH3	---	(Yang *et al.*, 1999b)
YAP	development (Hippo pathway)	SH3	---	(Espanel and Sudol, 2001)
APCL	cytoskeletal regulation	ARD-SH3	---	(Nakagawa *et al.*, 2000)
APP-BP1	cell cycle regulation (neddylation pathway)	N-terminus (aa 332–483) and Pro-ARD-SH3	inhibits cell proliferation and protects against APP-BP1-induced apoptosis	(Chen *et al.*, 2003)
HCV core protein	hepatitis C virus core protein	ARD-SH3	---	(Cao *et al.*, 2004)
IRS-1	insulin receptor substrate	ARD-SH3	inhibits insulin-induced tyrosine phosphorylation of IRS-1	(Hakuno *et al.*, 2007)
DDA3	mitotic spindle regulation	N-terminus (aa 1–450) and ARD-SH3	---	(Sun *et al.*, 2008)
DDX42	ATP-dependent RNA helicase	N-terminus (aa 415–489) and ARD-SH3	---	(Uhlmann-Schiffler *et al.*, 2009)
p300	acetyl transferase, transcriptional co-activator	not mapped	complex formation of ASPP2-p53-p300 enhances p53 transcriptional activity on proapoptotic genes	(Gillotin and Lu, 2011)
CagA	*Helicobacter pylori* effector protein, induces EMT	not mapped	inhibits p53 accumulation and transcriptional activity	(Buti *et al.*, 2011)
Bcl-W	apoptosis inhibition	ARD-SH3	---	(Katz *et al.*, 2008)
Bcl-X_L	apoptosis inhibition	ARD-SH3	---	(Katz *et al.*, 2008)
Par-3	cell polarity, tight/adherens junction formation	N-terminus (aa 2-353)	necessary for epithelial cell polarity, controls neuronal progenitor proliferation and polarity	(Cong *et al.*, 2010; Sottocornola *et al.*, 2010)
HRas	GTPase, growth factor signalling	N-terminus (aa 1-100)	promotes membrane localisation, promotes Ras signalling (senescence/apoptosis)	(Wang *et al.*, 2013a; Wang *et al.*, 2013b)

EMT: epithelial to mesenchymal transition

Besides structural and functional similarities, ASPP1 and ASPP2 are also regulated by the same family of transcription factors in a similar fashion. E2F transcription factors which are critical for the control of cell cycle, proliferation and apoptosis were shown to bind the promoters of endogenous ASPP1 and ASPP2 and to upregulate the expression of both proteins (Chen *et al.*, 2005; Fogal *et al.*, 2005; Hershko *et al.*, 2005). In breast cancer cell lines apoptosis induced by the chemotherapeutic agent resveratrol was found to depend on an E2F-1 mediated increase of ASPP1 emphasising the importance of this regulatory mechanism (Shi *et al.*, 2011).

1.2.2.2 Stimulation of p53-dependent apoptosis by ASPP1 and ASPP2

The apoptosis-stimulating function is best characterised for ASPP2 although the precise mechanism has not been elucidated yet. The solution structure of the ARD-SH3 region of ASPP2 in complex with p53 revealed that the binding site for ASPP2 is located in the p53 core domain and overlaps the DNA-binding domain (Gorina and Pavletich, 1996). Because of the overlapping binding sites the formation of a ternary complex of ASPP2, p53 and DNA seems unlikely and could indeed be excluded from competitive binding studies (Tidow *et al.*, 2006; Patel *et al.*, 2008).

Moreover, the predominantly cytoplasmic localisation of ASPP1 and ASPP2 argues against a direct effect on the transactivation function of p53 but rather suggests an indirect signal transduction pathway through which proapoptotic ASPPs trigger p53-dependent apoptosis. Supporting this hypothesis, several studies have shown that the ASPP2-mediated stimulation of apoptosis was decreased upon co-expression of other interaction partners which implies a competition for binding of different proteins to the ARD-SH3 region of ASPP2 (Cao *et al.*, 2004; Takahashi *et al.*, 2005; Sun *et al.*, 2008).

Besides the highly conserved C-terminus responsible for the interaction with p53, ASPP1 and ASPP2 show a high sequence similarity in the N-terminal 100 amino acids which were shown to adopt a β-Grasp ubiquitin-like fold (Fig. 5) and to share some sequence homology with Rat sarcoma (Ras) association domain (RAD) containing proteins (Tidow *et al.*, 2007). Very recently, the interaction of ASPP1 and ASPP2 with Ras via this domain was demonstrated to potentiate Ras signalling (Wang *et al.*, 2013a).

Ras small GTPases are well-known oncogenes in human cancer as mutations rendering Ras permanently active occur frequently leading to uncontrolled proliferation of tumor cells via various cellular signalling pathways (Pylayeva-Gupta *et al.*, 2011). In addition, Ras has also been demonstrated to possess the opposing function and induce apoptosis and senescence which can be mediated by p53-dependent signalling pathways (Spandidos *et al.*, 2002; Overmeyer and Maltese, 2011). ASPP2 has previously been shown to act as a mediator of Ras-induced senescence via interaction between Ras and the N-terminus of ASPP2 (Wang *et al.*, 2011; Wang *et al.*, 2013b). Recently, it could be demonstrated that this interaction is also involved in the stimulation of p53-dependent apoptosis via ASPP1 and ASPP2 (Wang *et al.*, 2013a).

1.2.2.3 Mouse models of ASPP1 and ASPP2 deficiency

Consistent with the role of ASPP2 in the regulation of apoptosis via p53 family members, heterozygous mice are more susceptible to spontaneous tumor development compared to wild-type mice (Kampa *et al.*, 2009). Moreover, the tumor suppressor function of ASPP2 *in vivo* was shown to require the presence of p53 as tumor development in mice was unaffected by ASPP2 gene dosage in the absence of p53 (Vives *et al.*, 2006). The homozygous deletion of ASPP2 which revealed a new function of the protein in the regulation of cell polarity was carried out in another genetic background because all pups of the two mouse models mentioned above died before weaning. ASPP2 knockout mice showed a hydrocephalus and retinal dysplasia due to the loss of tight junction integrity at the choroid plexus and abnormal growth of neuroepithelial cells (Sottocornola *et al.*, 2010). These defects could be connected to the disorganised localisation of components of the apical junctional complex (AJC) which is involved in the regulation of cell-cell adhesion, epithelial barrier function and cell polarity. The AJC is composed of tight and adherens junctions which are formed by protein subcomplexes (Martin-Belmonte and Perez-Moreno, 2011). One of these complexes responsible for the establishment of cell polarity is the Par complex consisting of the two scaffolding proteins partitioning defective 3 homolog (Par-3) and partitioning defective 6 homolog (Par-6) and the atypical protein kinase C (aPKC). ASPP2 could be shown to form an alternative cell polarity complex with Par-3 *in vivo* whose disruption causes the defects in neuronal development observed in the ASPP2 knockout mice (Sottocornola *et al.*, 2010). The interaction of ASPP2 and Par-3 could also be detected *in vitro* in human cancer cell lines and the cell-cell contact localisation was shown to be interdependent as depletion of one of the

interaction partners disrupted the junctional localisation of the other protein (Sottocornola *et al.*, 2010). Interestingly, the Par-3-binding domain of ASPP2 is located within the N-terminus of the protein and does not comprise the ARD-SH3 domain which is responsible for binding of most of the interaction partners, including p53 (Table 2) (Cong *et al.*, 2010). To date, it is unclear, whether the control of cell polarity and neuronal progenitor proliferation via ASPP2 are p53-dependent because the combined knockout mice are embryonic lethal (Sottocornola *et al.*, 2010).

In contrast to the ASPP2 heterozygous mice, the phenotype of ASPP1 knockout mice was shown to be independent of p53 function. These mice manifest delayed lymphatic vessel assembly during embryogenesis. The mechanism involving ASPP1 in this developmental malfunction is not clarified to date (Hirashima *et al.*, 2008).

Taken together, the different mouse models demonstrate that, despite redundant functions in p53 regulation observed *in vitro*, ASPP1 and ASPP2 regulate different signalling pathways pointing to unique functions of each protein *in vivo*. This is supported by several studies reporting further p53-independent functions of the proteins *in vitro* (Aylon *et al.*, 2010; Liu *et al.*, 2010a; Vigneron *et al.*, 2010).

1.2.2.4 ASPP1 and ASPP2 - beyond p53 regulation

Besides regulation of p53 function, ASPP1 was shown to affect the Hippo signalling pathway which controls cell proliferation and apoptosis independent of p53 (Aylon *et al.*, 2010; Vigneron *et al.*, 2010). The Hippo signalling pathway is essential for organ size control during mammalian development. The inhibition of cell proliferation and induction of apoptosis are mediated through the regulation of the transcriptional co-activators Yes associated protein (YAP) and transcriptional co-activator with PDZ-binding motif (TAZ) which can associate with different transcription factors upon activation, e.g. members of the TEA domain (TEAD) family and the tumor suppressor p73 (Halder and Johnson, 2011). YAP and TAZ are inhibited by phosphorylation via a kinase cascade when the Hippo pathway is activated which leads to the inhibition of cell proliferation. ASPP1 has been shown to act on this pathway via two of these kinases, large tumor suppressor 1 and 2 (LATS1 and LATS2), which catalyse the phosphorylation of YAP and TAZ. On the one hand, ASPP1 can inhibit the kinase activity of LATS1 in the cytoplasm leading to the activation of YAP and TAZ (Vigneron *et al.*, 2010). One consequence of the activation of YAP by ASPP1 is the downregulation of LATS2 which

reduces p53 transactivation function on the p21 promoter thereby inhibiting cell cycle arrest and senescence induction (Vigneron and Vousden, 2011). On the other hand, phosphorylation of ASPP1 by LATS2 can trigger the nuclear translocation of a LATS2/ASPP1 complex under oncogenic stress conditions which promotes apoptosis of polyploid cells in a p53-dependent manner (Aylon *et al.*, 2010).

ASPP2 has also been shown to be implicated in the activation of the Hippo pathway through enhanced dephosphorylation of TAZ which is catalysed by one of the ASPP2 interaction partners, protein phosphatase 1 (PP1) (Table 2) (Liu *et al.*, 2010a). Moreover, a direct interaction of YAP and ASPP2 has been reported, but the biological relevance of this interaction is still unclear (Table 2) (Espanel and Sudol, 2001).

As listed in Table 2, a multitude of other interaction partners were identified for ASPP2 with partially unknown function to date suggesting that the protein is involved in numerous other signalling pathways. As the biological relevance of most of these interactions could not be revealed yet, they will not be discussed further in detail.

1.2.3 iASPP

1.2.3.1 Structure, function and regulation

Similar to the identification of ASPP2, a truncated iASPP form was first identified in a yeast two-hybrid screen. The C-terminal 351 amino acids of the full length protein were found to interact with the NF-κB subunit p65 (RelA) and to inhibit NF-κB-dependent gene expression (Yang *et al.*, 1999a). Thus, the potential splice variant of iASPP was termed RelA-associated inhibitor (RAI) (Fig. 5). Full length iASPP was identified together with its *C. elegans* homolog ape-1 which were both found to inhibit apoptosis induced by p53 (Bergamaschi *et al.*, 2003). In contrast to the full length protein, expression of the splice variant RAI could not be detected in several cancer cell lines suggesting that it is either restricted to certain tissues or represents a truncated version of iASPP not occurring *in vivo* (Slee *et al.*, 2004). However, RAI has been shown to localise almost exclusively to the nucleus while iASPP is partially located to the cytoplasm which indicates that the N-terminus of the protein controls the subcellular localisation enabling iASPP-dependent signalling in both cellular compartments (Slee *et al.*, 2004).

1.2.3.2 Inhibition of p53-dependent apoptosis and cell cycle arrest by iASPP

Fig. 6: Domain structure of p53. The tumor suppressor p53 consists of an N-terminal transactivation domain (TAD), a proline-rich region (Pro), a central core DNA-binding domain which is separated from the tetramerisation domain (TET) by a linker region (L). The C-terminus of p53 contains a regulatory domain (REG). ASPP interaction sites referred to in the text are indicated by asterisks.

To date, little is known about the regulation of iASPP but it could be demonstrated that activation of NF-κB triggers the expression in hepatocellular carcinoma cells via a putative NF-κB binding site in the iASPP promoter (Lu *et al.*, 2010).

Initially, suppression of iASPP in human breast cancer and osteosarcoma cell lines was shown to stimulate apoptosis in a p53-dependent manner (Bergamaschi *et al.*, 2003). This could be verified in other cancer cell lines of different origin, e.g. lung (Li *et al.*, 2012) and hepatocellular carcinoma (Lu *et al.*, 2010). Besides regulation of apoptosis, iASPP was also found to stimulate proliferation of cancer cells through inhibition of p53-dependent cell cycle arrest (Chen *et al.*, 2010; Li *et al.*, 2011).

Moreover, increased chemosensitivity of cancer cells has been reported upon depletion of iASPP (Liu *et al.*, 2009; Lu *et al.*, 2010). These effects could also be confirmed in a xenograft mouse model with human hepatocellular carcinoma cells where upregulation of iASPP enhanced tumor growth and chemoresistance while suppression of the protein had the opposite effect (Lu *et al.*, 2010).

As for ASPP2, direct interaction of the iASPP ARD-SH3 region with the p53 DNA-binding domain could be detected in cancer cells (Bergamaschi *et al.*, 2003) although subtle differences were observed in the binding interfaces. While ASPP2 preferentially binds to the core domain of p53, iASPP interacts with a linker region adjacent to the core (Fig. 6) (Ahn *et al.*, 2009). Moreover, the interaction interfaces of ASPP2 and iASPP were found to differ in the charge of residues exposed to the surface of the proteins which might provide differences in protein interactions (Benyamini and Friedler, 2011). Although both proteins show a similar binding affinity for p53, iASPP was found to have a 3-fold higher affinity for the p53 family members p63 and p73 which were also shown to be regulated by iASPP (Robinson *et al.*,

2008; Cai *et al.*, 2012). Besides the DNA-binding domain, a second region for ASPP interaction located in the proline-rich region of p53 could be identified (Fig. 6). A common p53 polymorphism in this region at codon 72 (proline to arginine) decreases binding of iASPP to a greater extent than binding of ASPP2 confirming the differences in the interaction interfaces of the proteins (Bergamaschi *et al.*, 2006). In addition to regulation of p53 activity, iASPP is also involved in p53-independent signalling pathways with a similar outcome triggering cellular proliferation on one hand and suppressing apoptotic responses on the other.

1.2.3.3 iASPP knockout mouse model

One example for p53-independent signalling of iASPP is derived from a knockout mouse model which identified iASPP as a key player in the regulation of epithelial stratification (Notari *et al.*, 2011). iASPP was shown to regulate this process via inhibition of the transcriptional activity of p63 which acts as a master transcription factor in epithelial development. As in the case of ASPP1 and ASPP2, the knockout mouse model for iASPP highlights the importance of p53-independent functions of the protein. Indeed further signalling pathways mediated by iASPP where p53 is dispensable were identified *in vitro*.

1.2.3.4 iASPP - beyond p53 regulation

Several studies report that silencing of iASPP inhibits proliferation of cancer cells in a p53-independent manner. iASPP suppression in p53-defective prostate cancer cells inhibited growth, *in vitro* colony-forming capacity of the cells and even tumorigenesis *in vivo* due to an increase in apoptosis (Zhang *et al.*, 2011). Moreover, a decreased expression of iASPP in p53-deficient bladder cancer cell lines has been reported to inhibit proliferation (Liu *et al.*, 2011). In ovarian cancer cell lines iASPP silencing increased not only paclitaxel-induced apoptosis but also mitotic catastrophe, i.e. an alternative cell death pathway, irrespective of the p53 status of the cells (Jiang *et al.*, 2011). Furthermore, iASPP suppression in keratinocytes was shown to inhibit proliferation through induction of a differentiation pathway suggesting a role of iASPP in stem cell maintenance (Chikh *et al.*, 2011). These effects might at least in part be associated to the modulation of p63 and p73, as iASPP has been shown to stimulate the activity of these transcription factors leading to the induction of proapoptotic proteins (Cai *et al.*, 2012). Additionally, an interaction between iASPP and PP1 which was previously shown to be bound by ASPP2 has been reported, although the

biological relevance of this interaction is unclear to date (Llanos *et al.*, 2011). iASPP was also found to affect Ras signalling. In contrast to ASPP1 and ASPP2, iASPP functions as an oncoprotein in this context and enhances the transforming activity of Ras in a p53-dependent manner (Bergamaschi *et al.*, 2003). Taken together, the studies suggest that iASPP is an interesting target in cancer therapy as suppression of the protein could induce an anti-proliferative and proapoptotic program in cancer cells irrespective of the p53 status.

1.2.4 ASPPs and cancer

In line with ASPPs being involved in central cellular signalling pathways regulating cellular proliferation as well as apoptotic responses, alterations of ASPP expression levels and regulation have frequently been observed in human tumor tissues.

Consistent with the *in vitro* studies revealing the oncogenic potential of iASPP, the expression levels of the protein were shown to be increased *in vivo* in a multitude of human tumor samples including breast cancer (Bergamaschi *et al.*, 2003), prostate cancer (Zhang *et al.*, 2011), non-small cell lung cancer (Chen *et al.*, 2010), glioblastoma (Li *et al.*, 2011), acute leukemia (Zhang *et al.*, 2005) and hepatocellular carcinoma (Lu *et al.*, 2010). For ovarian cancer (Jiang *et al.*, 2011), head and neck squamous cell carcinoma (HNSCC) (Liu *et al.*, 2012) and squamous cell cervical cancer (Cao *et al.*, 2013) high iASPP expression levels were correlated with a poor prognosis for the patients or with chemoresistance of the cancer cells. One study even suggests an iASPP polymorphism (A67T) potentially predisposing smokers to lung cancer development (Deng *et al.*, 2010). In summary, the elevated expression observed in a multitude of different cancer types demonstrates the potential of iASPP as prognostic tumor marker and a possible target for cancer treatment.

In contrast to iASPP, the proapoptotic ASPP family members were frequently shown to be downregulated in tumor samples, e.g. in endometrial adenocarcinomas (Liu *et al.*, 2010b). In non-small cell lung cancer samples the decrease of ASPP1 and ASPP2 mRNA was found to be even more pronounced in samples expressing wild-type p53 (Li *et al.*, 2012). Reduced transcription of ASPP1 and ASPP2 could be shown to be mediated by aberrant DNA methylation in various p53 wild-type cancer cell lines (Liu *et al.*, 2005) and in hepatitis B virus-positive hepatocellular carcinoma (Zhao *et al.*, 2010). For ASPP1, inactivation by aberrant promoter methylation has also been described to correlate with poor prognosis or metastasis in acute lymphoblastic leukemia (Agirre *et al.*, 2006) and non-small cell lung

cancer (Wei *et al.*, 2011), respectively. Moreover, downregulation of ASPP1 has been reported in leukemia cell lines (Liu *et al.*, 2004) and gestational trophoblastic disease (Mak *et al.*, 2011). For ASPP2, decreased mRNA expression was found to correlate with poor prognosis in lymphoma (Lossos *et al.*, 2002) and a frameshift mutation was detected in one gastric and two colorectal cancer samples with mircosatellite instability (Park *et al.*, 2010). Moreover, a high expression of ASPP2 in cancer cells correlates with sensitivity to cisplatin and irradiation (Mori *et al.*, 2000). Finally, the ASPP2-p53 interaction interface reveals that all the contact residues of p53 are frequently mutated in human cancers suggesting that the ASPP2-dependent stimulation of apoptosis might selectively be switched off in p53 wild-type cancer cells (Gorina and Pavletich, 1996).

In summary these studies confirm the tumor suppressive roles of ASPP1 and ASPP2 on one hand and the oncogenic potential of iASPP on the other. In general, targeting the ASPP protein family may be a promising new approach in cancer therapy. For example, a 37 amino acid peptide derived from the DNA-binding domain of wild-type p53 was shown to stimulate cancer cell death irrespective of the p53 status by disruption of an iASPP-p73 complex releasing p73 from iASPP-mediated suppression which restores the proapoptotic function (Bell and Ryan, 2008). This approach provides an interesting new mechanism through which p53 wild-type and mutant tumors could be targeted in cancer therapy by inhibition of iASPP.

1.3 Aim of the study

As demonstrated by recent findings, the members of the ASPP family are important for several cellular signalling pathways which affect tissue homeostasis and developmental processes as well as tumor development and progression. A database comparison revealed potential hydroxylation sites for FIH-1 in the ARD of all three members of the protein family. The scope of this study was to determine whether ASPPs are modified by FIH-1 at the posttranslational level, because hypoxic conditions are often encountered by the organism in development as well as in pathological processes such as tumor formation. As ASPPs are implicated in these processes, it was of great interest to determine whether ASPPs are hydroxylated by FIH-1 and consequently affected by insufficient oxygen supply.

To date, the functional consequences of ARD hydroxylation could not be revealed. As ASPPs are involved in numerous signalling pathways and multiple protein interactions the hydroxylation of these proteins may be particularly suitable to study the impact of FIH-1-dependent ARD modification. The finding that FIH-1 suppresses the p53-p21 signalling axis together with the potential hydroxylation site suggests that ASPPs are targeted by FIH-1 to modulate p53 signalling.

Furthermore, a connection between intracellular oxygen-sensing mechanisms and ASPP-dependent signalling pathways could explain hypoxia-dependent effects on physiological processes which are not mediated by HIF on the transcriptional level. Consequently, we investigated whether ASPPs are targeted for hydroxylation by FIH-1 and examined the functional consequences of the protein modification.

2 Material and Methods

2.1 Material

2.1.1 Reagents and consumables

Reagents and enzymes used in this study were all obtained in p.a. quality. Radiochemicals were from Perkin-Elmer (Waltham, Massachusetts, USA). Laboratory equipment and consumables not mentioned met laboratory standards.

2.1.2 Technical devices

Technical devices were from the companies listed in Table 3.

Table 3: Technical devices used in this study

Equipment	Companies
Laser scanning microscope Zeiss LSM510	Carl Zeiss (Oberkochen, Germany)
Fusion-FX7 chemiluminescence documentation system	Peqlab (Erlangen, Germany)
Tri-Carb2900R liquid scintillation counter	Perkin-Elmer (Waltham, Massachusetts, USA)
Hypoxic working chamber	Toepffer Lab System (Göppingen, Germany)
FLx800 fluorescence reader	Biotek (Winooski, Vermont, USA)
Epoch spectrophotometer	Biotek (Winooski, Vermont, USA)
Sequencing service	LGC Genomics (Berlin, Germany); Microsynth (Balgach, Switzerland)

2.1.3 Buffers and media

Media and buffers frequently used in this study are listed in Table 4.

Table 4: Buffers and media

PBS	138 mM	Tris (pH 7.4)
	8.1 mM	Na_2HPO_4
	2.7 mM	KCl
	1.5 mM	KH_2PO_4
TBS	20 mM	Tris (pH 7.4)
	137 mM	NaCl
Running buffer (SDS-PAGE)	25 mM	Tris (pH 7.4)
	0.192 M	glycine
	0.1% (w/v)	SDS
Transfer buffer (Western blotting)	25 mM	Tris (pH 7.4)
	0.192 M	glycine
Stacking gel buffer (5%)	5% (w/v)	acrylamide
	125 mM	Tris (pH 6.8)
	0.1% (w/v)	SDS
	0.05% (w/v)	APS
	0.1% (v/v)	TEMED
Separating gel buffer	5 – 12.5% (w/v)	acrylamide
	375 mM	Tris (pH 8.8)
	0.1% (w/v)	SDS
	0.05% (w/v)	APS
	0.05% (v/v)	TEMED
SDS sample buffer	62.5 mM	Tris (pH 7.4)
	2% (w/v)	SDS
	3% (v/v)	β-mercaptoethanol
	10% (v/v)	glycerol
	0.25 mg/ml	bromphenol blue
	25 mM	DTT
LB-medium (pH 7.0)	10 g/l	tryptone
	5 g/l	yeast extract
	10 g/l	NaCl
LB-agar		LB-medium (pH 7.0)
	15 g/l	agar

Cell culture media were obtained from Life Technologies (Darmstadt, Germany) and Promocell (Heidelberg, Germany) and supplemented with 100 U/ml penicillin, 100 µg/ml streptomycin, 2 mM glutamine and 10% (v/v) FBS (Life Technologies, Darmstadt, Germany). Antibiotics used for plasmid selection are listed in Table 5.

Table 5: Antibiotics used for plasmid selection

Antibiotic	Concentration
ampicillin	100 µg/ml
kanamycin	40 µg/ml
chloramphenicol	50 µg/ml

2.1.4 Bacterial strains and eukaryotic cell lines

All bacterial strains and eukaryotic cell lines used in this study are listed in Table 6 and 7, respectively.

Table 6: Bacterial strains

Strain	Characteristics	Source/Reference
XL1-blue competent *E. coli*	*rec*A1 *end*A1 *gyr*A96 *thi*-1 *hsd*R17 *sup*E44 *rel*A1 *lac* [F' *pro*AB*lacI*^{q}ZΔM15 Tn10 (Tetr)]	Agilent Technologies (Santa Clara, California, USA) Cat. No.: 200228
BL21-CodonPlus(DE3)-RIPL competent *E. coli*	*E. coli* B F^{-}ompT*hsd*S(r_B^-, m_B^-) *dcm*$^{+}$Tet^{r}*gal*λ(DE3) *end*AHte [*arg*U*pro*LCam^{r}] [*arg*U*ile*Y*leu*W Strep/Spec^{r}]	Agilent Technologies (Santa Clara, California, USA) Cat. No.: 230280
One Shot Stbl3™ competent *E. coli*	F^{-}*mcr*B*mrr*h*sd*S20(r_B^-, m_B^-) *rec*A13 *sup*E44 *ara*-14 *gal*K2 *lac*Y1 *pro*A2 *rps*L20(Str^{R}) *xyl*-5 λ^{-}*leumtl*-1; *end*A1^{+}	Life Technologies (Darmstadt, Germany) Cat. No.: C7373-03

Table 7: Eukaryotic cell lines

Eukaryotic cell line	Origin	Characteristics	Medium	Selection	Source
HCT116	human colorectal carcinoma	p53 wild-type	McCoy's 5A	6 µg/ml puromycin	Vogelstein, B. ATCC #CCL-247
DLD-1	human colorectal carcinoma	p53 mutation	DMEM high glucose	2 µg/ml puromycin	ATCC #CCL-221
CaCo-2	human colorectal carcinoma	p53 truncation	DMEM high glucose	2 µg/ml puromycin	ATCC #HTB-37
H441	human lung carcinoma	p53 mutation	RPMI 1640	2 µg/ml puromycin	ATCC #HTB-174
HEK293T	human embryonic kidney	SV40 T-antigen	DMEM high glucose	2 µg/ml puromycin	DSMZ #ACC-635

2.1.5 Plasmids, shRNA sequences and PCR primers

All shRNA sequences, plasmids and PCR primers used in this study are listed in Table 8, 9 and 10, respectively. PCR primers were from Sigma (Munich, Germany) or Microsynth (Balgach, Switzerland).

Table 8: shRNA sequences

shRNA	Sequence	Reference
shFIH-1	GCCCTTGTTGAACACAATGAT corresponding to nucleotides 1086-1106 of the FIH-1 mRNA (GenBank NM_017902)	Sigma (Munich, Germany); TRCN0000064823
shASPP2	GCCTTTCTTATCTAATCCTTA corresponding to nucleotides 2551-2571 of the ASPP2 mRNA (GenBank NM_005426)	Sigma (Munich, Germany); TRCN0000061797
shPar-3	GCCATCGACAAATCTTATGAT corresponding to nucleotides 3112-3132 of the Par-3 mRNA (GenBank NM_0019619)	Sigma (Munich, Germany); TRCN0000118134

Table 9: Plasmids

Plasmid	Characteristics/Insert	Reference
pcDNA3.1/ASPP2-V5	mammalian expression plasmid containing C-terminal V5-tagged human ASPP2 mRNA (GenBank: AJ318888)	(Samuels-Lev *et al.*, 2001)
pET28a(+) FIH-1	bacterial expression plasmid containing N-terminal His-tagged full length FIH-1 mRNA (NM_017902)	(Hewitson *et al.*, 2002)
pcDNA3 FIH-1	mammalian expression plasmid containing full length FIH-1 mRNA (NM_017902)	(Metzen *et al.*, 2003)
pET32a HIF-1α	bacterial expression plasmid coding for N-terminal His-tagged HIF-1α aa 737-826	(Linke *et al.*, 2004)
pET32a HIF-1α N803A	bacterial expression plasmid coding for N-terminal His-tagged HIF-1α aa 737-826 with a point mutation N803A	(Linke *et al.*, 2004)
pMD2.G	mammalian expression vector coding for lentiviral envelope gene products	Addgene; #12259
psPAX2	mammalian expression vector coding for lentiviral packaging gene products	Addgene; #12260
pLKO.1-puro	pLKO.1 control plasmid without shRNA sequence or stuffer	Addgene; #10879
pLKO.1 shscrambled	pLKO.1 control plasmid containing scrambled shRNA sequence	Addgene; #1864
pGEX-4T-1 HIF-1α	bacterial expression plasmid coding for N-terminal GST-tagged HIF-1α aa 737-826	this study
pGEX-4T-1 HIF-1α N803A	bacterial expression plasmid coding for N-terminal GST-tagged HIF-1α aa 737-826 with a point mutation N803A	this study
pGEX-4T-1 ASPP2	bacterial expression plasmid coding for N-terminal GST-tagged ASPP2 aa 852-1091	this study
pGEX-4T-1 ASPP2 N986A	bacterial expression plasmid coding for N-terminal GST-tagged ASPP2 aa 852-1091 with a point mutation N986A	this study
pGEX-4T-1 ASPP2 N986T	bacterial expression plasmid coding for N-terminal GST-tagged ASPP2 aa 852-1091 with a point mutation N986T	this study
pET24a(+) N-His ASPP2	bacterial expression plasmid coding for N-terminal His-tagged ASPP2 aa 852-1091	this study
pET24a(+) N-His ASPP2 N986A	bacterial expression plasmid coding for N-terminal His-tagged ASPP2 aa 852-1091 with a point mutation N986A	this study
pET24a(+) N-His ASPP2 N986T	bacterial expression plasmid coding for N-terminal His-tagged ASPP2 aa 852-1091 with a point mutation N986T	this study
pET24a(+) N-His ASPP2 N984T	bacterial expression plasmid coding for N-terminal His-tagged ASPP2 aa 852-1091 with a point mutation N984T	this study
pET24a(+) N-His ASPP2 N984T/N986T	bacterial expression plasmid coding for N-terminal His-tagged ASPP2 aa 852-1091 with the point mutations N984T and N986T	this study
pET24a(+) C-His ASPP2	bacterial expression plasmid coding for C-terminal His-tagged ASPP2 aa 852-1091	this study

Table 10: PCR primers

Primer	Sequence 5'→ 3'	Modification
N-His ASPP2 F	ATGGATCCCACCACCACCACCACCACAATCCAGAGGCTCCAC ATGT	BamHI site
N-His ASPP2 R	TAGAAGCTTTCAGTCTTCCCTGTGGATGATTG	HindIII site
C-His ASPP2 F	ATGGATCCAATCCAGAGGCTCCACATGT	BamHI site
C-His ASPP2 R	TAGAAGCTTGTCTTCCCTGTGGATGATTG	HindIII site
GST-ASPP2 F	ATGGATCCAATCCAGAGGCTCCACATGT	BamHI site
GST-ASPP2 R	TAGCTCGAGTCAGTCTTCCCTGTGGATGATTG	XhoI site
GST-HIF-1α F	TAGGATCCTTATTACAGCAGCCAGACG	BamHI site
GST-HIF-1α R	TTAGTCGACTCAGTTAACTTGATCCAAAGC	SalI site
ASPP2 N986A F	CCTGGTACAGTTTGGTGTAAATGTAGCGGCTGCTGATAG	point mutation
ASPP2 N986A R	GAGTCCATCCATCACTATCAGCAGCCGCTACATTTACAC	point mutation
ASPP2 N986T F	CCTGGTACAGTTTGGTGTAAATGTAACCGCTGCTGATAG	point mutation
ASPP2 N986T R	GAGTCCATCCATCACTATCAGCAGCGGTTACATTTACAC	point mutation
ASPP2 N984T F	AAGTTCCTGGTACAGTTTGGTGTAACCGTAAATGCTGCT	point mutation
ASPP2 N984T R	TCCATCACTATCAGCAGCATTTACGGTTACACCAAACTG	point mutation
ASPP2 N984T/N986T F	AAGTTCCTGGTACAGTTTGGTGTAACCGTAACCGCTGCT	point mutation
ASPP2 N984T/N986T R	TCCATCACTATCAGCAGCGGTTACGGTTACACCAAACTG	point mutation

2.1.6 Antibodies

The primary and secondary antibodies used in this study for immunodetection of proteins are listed in Table 11 and 12.

Table 11: Primary antibodies

Antigen	MW	Product number/clone	Company
ASPP2	170/150 kDa	#611354/clone 19/53BP2	BD Biosciences (Heidelberg, Germany)
Par-3	180/150/100 kDa	#07-330	Millipore (Billerica, Massachusetts, USA)
HIF-1α	120 kDa	#610959/clone 54/HIF-1α	BD Biosciences (Heidelberg, Germany)
β-actin	42 kDa	#A2103	Sigma (Munich, Germany)
GAPDH	36 kDa	#G9545	Sigma (Munich, Germany)
FIH-1	40 kDa	#NB100-428	Novus Biologicals (Littleton, USA)
p53	53 kDa	#OP43/clone DO-1	Merck (Darmstadt, Germany)
p53	53 kDa	#04-1083/clone Y5	Millipore (Billerica, Massachusetts, USA)
p21	21 kDa	#556431/ clone SXM30	BD Biosciences (Heidelberg, Germany)
Bcl-2	26 kDa	#sc-783/clone C21	Santa Cruz Biotechnology (Dallas, Texas, USA)
V5	---	#V8137	Sigma (Munich, Germany)

MW: molecular weight

Table 12: Secondary antibodies

Conjugate	Specificity	Product number	Company
HRP	mouse	PO447	DAKO (Glostrup, Denmark)
HRP	rabbit	PO448	DAKO (Glostrup, Denmark)
Atto 647N	mouse	50185	Sigma (Munich, Germany)
Atto 647N	rabbit	40839	Sigma (Munich, Germany)
Alexa Fluor 488	mouse	A-11017	Life Technologies (Darmstadt, Germany)
Alexa Fluor 488	rabbit	A-11070	Life Technologies (Darmstadt, Germany)

2.2 Methods

2.2.1 Transformation of bacteria

Heat shock transformation of competent bacteria listed in Table 6 was performed according to the instructions of the manufacturer.

2.2.2 Preparation of plasmid DNA

XL1-blue *E. coli* were used for general preparation of plasmid DNA. Preparation of DNA containing unstable inserts, e.g. lentiviral DNA containing direct repeats, was performed in One Shot Stbl3^{TM} *E. coli*. Isolation of plasmid DNA was carried out as recommended by the manufacturer using the plasmid purification kits from Qiagen (Hilden, Germany) for maxi, Promega (Madison, Wisconsin, USA) for midi and Thermo Fisher Scientific (Waltham, Massachusetts, USA) for mini preparations.

2.2.3 Recombinant protein expression

Table 13: Expression and storage conditions for recombinant proteins

Protein	Induction	Temperature	Expression time	Storage
His-HIF-1α	1 mM IPTG	37°C	4 h	-80°C; 10% glycerol; stable
His-FIH-1	1 mM IPTG	30°C	6 h	-20°C; 50% glycerol; stable
His-ASPP2	0.5 mM IPTG	20°C	16 h	4°C; unstable
GST	1 mM IPTG	37°C	6 h	-80°C; 10% glycerol; stable
GST-HIF-1α	1 mM IPTG	30°C	6 h	-80°C; 10% glycerol; stable
GST-ASPP2	1 mM IPTG	30°C	6 h	-80°C; 10% glycerol; stable

Protein expression was performed in BL21-CodonPlus (DE3)-RIPL competent *E. coli* cells grown in LB-medium. First an overnight culture of the transformed bacteria was grown at

37°C and 220 rpm in 5 ml selection medium containing the corresponding antibiotic and chloramphenicol in the appropriate concentration (Table 5). Subsequently a larger culture of 100-500 ml selection medium without chloramphenicol was inoculated from the overnight culture and protein expression induced at OD600 = 0.4-0.6 by addition of IPTG. Specific expression conditions for the different recombinant proteins are listed in Table 13. Following expression, cultures were collected by centrifugation, the supernatant discarded and cell pellets were either directly subjected to purification or stored at -20°C until purification. Storage conditions for recombinant proteins following purification are listed in Table 13. For analysis of protein expression culture samples taken before induction and after expression were prepared in SDS sample buffer and analysed by SDS-PAGE and subsequent Coomassie staining (staining buffer: 0.1% (w/v) Coomassie Brilliant Blue R-250, 45% (v/v) methanol, 10% (v/v) acetic acid; destaining buffer: 10% (v/v) methanol, 10% (v/v) acetic acid).

2.2.4 Polymerase Chain Reaction (PCR)

2.2.4.1 Standard PCR

Standard reactions for amplification of DNA fragments were performed in a mixture containing template plasmid DNA (20 pg/µl), primer oligonucleotides (forward and reverse, 1 µM each), dNTP (200 µM each), DMSO (5% (v/v)) and Pfu- or Taq-Polymerase (0.05 U/µl). Buffers containing $MgCl_2$ or $MgSO_4$ were added as recommended by the manufacturer of the polymerases (Thermo Fisher Scientific, Waltham, Massachusetts, USA). Cycling conditions for standard PCR were: 1 x (3 min 95°C); 33 x (30 sec 95°C; 30 sec 58°C; 30 sec – 3 min (depending on the length of the amplicon) 72°C); 1 x (10 min 72°C). PCR reactions were performed in a TRIO thermal cycler (Biometra, Göttingen, Germany) and resulting PCR products were purified by gel extraction using the QIAEX II kit (Qiagen, Hilden, Germany) or the GeneJET gel extraction kit (Thermo Fisher Scientific).

2.2.4.2 Overlap PCR for mutagenesis

To generate amino acid exchanges in expressed proteins, the corresponding DNA sequences were mutated by means of overlap PCR (Ho *et al.*, 1989). In addition to the external primers used for amplification of the whole template DNA, internal primers containing the appropriate base pair exchanges of about 35 bp length overlapping the mutation site about 10 bp in each

direction were used for two initial PCR reactions under standard conditions generating two fragments, one upstream (external forward, internal reverse primer) and one downstream (internal forward, external reverse primer) relative to the mutation site. Following purification of these fragments by gel extraction using the QIAEX II kit or the GeneJET gel extraction kit a new PCR reaction was performed with the external primers. Both fragments were used as template DNA in equimolar concentrations and standard PCR conditions were modified slightly decreasing the annealing temperature to 55°C.

2.2.5 *In vitro* DNA recombination

DNA restriction digestion and ligation reactions were carried out as recommended by the manufacturer of the enzymes, Thermo Fisher Scientific (Waltham, Massachusetts, USA).

2.2.6 Agarose gel electrophoresis

Agarose gel electrophoresis for analysis and purification of DNA was performed in 1 x TAE buffer (40 mM Tris, 20 mM acetic acid, 1 mM EDTA) using the MINI GEL II system (VWR, Darmstadt, Germany). DNA was stained using the Sybr Green nucleic acid stain (Life Technologies, Darmstadt, Germany). For visualisation and documentation of DNA the Fusion-FX7 documentation system from Peqlab (Erlangen, Germany) was used. Purification of DNA fragments from agarose gels was conducted using the QIAEX II kit or the GeneJET gel extraction kit as recommended by the manufacturer. As a molecular weight standard the GeneRuler 1 kb DNA ladder from Thermo Fisher Scientific (Waltham, Massachusetts, USA) was used.

2.2.7 Cell culture

2.2.7.1 Culture conditions for eukaryotic cell lines

Mammalian cell lines were cultured in a humidified incubator at 37°C under 5% CO_2 and 21% oxygen. For maintenance of adherent cultures, cells were trypsinised by incubation with 0.25% trypsin/EDTA solution (Life Technologies, Darmstadt, Germany). Centrifugation steps were generally performed at room temperature for 3 min and 280 x g. Adherent cells were grown to a maximal confluence of 70-90%. For quantification, cells were counted either

manually using a counting chamber or automatically using the Cellometer Auto T4 from Peqlab (Erlangen, Germany).

2.2.7.2 Cryopreservation of eukaryotic cell lines

For cryopreservation, cells were resuspended in FBS containing 10% DMSO following centrifugation at 4°C for 3 min and 280 x g. Tubes with cells were immediately placed in an isopropanol-filled freezing jar and incubated overnight at -80°C. Subsequently cells were either stored for up to 6 months at -80°C or transferred into liquid nitrogen the next day.

2.2.7.3 Transfection of cell cultures

Transient transfections were performed using GeneJuice (Merck, Darmstadt, Germany) in a ratio of 3:1 (µl reagent:µg DNA) as recommended by the manufacturer. Alternatively, to maximise yield of the overexpressed protein, transient transfections were performed using TurboFect (Thermo Fisher Scientific, Waltham, Massachusetts, USA) in a ratio of 2:1 (µl reagent:µg DNA) as recommended by the manufacturer.

2.2.7.4 Lentivirus production in HEK293T cells

Production of lentivirus was performed in HEK293T cells. 7.5-8 x 10^5 cells were seeded in 25 cm^2 flasks. At a confluence of 50-70% (usually overnight incubation) cells were transfected as outlined above using GeneJuice. The transfection mixture contained three different plasmids necessary for virus production: 6 µg of the pLKO.1 vector expressing shRNA to suppress the target gene, 4 µg psPAX2, the packaging plasmid, and 2 µg pMD2.G, the envelope vector. Transfected cells were grown for 48-60 h and the supernatant containing the viral particles passed through a 0.45 µm filter for purification. The virus solution was either directly used or stored at -80°C in 2 ml aliquots until use for transduction.

2.2.7.5 Lentiviral transduction of cell cultures

For transduction, 2x10^5 adherent cells were seeded in 25 cm^2 flasks with 2x10^6 transduction units in 2 ml DMEM and 8 µg/ml polybrene to support adherence of the viral particles to the cells. After 24 h incubation the virus solution was replaced by full growth medium. Following an expression period of 48 h cells were selected with a high concentration of puromycin for at least 3 days. The concentrations used for selection which were determined for each individual cell line by dose-response measurements, are listed in Table 7. Following selection, cells were maintained in normal culture medium in the absence of selection pressure. Stability of the

transient knockdown was monitored by Western blotting in parallel to the experiments performed.

2.2.7.6 Irradiation, chemotherapeutic and hypoxic treatment of cell cultures

For chemotherapeutic treatment and irradiation, adherent cells were grown to a confluence of 50-60%. Before stimulation, growth medium was exchanged. After treatment cells were grown for the indicated time. Chemotherapeutic agents were applied for the whole incubation time. Irradiation was performed using an Isovolt 320 (Pantak-Seifert, East Haven, Connecticut, USA) running at 320 kV and 10 mA with a 1.65 aluminium filter. The effective photon energy was approximately 90 kV with a dose rate of about 2.76 Gy/min. For subsequent analysis, cells were lysed as indicated for the corresponding method. Hypoxic incubations were performed using a Hypoxic working chamber (Toepffer Lab System, Göppingen, Germany). Anoxic incubations were performed in the GasPak™ system (BD Biosciences, Heidelberg, Germany).

2.2.7.7 Proliferation measurement

To measure cell proliferation cells were seeded into 96-well plates at low density ($2x10^3$ cells per well). After 1, 4 and 7 days of growth cells were incubated with 0.5 mg/ml thiazolyl blue tetrazolium bromide (MTT) for 2 - 4 h at 37°C and lysed with MTT lysis buffer (50% (v/v) N,N-dimethylformamide, 20% (w/v) SDS, 0.01% acetic acid, 0.01 M HCl) to solubilise formazan crystals. Following lysis absorbance was measured at 540 nm with 700 nm as reference wave length in an Epoch multimode reader (Biotek, Winooski, Vermont, USA). As a second assay for proliferation, cells were seeded into 6-well plates at low density and counted after 1, 4 and 7 days of growth using the Cellometer Auto T4.

2.2.7.8 Scratch assay

Cellular migration was measured by scratch assay. In brief, cells were grown to confluent monolayers in culture dishes coated with rat collagen-I (Biozol, Eching, Germany) before scratching. Closure of the introduced wounds was quantified as reduced distance between the edges over time. At the indicated time points images were taken using a Zeiss Axiovert 200 M microscope (Carl Zeiss, Oberkochen, Germany). Distances were measured at 11 different positions of each scratch for statistical analysis. Representative data from at least three independent experiments are shown.

2.2.7.9 Adhesion assay

For quantification of cellular adhesion $4x10^4$ HCT116 or H441 cells were seeded into collagen-coated 96-well plates. Following an adhesion period of 2 h at 37°C in serum-free medium containing 0.5% BSA the plate was washed twice with PBS to remove floating cells. For fluorescent detection adherent cells were incubated with 2.5 µM calcein-AM and fluorescence quantified every 5 min at an excitation of 485 nm and emission wavelength of 525 nm over 2 h in a FLx800 fluorescence reader. Replicate values (n = 10 per experiment) of a single time point in the linear range of the reaction were plotted for analysis of the results.

2.2.7.10 Pulse-chase labelling of cellular proteins

For pulse-chase labelling of cellular proteins with ^{35}S-methionine, HCT116 cells were starved with medium lacking methionine for 15 min. Labelling of the cellular proteins was achieved by incubation with EasyTag™ L-[^{35}S]-Methionine (NEG709A) (Perkin-Elmer) at a dose of 7 µCu per cm^2 adherent cell culture for 40 min. Subsequently, residual ^{35}S-methionine was removed by washing with PBS and the cells were incubated with medium containing non-labelled methionine for different time points to monitor degradation of the protein of interest. For generation of total cell extracts the culture dishes were chilled to 4°C, the culture medium removed and cells washed with PBS. Subsequently the cells were lysed in 1 ml NP-40 buffer (50 mM Tris pH 7.5; 150 mM NaCl; 0.5% NP-40; 2 mM EDTA) containing protease inhibitor cocktail (Roche, Mannheim, Germany) per 21 cm^2 culture dish. For immunoprecipitation 900 µl cell lysate were incubated with the indicated antibody for 2 h at 4°C and immune complexes were recovered by incubation with protein G sepharose beads (Sigma, Munich, Germany) for 1 h at 4°C. The beads were washed 10 times with at least 20 volumes NP-40 buffer, resuspended in SDS sample buffer and boiled for 7.5 min at 95°C. After removal of the beads by centrifugation, the supernatant was analysed by SDS-PAGE. As a control for labelling, 1 µl of the crude cell lysate was boiled with SDS sample buffer for 7.5 min at 95°C and subjected to SDS PAGE. The gel was fixed in TCA solution (10% (v/v) TCA; 10% (v/v) acetic acid; 30% (v/v) ethanol) and, following amplification of the signal by incubation in 1 M sodium salicylate, dried using a MGD-4534 gel dryer (VWR, Darmstadt, Germany). Radioactively labelled proteins were visualised by autoradiography. Representative data from two independent experiments are shown.

2.2.8 Purification of recombinant proteins

2.2.8.1 Nickel affinity purification

Cell pellets derived from bacterial protein expression were lysed in 20 mM Tris-HCL (pH 8), 150 mM NaCl containing 1 x CelLytic™ B (Sigma, Munich, Germany), 0.2 mg/ml lysozyme and protease inhibitor cocktail (Roche, Mannheim, Germany). Lysates were cleared by centrifugation and the salt concentration of the cleared lysate was increased to 500 mM NaCl. After addition of 5 mM imidazole, 0.5 mM DTT and 1 mM PMSF lysates were incubated with Ni-NTA Agarose (Qiagen, Hilden, Germany) at 4°C for 1 h. Before addition of the lysate, the agarose was prepared by 4 washing steps with 4 volumes of washing buffer (20 mM Tris-HCL (pH 8), 500 mM NaCl, 10 mM imidazole). After incubation with the lysate, the agarose was washed twice with 10 volumes washing buffer and bound protein eluted with 20 mM Tris-HCL (pH 8), 500 mM NaCl, 250 mM imidazole. After affinity purification protein solutions were directly desalted using PD-10 columns (GE Healthcare, Munich, Germany) and concentrated using the appropriate Amicon centrifugal filter device (Millipore, Billerica, Massachusetts, USA). Protein concentrations were measured at 280 nm and the purity of the proteins was estimated on Coomassie-stained SDS-PAGE gels. Depending on the stability, purified proteins were stored at -20 to -80°C in 10-50% glycerol (Table 13).

2.2.8.2 Glutathione affinity purification

For glutathione affinity purification cell pellets of bacterial cultures expressing the protein of interest were lysed in PBS containing 1 x CelLytic™ B, 0.2 mg/ml lysozyme and protease inhibitor cocktail. Lysates were cleared by centrifugation and incubated with glutathione sepharose 4B (GE Healthcare, Munich, Germany) at 4°C for 1 h. Before addition of the lysate, sepharose was prepared by four washing steps with 4 volumes of PBS. After incubation with the lysate, the sepharose was washed twice with 10 volumes PBS and bound protein eluted with a 20 mM Tris-HCL buffer (pH 8.8) containing 150 mM NaCl and 25 mM reduced Glutathione. After affinity purification protein solutions were directly desalted using PD-10 columns and concentrated using the appropriate Amicon centrifugal filter device. Protein concentrations were measured at 280 nm and the purity of the proteins was estimated on Coomassie-stained SDS-PAGE gels. Depending on the stability, purified proteins were stored at -20 to -80°C in 10-50% glycerol (Table 13).

2.2.9 *In vitro* transcription and translation of proteins

In vitro transcription and translation was performed directly before use of the protein according to the manufacturers instructions using rabbit reticulocyte lysate (L1170; Promega, Madison, Wisconsin, USA). For radioactive labelling of generated proteins EasyTag™ L-[^{35}S]-Methionine (NEG709A) was added to the reaction as recommended by the manufacturer. *In vitro* transcription and translation of FIH-1 was conducted using the expression plasmid pET28a(+) FIH-1.

2.2.10 Hydroxylase activity assay

FIH-1 activity was quantified via the hydroxylation-coupled decarboxylation of 2-oxo[1-^{14}C]glutarate (NEC597) (Perkin-Elmer). $Ca(OH)_2$ soaked filter papers were placed in the top of the sample tubes leading to the precipitation of ^{14}C-labelled $^{14}CO_2$ released from the reactions. Hydroxylation was assessed in a final volume of 40 µl containing 7.5 µM His-FIH-1, 10-300 µM substrate, 0.3% (w/v) BSA (3 mg/ml); 50 mM Tris-HCL (pH 7); 0.5 mM DTT; 4 mM ascorbate; 20 µM $FeSO_4$; 40 µM 2-oxo[1-^{14}C]glutarate. After reaction at 37°C for the indicated time-period the filter paper was dried and subjected to scintillation counting using Ultima Gold XR (Perkin-Elmer, Waltham, Massachusetts, USA) in a Tri-Carb2900R liquid scintillation counter (Perkin-Elmer). Peptides for hydroxylase activity assays were from Thermo Fisher Scientific (Waltham, Massachusetts, USA). Representative data from at least three independent experiments are shown.

2.2.11 Sample preparation for mass spectrometry (MS) analysis

Samples for MS analysis were prepared from HEK293T cells transiently transfected with pcDNA3.1/ASPP2-V5 for 24 h using TurboFect. Cells were lysed in RIPA lysis buffer (50 mM Tris pH 7.5, 150 mM NaCl, 0.1% SDS, 1% NP-40, 0.5% sodium desoxycholate, 2 mM EDTA) containing protease inhibitor cocktail. 1 mg protein of the cell extract was subjected to immunoprecipitation of ASPP2 using 10 µg specific antibody. Immunoprecipitates were separated on a reducing 5% SDS gel which was stained by colloidal Coomassie staining. First, the gel was fixed in 50% (v/v) methanol, 2% (v/v) phosphoric acid for 30 min. Following three washing steps with distilled water, the gel was incubated in 35% (v/v) methanol, 2% (v/v) phosphoric acid, 17% (w/v) ammoniumsulfate for 1 h. Staining

was performed overnight after addition of 0.1% (w/v) Coomassie Brilliant Blue 250 G. Destaining was carried out in distilled water as required for visualisation of the bands. Subsequently bands were excised and subjected to LC-MS/MS analysis.

2.2.12 LC-MS/MS analysis

LC-MS/MS analyses were performed in cooperation by Dr. Katja Kuhlmann at the Medical-Proteome Center at the Ruhr-University Bochum. The analysis was performed as previously described (Janke *et al.*, 2013). In brief, excised protein bands, were destained by alternating incubation with 10 mM NH_4HCO_3 and 5 mM NH_4HCO_3/50% acetonitrile (ACN) (v/v) for 10 min each, three times. Following reduction with 10 mM DTT for 45 min at 56°C, proteins were alkylated with 55 mM iodoacetamide for 30 min at room temperature in the dark. For in-gel digestion, bands were incubated overnight with 150 ng chymotrypsin (Promega, Madison, Wisconsin, USA) each in 10 mM ammonium bicarbonate. Subsequently, peptides were extracted twice from the gel by addition of 15 µl 0.05 TFA/50% ACN (v/v). ACN was removed from the combined extracts *in vacuo*. Peptide separation was performed using an Ultimate 3000 RSLCnano HPLC system (Thermo Fisher Scientific, Waltham, Massachusetts, USA) online-coupled to a QExactive mass spectrometer (Thermo Fisher Scientific, Waltham, Massachusetts, USA). The Mascot search engine (Matrix Science) was used to search MS/MS spectra against the Uniprot complete proteome set for homo sapiens (26.10.2012, 68.109 entries) with a precursor tolerance of 5 ppm, a fragment tolerance of 20 mmu, chymotrypsin specificity with three missed cleavages allowed, cysteine-carbamidomethylation as fixed modification and oxidation of methionine and hydroxylation of asparagine as variable modifications. Peptide identifications were filtered by the peptide validator algorithm of ProteomeDisvoverer 1.3 at 1% false discovery rate on peptide level. MS/MS spectra for ASPP2 hydroxylated or non-hydroxylated peptides were inspected manually in addition to database searching. Elution profile areas from extracted ion chromatograms (5 ppm mass tolerance) of the respective masses were calculated in XCalibur (Thermo Fisher Scientific, Waltham, Massachusetts, USA) for quantitative comparison of peptides. Representative data from three independent experiments are shown.

2.2.13 *In vitro* protein interaction

For detection of *in vitro* interaction with FIH-1, non-labelled recombinant substrates were treated as for the decarboxylation assay, except usage of 20 µM ZnAc instead of $FeSO_4$ and 40 µM NOG instead of radioactively labelled 2-OG. Following incubation with 10 µl *in vitro* transcribed and translated ^{35}S-labelled FIH-1 at 37°C for 2 h, 50 µl Glutathione Sepharose 4B, prepared by three washing steps in at least 10 volumes of 50 mM Tris-HCl pH 7, were added to the samples and the final volume adjusted to 1 ml with 50 mM Tris-HCl pH 7. After incubation for 1 h at 4°C the beads were washed 4 times with 50 mM Tris pH 7, resuspended in SDS sample buffer and boiled for 7.5 min at 95°C. After removal of the beads by centrifugation, the supernatant was split up for analysis either by reducing SDS-PAGE and autoradiography to detect labelled proteins or by SDS-PAGE and Coomassie staining (see 2.2.3) to detect non-labelled proteins, respectively. Representative data from three independent experiments are shown.

2.2.14 Determination of protein concentration

The protein concentration of cell extracts was measured spectrophotometrically at 562 nm using the bicinchoninic acid (BCA) Protein Assay kit from Thermo Fisher Scientific (Waltham, Massachusetts, USA) as recommended by the manufacturer. Bovine serum albumin (BSA) was used as standard.

2.2.15 Immnunoprecipitation of protein complexes

To perform co-immunoprecipitation experiments cells were lysed in NP-40 lysis buffer (2.2.7.10) containing protease inhibitor cocktail for generation of whole cell extracts. Following incubation of a defined protein amount of the cell lysates with the indicated antibodies for 2 h at 4°C co-immunoprecipitation was performed by incubation with protein G sepharose beads for 1 h at 4°C. The beads were washed 10 times with at least 20 volumes NP-40 buffer, resuspended in SDS sample buffer and boiled for 7.5 min at 95°C. After removal of the beads by centrifugation, the supernatant was analysed by SDS-PAGE and immunoblotting. For crosslinking of the protein complexes prior to immunoprecipitation cells were incubated with DSP (dithiobis[succinimidylpropionate]) (Thermo Fisher Scientific, Waltham, Massachusetts, USA) at a final concentration of 2 mM for 30 min at room

temperature. The reaction was stopped by incubation with 20 mM glycine (pH 7.5) for 30 min and following two washing steps with PBS, cells were lysed and whole cell lysates subjected to immmunoprecipitation as described above.

2.2.16 SDS polyacrylamide gel electrophoresis (PAGE) and Western blotting

For Western blotting whole cell extracts were prepared in RIPA lysis buffer (2.2.11) containing protease inhibitor cocktail. Defined protein amounts (25 µg – 50 µg) were prepared in SDS sample buffer and boiled for 7.5 min at 95°C. Proteins were separated using reducing 7.5 – 10% SDS gels and transferred onto PVDF membranes. Unspecific binding sites on the membranes were blocked by incubation in TBST (TBS, 0.1% Tween 20) containing 5% skimmed milk. Incubation steps with primary and HRP-conjugated secondary antibodies were performed as recommended by the manufacturer (Table 11 and 12). Detection of the HRP-conjugated secondary antibodies was conducted with an ECL kit (GE Healthcare, Munich, Germany) using the FX7 chemoluminescence documentation system. Representative data from at least three independent experiments are shown.

2.2.17 Caspase-3 activity assay

Cleavage of the caspase-3-specific substrate sequence DEVD from acetyl Asp-Glu-Val-Asp 7-amido-4-methylcoumarin (Ac-DEVD-Amc, Sigma, A1086), resulting in the release of the fluorescent 7-amino-4-methylcoumarin (Amc), was quantified as an indicator of apoptosis. Cells were treated as indicated and lysed in NP-40-buffer (50 mM Tris pH 7.3, 150 mM NaCl, 1% (v/v) NP-40) containing protease inhibitor cocktail. 50 µg of the cell lysates were incubated with a final concentration of 50 µM Ac-DEVD-Amc in caspase substrate buffer (50 mM HEPES pH 7.3, 100 mM NaCl, 10% (w/v) sucrose, 0.1% (w/v) CHAPS (3-[(3-cholamidopropyl)dimethylammonio]-1-propanesulfonate hydrate), 10 mM DTT) at 37°C. For quantification of caspase activity fluorescence was measured every 10 min at an excitation of 360 nm and emission wavelength of 460 nm over 4 h in a FLx800 fluorescence reader. For analysis of the result values of a single time point in the linear range of the reaction were plotted. Representative data from three independent experiments are shown.

2.2.18 Immunofluorescence microscopy

For immunofluorescence staining cells were grown to confluence on glass plates coated with rat collagen-I. Cells were washed once with PBS, fixed with 4% paraformaldehyde in PBS for 30 min and permeabilised with 0.5% Triton X-100 in PBS for 3 minutes. Afterwards, unspecific binding sites were blocked with blocking buffer (2% BSA in PBS) for 15 min and incubated with primary antibodies in blocking buffer for 2 hours. Following 2 washing steps with blocking buffer, cells were incubated with Alexa Fluor 488 and Atto 647-conjugated secondary antibodies in blocking buffer for 1 h. Cells were washed twice with PBS, counterstained with 50 µg/µl DAPI (4′,6-diamidino-2-phenylindole), washed another three times with PBS and mounted using DAKO mounting medium (DAKO, Glostrup, Denmark). Slides were analysed using a Zeiss LSM510 confocal microscope with a 63x/1.2 NA oil immersion lens (Carl Zeiss, Oberkochen, Germany). Representative data from at least three independent experiments are shown.

2.2.19 Statistical analysis

Statistical analyses were performed using GraphPad Prism 5 software. Statistical significance between two groups was tested by Students t-test. Comparisons of more than two groups were performed by one-way ANOVA analysis.

3 Results

3.1 Sequence similarities between ASPPs and known FIH-1 substrates

Previous reports identified several ARD-containing proteins as substrates for FIH-1 (chapter 1.1.4.2, Table 1). As the high conservation of the ARD suggested further unknown substrates, we compared the previously identified FIH-1 hydroxylation sites to obtain a consensus motif for hydroxylation by the enzyme suitable for a database search for new FIH-1 substrates. An alignment of the protein sequences comprising 20 upstream and 19 downstream amino acids relative to the hydroxylation site revealed the consensus sequence "AAXXXXXXXXXXLLXXGADVNAXDXXGXXPLHXAXXXXXX" indicating residues which are conserved in at least 50% of the sequences (X meaning any residue). The consensus for the FIH-1 hydroxylation site did not change upon addition of substrates identified while our study was in progress (Fig. 7).

The motif revealed that only 16 out of the 40 residues aligned are conserved among 50% of the sequences which demonstrates very low substrate specificity for the enzyme. Confirming the high variation in the hydroxylation site tolerated by FIH-1 none of the amino acid residues in the alignment was found 100% conserved among all substrates currently known. Even the hydroxylated amino acid can vary as the enzyme was recently found to hydroxylate aspartate and histidine residues as well if these are positioned appropriately in the ARD of the substrate (Yang *et al.*, 2011a; Yang *et al.*, 2011b).

The consensus sequence perfectly matches the human ARD consensus. Thus, it was not surprising that a database search for similar protein sequences resulted in matches with several ARD-containing proteins. Besides significant similarities in the previously identified FIH-1 substrates we found the consensus sequences matching a number of other proteins, including all members of the ASPP protein family. The matching values for ASPPs were in part even higher than for some of the experimentally confirmed FIH-1 substrates strongly suggesting hydroxylation of ASPPs at the sites retrieved from the database search: ASPP1 N948, ASPP2 N986 and iASPP N687.

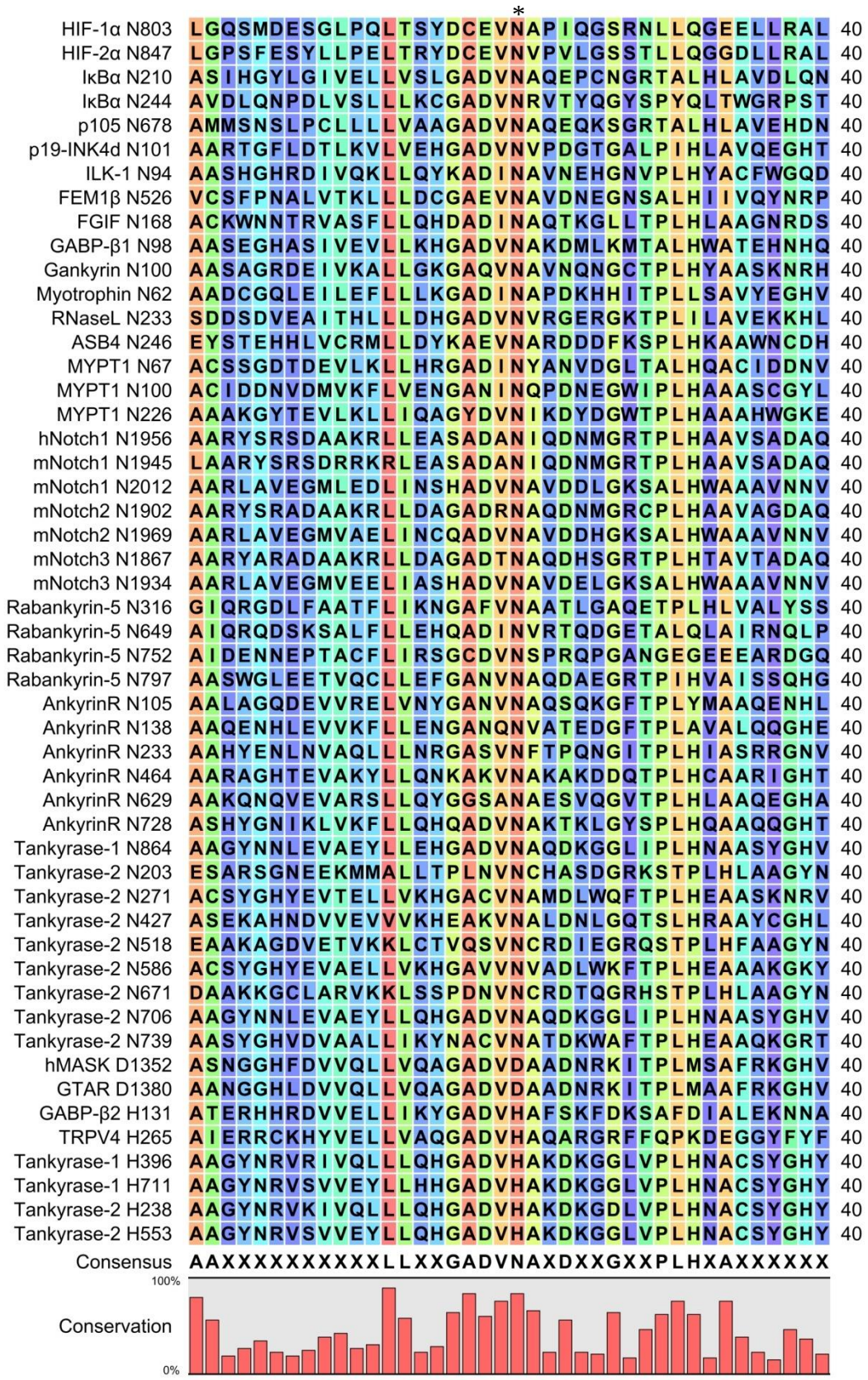

Fig. 7: Alignment of FIH-1 substrates previously identified. Alignment of protein sequences currently known to be hydroxylated by FIH-1. Conservation of the residues is indicated by differential colouring ranging from red for highly conserved amino acids over yellow, green and light-blue to dark-blue for less conserved residues. The consensus sequence shows amino acids which are at least 50% conserved among all sequences. Residues showing less than 50% conservation in the consensus sequences are marked with X. Alignment was created using the CLC Bio sequence viewer 6. The FIH-1 hydroxylation site is indicated by an asterisk.

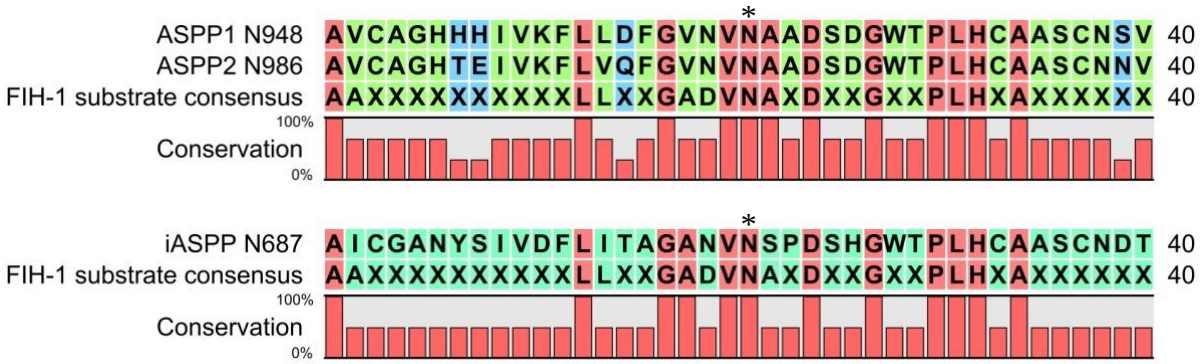

Fig. 8: Alignments of ASPPs and the FIH-1 substrate consensus sequence. Putative hydroxylation sites of ASPP family members aligned with the consensus sequence containing amino acids conserved in 50% of all FIH-1 substrates. Residues showing less than 50% conservation in the consensus sequence are marked with X. Alignment was created using the CLC Bio sequence viewer 6. The putative FIH-1 hydroxylation sites are indicated by asterisks.

Alignments of these putative hydroxylation sites of ASPPs with the FIH-1 substrate consensus sequence revealed a high homology with slight differences between the family members. For ASPP2 and iASPP 12 of the 16 specified amino acids of the 50% consensus were identical while ASPP1 even showed 13 identities (Fig. 8).

Importantly, a leucine residue 8 amino acids upstream of the potential target asparagine is conserved among all ASPPs. This residue was found to be the most conserved in the vicinity of the FIH-1 hydroxylation site among all substrates (Fig. 7) and it was previously shown to be important for interaction with the enzyme (Linke *et al.*, 2007).

The sequence alignments of ASPPs and the FIH-1 substrate consensus not only revealed putative hydroxylation sites but also demonstrated a higher conservation level between the proapoptotic ASPPs as compared to iASPP. An alignment of the putative FIH-1 sites of all ASPP family members shows that only five amino acids in the immediate vicinity of the potential target asparagine (positions -20 to +19) differ between ASPP1 and ASPP2 while iASPP showed a substantially higher degree of variation as compared to the proapoptotic ASPPs (Fig. 9).

Fig. 9: Alignment of putative FIH-1 hydroxylation sites in ASPPs. Protein sequence alignment of the putative hydroxylation sites, ASPP1 N948, ASPP2 N986 and iASPP N687. Residues conserved in all sequences are coloured in red. Amino acids conserved among ASPP1 and ASPP2 are coloured in green and residues that differ in all sequences are shown in blue. Alignment was created using the CLC Bio sequence viewer 6. The putative FIH-1 hydroxylation site is indicated by an asterisk.

These differences imply a differential regulation of pro- and antiapoptotic family members. Therefore it is interesting to determine whether both groups can be targeted by FIH-1 or whether hydroxylation is restricted to distinct ASPPs.

3.2 FIH-1-dependent hydroxylation of ASPPs *in vitro*

3.2.1 ASPP2 derived FIH-1 substrates

As ASPP2 showed a high similarity with the FIH-1 consensus sequence and is involved in a variety of signalling pathways we decided to perform our initial experiments with this ASPP family member. First, we wanted to determine whether ASPP2 can serve as a substrate for FIH-1 *in vitro*. Therefore, we used a hydroxylase activity assay where enzyme activity can be quantified via decarboxylation of the ^{14}C-labelled co-substrate 2-OG leading to the release of $^{14}CO_2$ which can be precipitated as an indicator of hydroxylase activity (Linke *et al.*, 2007).

The *in vitro* hydroxylation reaction was performed using enzyme and substrate regions purified from a bacterial expression system. As positive and negative controls His-tagged HIF-1α fragments (His-HIF-1α) of nearly 100 amino acid length (aa 737-826) containing or lacking the FIH-1 hydroxylation site (Linke *et al.*, 2004) were used (Fig. 10). To obtain similar protein fragments for ASPP2, amino acids 852-1091 were cloned into the bacterial expression plasmid pET24a(+) with an N-terminal His-tag by PCR (Fig. 10). Alternatively, the His-tag was positioned at the C-terminus by PCR cloning. The ASPP2 test substrate was designed to contain approximately 100 amino acids up- and downstream of the putative FIH-1 hydroxylation site to achieve the least artificial conditions possible and to enable proper folding of the ARD containing the target asparagine. As the enzyme was also purified via a His-tag, all substrates including HIF-1α were also cloned into pGEX-4T-1 by PCR for bacterial expression of N-terminal GST-tagged proteins (Fig. 10). These fusion proteins were not used in the hydroxylase activity assay because the large GST-tag was expected to interfere with the reaction. However, the GST-tag also allowed potential studies of enzyme-substrate interaction by *in vitro* pull-down assays.

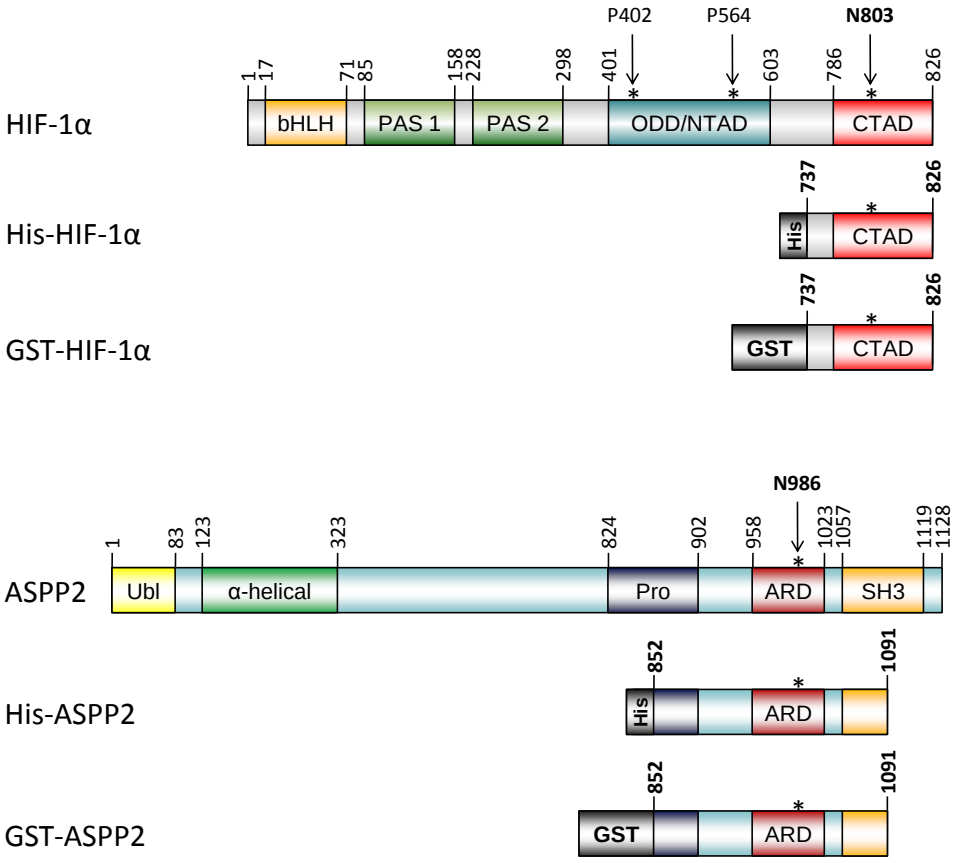

Fig. 10: ASPP2 and HIF-1α sequences used for *in vitro* hydroxylase activity assessment and interaction assays. The sequences are shown as positioned in the full length protein. N-terminal protein tags are indicated. His, histidine-tag; GST, GST-tag; Ubl, ubiquitin-like fold; Pro, proline-rich region; ARD, ankyrin repeat domain; SH3, Src-homology 3 domain; bHLH, basic-helix-loop-helix domain; PAS, Per-Arnt-Sim domain; ODD, oxygen-dependent degradation domain; NTAD, N-terminal transactivation domain; CTAD, C-terminal transactivation domain.

3.2.2 Protein expression and purification

For hydroxylase activity measurements, His-tagged full length FIH-1 (Hewitson *et al.*, 2002) and substrate proteins were expressed in BL21 (DE3) *E. coli* cultures and purified from lysates by nickel affinity purification (Fig. 11). As assessed on Coomassie-stained SDS-PAGE gels by quantification using ImageJ, purity of the proteins was approximately 95% for His-HIF-1α and 98% for His-ASPP2 fragments. For FIH-1, purity was more variable ranging from 65% to 85% in different enzyme preparations. The enzyme was stable over several months upon storage in 50% glycerol at -20°C, as well as the His-HIF-1α substrates which were stored in 10% glycerol at -80°C. In contrast, the His-ASPP2 substrates were unstable upon storage and therefore freshly prepared prior to each hydroxylase activity assay.

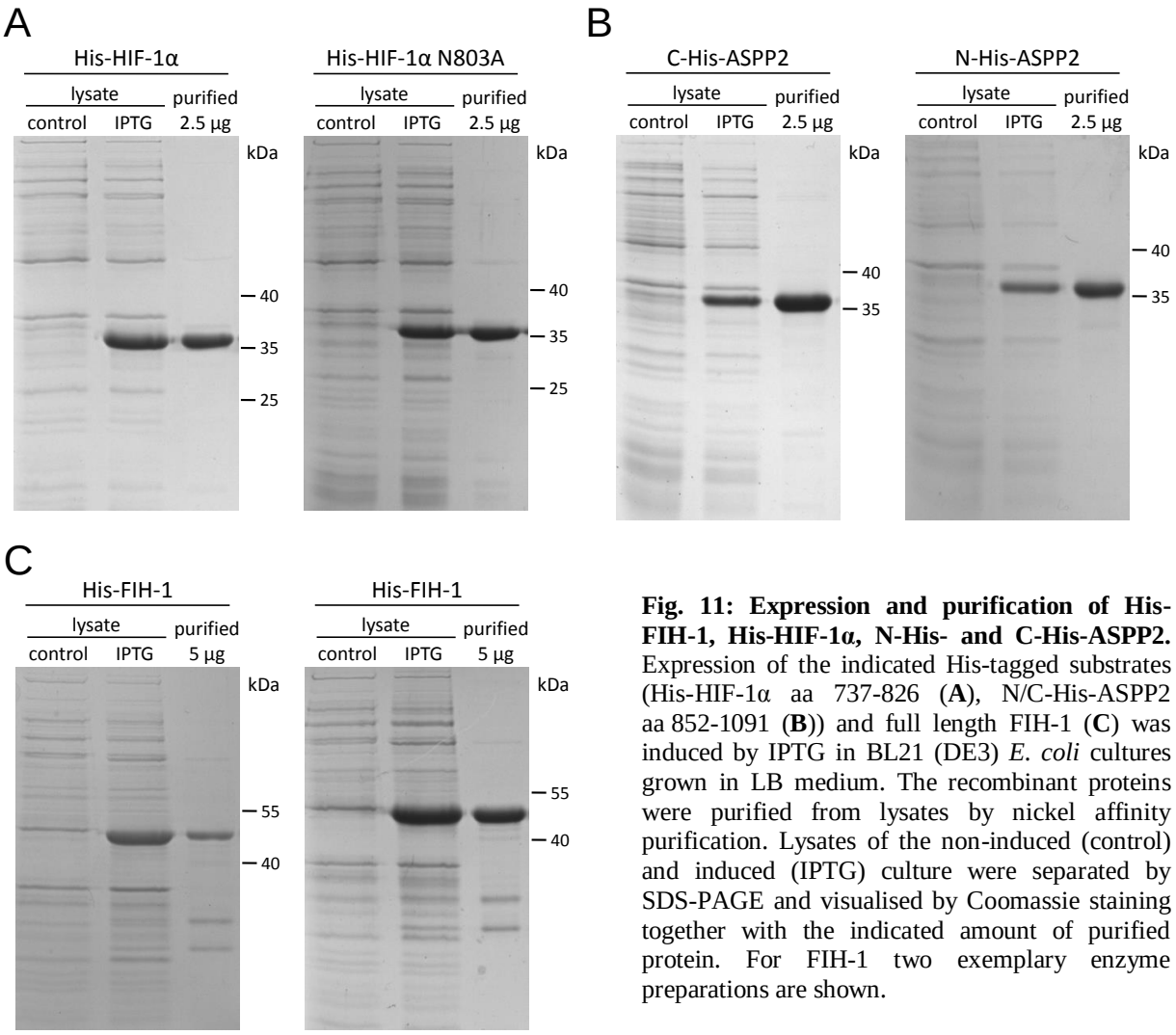

Fig. 11: Expression and purification of His-FIH-1, His-HIF-1α, N-His- and C-His-ASPP2. Expression of the indicated His-tagged substrates (His-HIF-1α aa 737-826 (**A**), N/C-His-ASPP2 aa 852-1091 (**B**)) and full length FIH-1 (**C**) was induced by IPTG in BL21 (DE3) *E. coli* cultures grown in LB medium. The recombinant proteins were purified from lysates by nickel affinity purification. Lysates of the non-induced (control) and induced (IPTG) culture were separated by SDS-PAGE and visualised by Coomassie staining together with the indicated amount of purified protein. For FIH-1 two exemplary enzyme preparations are shown.

3.2.3 FIH-1-dependent hydroxylation of ASPP2 *in vitro*

The hydroxylase activity assay was established using the well-characterised His-HIF-1α substrate containing the whole CTAD with the FIH-1 hydroxylation site N803 (aa 737-826) (Linke *et al.*, 2004). The reaction, monitored via release of $^{14}CO_2$ by scintillation counting, was found to be linear over more than 2 h (Fig. 12). To warrant maximal sensitivity for the following experiments on ASPP hydroxylation, the 2 h time point was chosen for subsequent analyses. Comparing the activity of FIH-1 on N- and C-terminal His-tagged ASPP2 test substrates at this time point to that of His-HIF-1α, we detected lower values for both His-ASPP2 substrates, but as compared to the negative control, His-HIF-1α where the hydroxylation site is substituted by alanine (N803A), values were significantly higher (Fig. 13 A).

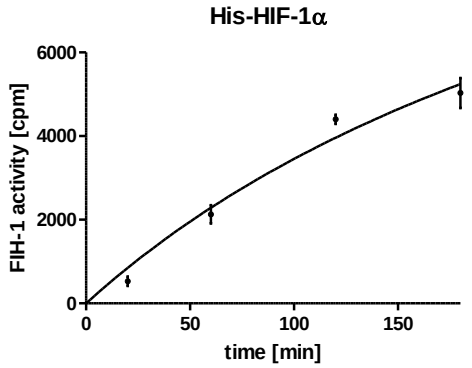

Fig. 12: Time course of FIH-1-dependent hydroxylation of His-HIF-1α. 50 µM His-HIF-1α was incubated with 7.5 µM His-FIH-1 in the presence of co-factors at 37°C. FIH-1 activity was quantified via release of $^{14}CO_2$ from the reaction by scintillation counting. Hydroxylation of His-HIF-1α by FIH-1 was monitored over a period of 3 h. Triplicate values for each time point normalised to control samples lacking the enzyme are plotted.

This is important because 2-oxoglutarate-dependent dioxygenases can also catalyse decarboxylation of the co-substrate in the absence of the primary substrate which is termed uncoupled activity (Koivunen *et al.*, 2004). In line with previous reports on other ARD-containing FIH-1 substrates (Cockman *et al.*, 2009b), the FIH-1-dependent hydroxylation of His-ASPP2 *in vitro* was less efficient as compared to His-HIF-1α containing the hydroxylation site (Fig. 13 A). Because the FIH-1 activity on His-ASPP2 was found to be higher with an N-terminal position of the His-tag, the N-His-ASPP2 substrate was used in mutation studies to identify the hydroxylated amino acid. First, the putative FIH-1 hydroxylation site identified in our database search, N986, was mutated to alanine or in a more structure conserving way to threonine by overlap PCR.

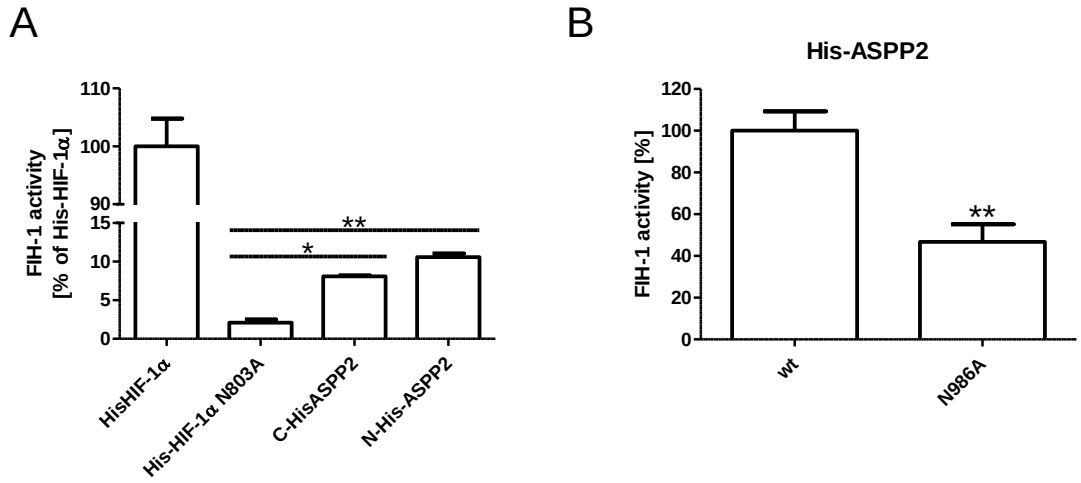

Fig. 13: ASPP2 is hydroxylated by FIH-1 *in vitro*. (**A**) FIH-1 activity on N- and C-terminal His-tagged ASPP2 test substrates as compared to His-HIF-1α wild-type and hydroxylation deficient (N803A) substrates used as positive and negative control, respectively. Activities are shown relative to His-HIF-1α. (**B**) FIH-1 activity on N-terminal His-ASPP2 substrate fragments containing (wt) and lacking (N986A) the putative FIH-1 hydroxylation site. Activities are shown relative to His-ASPP2 wt. (**A**, **B**) 50 µM substrate was incubated with 7.5 µM FIH-1 in the presence of co-factors at 37°C for 2 h. Enzyme activity was monitored via release of $^{14}CO_2$ from the reaction by scintillation counting. Triplicate values for each test substrate normalised to control samples lacking the enzyme are plotted. Significance was tested by one-way ANOVA (**A**) or Student's t-test (**B**) where * indicates $p < 0.05$ and ** indicates $p < 0.01$.

Comparing the N986A mutant to wild-type His-ASPP2 in the hydroxylase activity assay showed that the mutation indeed reduced, but not completely abrogated enzyme turnover (Fig. 13 B). As still almost 50% of the activity was detected, the presence of another hydroxylation site was examined for the test substrate. Indeed, the protein sequence of ASPP2 showed another asparagine two amino acids upstream of N986 (Fig. 9) which might be targeted by FIH-1 as well considering the low substrate specificity of the enzyme.

To test whether hydroxylation of N984 occurs, we generated a threonine single mutant for this residue (N984T) and a threonine mutant lacking both asparagines (N984T/N986T). All mutants were expressed in BL21 (DE3) *E. coli* cultures and purified from culture lysates by nickel affinity purification yielding a similar degree of purity ranging from 87% to 94% as assessed on Coomassie-stained SDS-PAGE gels (Fig. 14).

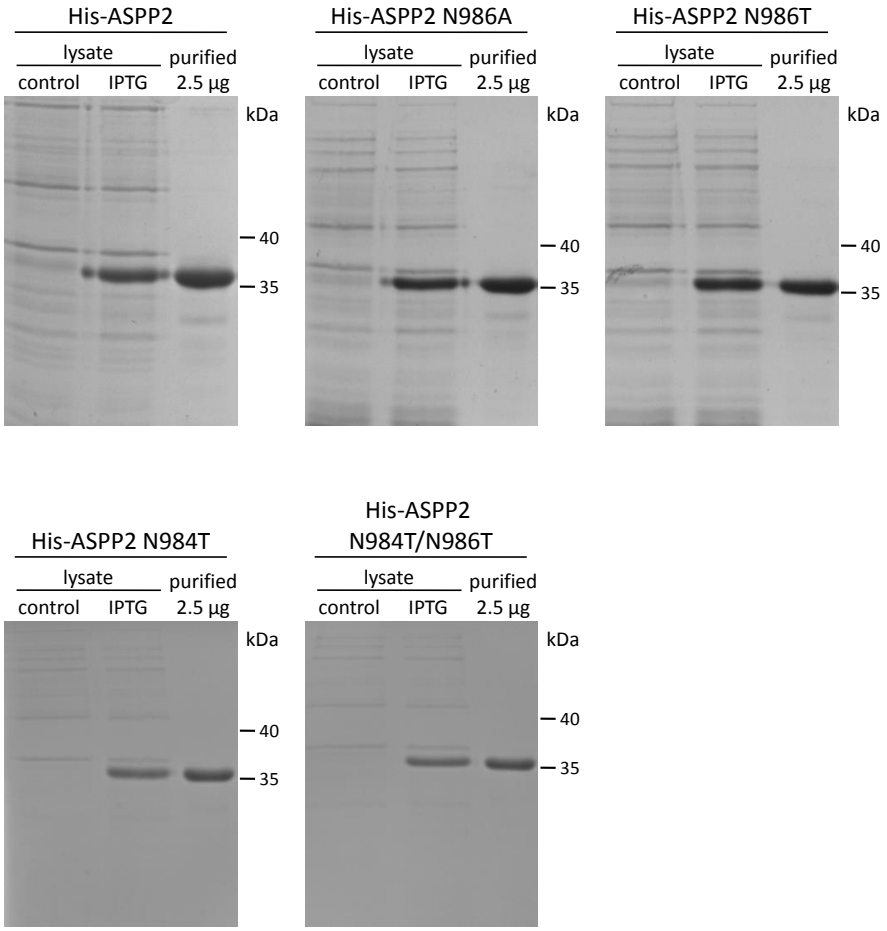

Fig. 14: Expression and purification of His-ASPP2 asparagine mutants. The indicated mutations were inserted into the expression plasmids by overlap PCR. Protein expression of the indicated N-terminal His-tagged ASPP2 test substrates was induced by IPTG in BL21 (DE3) *E. coli*. The recombinant proteins were purified from lysates by nickel affinity purification. Lysates of the non-induced (control) and induced (IPTG) culture were separated by SDS-PAGE and visualised by Coomassie staining together with 2.5 µg of the purified protein.

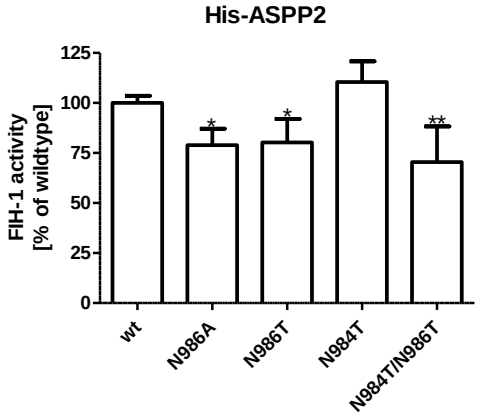

Fig. 15: FIH-1-dependent hydroxylation of His-ASPP2 asparagine mutants. The indicated N-terminal His-tagged ASPP2 test substrates in wild-type (wt) and mutant forms as indicated were incubated at a concentration of 50 µM with 7.5 µM FIH-1 in the presence of co-factors at 37°C for 2 h. Enzyme activity was monitored via release of $^{14}CO_2$ from the reaction by scintillation counting. Activities are shown relative to His-ASPP2 wt. Six-fold values for each mutant normalised to control samples lacking the enzyme are plotted. Significance between each mutant and wt was tested by one-way ANOVA where * indicates $p < 0.05$ and ** indicates $p < 0.01$.

Subjecting the mutants to the hydroxylase activity assay, we observed similar effects of alanine and threonine mutation. Both mutations of N986 reduced hydroxylation significantly and to the same extent, but the residual FIH-1 activity observed for this substrate preparation was even higher than observed in the proceeding experiment with 75% of the wild-type activity detected (Fig. 15). The slightly more pronounced decrease observed for the double mutant was not significant in comparison to the N986 single mutants demonstrating that the high background was not due to hydroxylation of N984 instead of N986. In line with this, the single mutant for N984 did not show significant differences as compared to the wild-type substrate. However, the high background could still be caused by another hydroxylation site present in the test substrate. On the other hand, as the His-ASPP2 proteins were found to be unstable in solution, degradation products or precipitates might interfere with the hydroxylation reaction. To obtain a system with lower background for the analyses we designed short peptides of ASPP2 and also iASPP for further *in vitro* studies on the hydroxylation of ASPPs.

3.2.4 ASPP peptide design

The ASPP peptides were designed according to previous studies on the hydroxylation of peptides by FIH-1. All the peptides previously reported to be hydroxylated by FIH-1 contained 20 amino acids comprising a relatively long region upstream to the hydroxylation site while only 3 to 5 downstream amino acids where included, e.g. aa 788-807 for HIF-1α (Cockman *et al.*, 2006). As this region also includes the most conserved residues of our consensus sequence, among which is the previously discussed leucine residue at the -8 position (chapter 3.1, Fig. 7), we designed our peptides based on this study containing 15 amino acids upstream of the target asparagine and 4 downstream residues (Fig. 16 A and B).

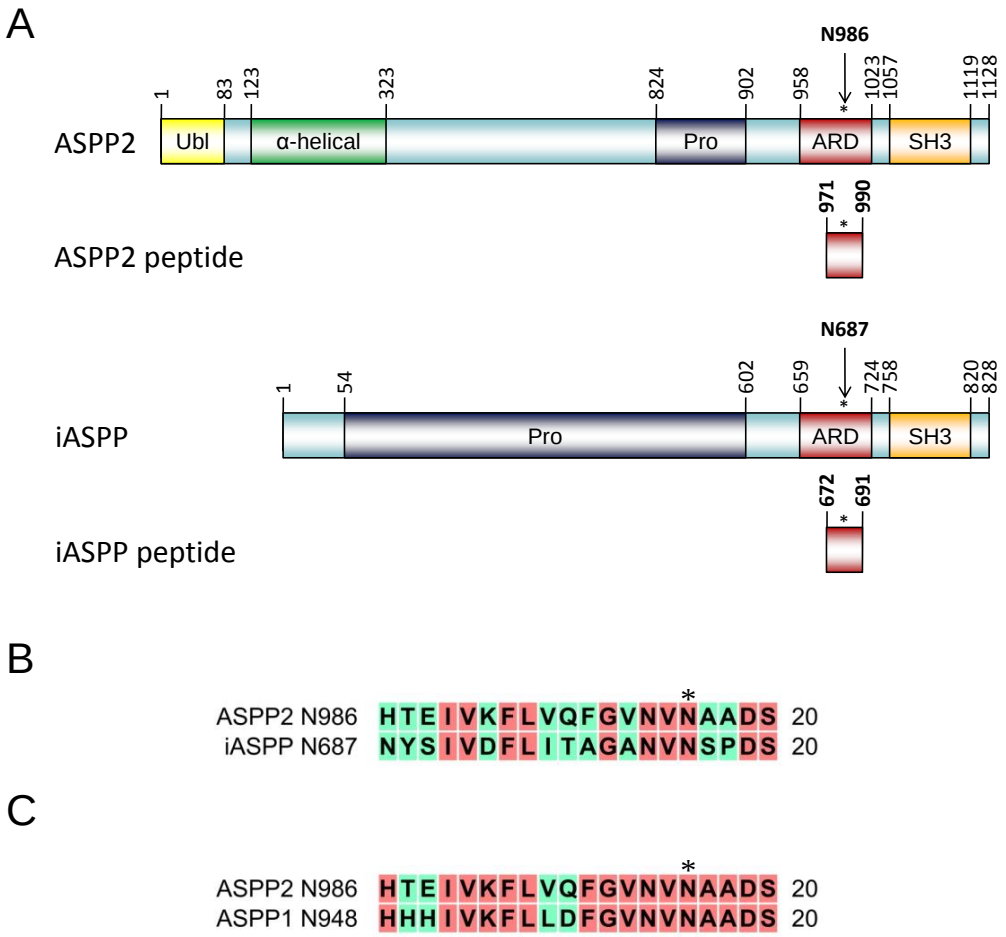

Fig. 16: ASPP peptide design. (**A**) Diagram showing the domain structure of ASPP2 and iASPP. Peptides designed for hydroxylase activity measurements are shown according to their position in the full length protein. (**B**, **C**) Protein sequence alignment of the ASPP2 peptide with the corresponding peptide for iASPP (**B**) and ASPP1 (**C**). Identical residues are coloured in red and different amino acids are shown in green. Putative FIH-1 hydroxylation sites are indicated by asterisks. Ubl, ubiquitin-like fold; Pro, proline-rich region; ARD, ankyrin repeat domain; SH3, Src-homology 3 domain.

Because ASPP1 shows a very high homology to the ASPP2 peptide with only 4 out of 20 amino acids differing in non-conserved regions of the FIH-1 substrate consensus, the ASPP2 peptide was tested as a representative of both proapoptotic ASPPs (Fig. 16 C). In contrast, iASPP showed substantially more variation with 10 different residues. Thus ASPP2 and iASPP peptides were generated in wild-type and mutant forms where the putative FIH-1 hydroxylation sites were substituted by alanine (ASPP2 N986A, iASPP N687A).

3.2.5 FIH-1-dependent hydroxylation of ASPP peptides *in vitro*

Subjecting the peptides for ASPP2 containing (wt) or lacking (N986A) the potential hydroxylation site to the hydroxylase activity assay we observed that mutation of N986 almost completely abrogated enzyme turnover confirming the previous finding that N986 is a single hydroxylation site in this region of the protein (Fig. 17 A). Moreover, increasing concentrations of wild-type but not mutant peptide specifically enhanced the activity of FIH-1 (Fig. 17 B). Comparing iASPP peptides containing (wt) or lacking (N687A) the potential hydroxylation site to ASPP2 peptides revealed that, in contrast to ASPP2, iASPP cannot serve as substrate for FIH-1 *in vitro*. Even increasing concentrations of the iASPP wild-type peptide up to 300 µM did not produce FIH-1 activity significantly exceeding background levels as determined by the use of the corresponding mutant (Fig. 17 C). Because the background activity we detected for the ASPP2 peptides was substantially lower than observed for the substrate protein fragments, the peptides were used to further characterise the hydroxylation of ASPP2 catalysed by FIH-1.

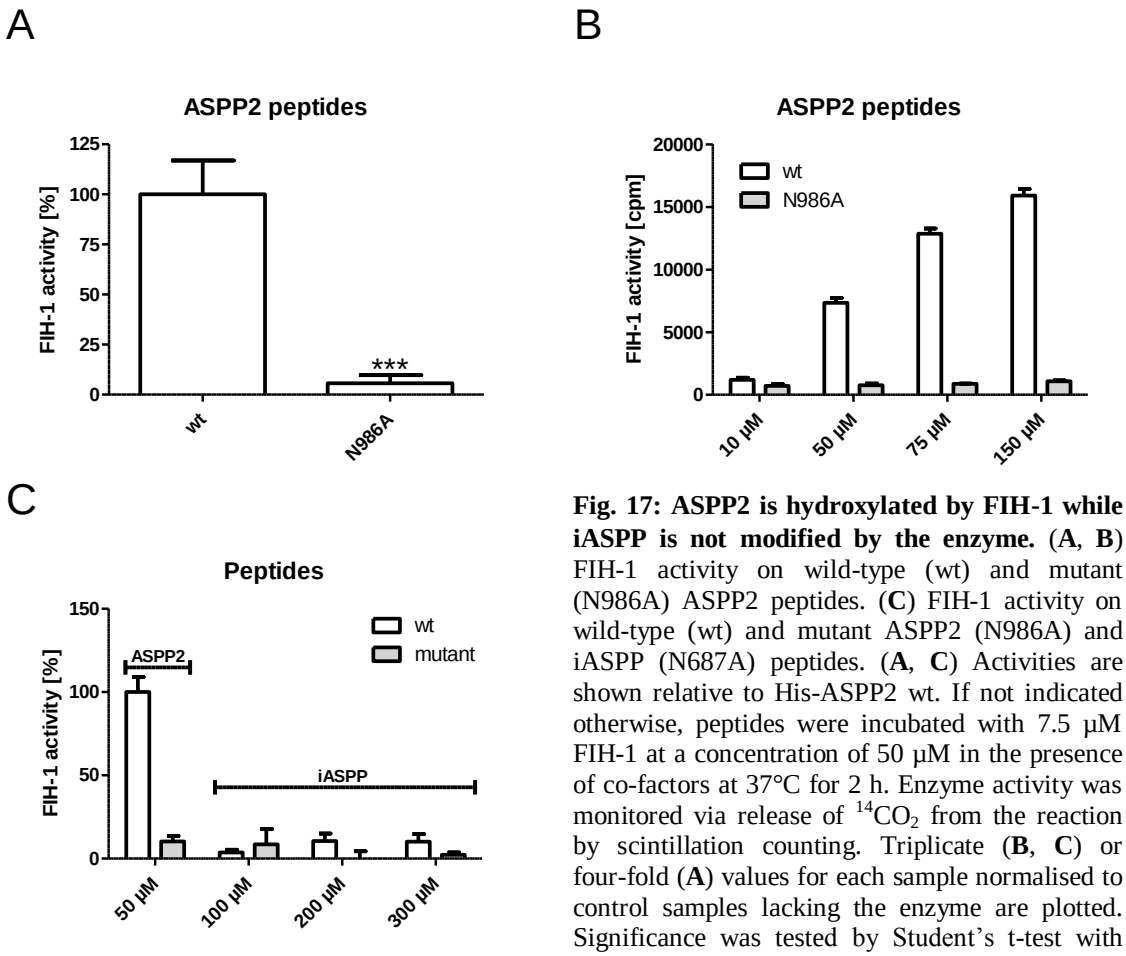

Fig. 17: ASPP2 is hydroxylated by FIH-1 while iASPP is not modified by the enzyme. (**A**, **B**) FIH-1 activity on wild-type (wt) and mutant (N986A) ASPP2 peptides. (**C**) FIH-1 activity on wild-type (wt) and mutant ASPP2 (N986A) and iASPP (N687A) peptides. (**A**, **C**) Activities are shown relative to His-ASPP2 wt. If not indicated otherwise, peptides were incubated with 7.5 µM FIH-1 at a concentration of 50 µM in the presence of co-factors at 37°C for 2 h. Enzyme activity was monitored via release of $^{14}CO_2$ from the reaction by scintillation counting. Triplicate (**B**, **C**) or four-fold (**A**) values for each sample normalised to control samples lacking the enzyme are plotted. Significance was tested by Student's t-test with *** indicating $p < 0.001$.

We determined the K_m value for the wild-type ASPP2 peptide to be 75 µM, which was comparable to those reported for other ARD-containing FIH-1 substrates identified so far (Fig. 18 A) (Wilkins *et al.*, 2009). The 2-OG competitor NOG specifically blocked enzyme turnover in a concentration-dependent manner for wild-type but not for mutant ASPP2 peptides (Fig. 18 B) which again demonstrates the specificity of the reaction. In summary, the *in vitro* data identify N986 as a single hydroxylation site in ASPP2. Although high background was detected in hydroxylase activity assays upon mutation of N986 using longer protein fragments, we did not identify other target amino acids for FIH-1.

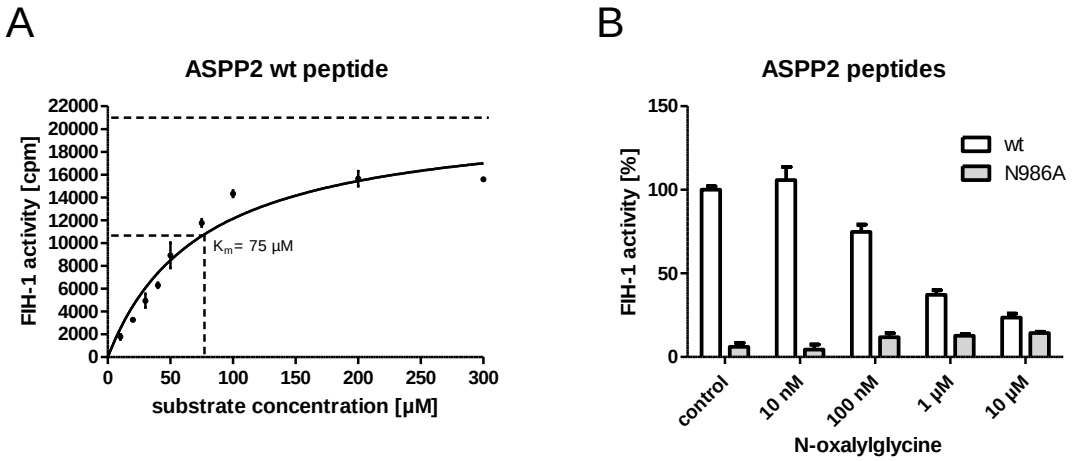

Fig. 18: Kinetics and specificity of FIH-1-dependent hydroxylation of ASPP2. (**A**) To determine the K_m value for the ASPP2 wild-type (wt) peptide increasing concentrations of the peptide were incubated with 7.5 µM FIH-1 in the presence of co-factors at 37°C for 2 h. (**B**) Competitive inhibition of FIH-1 activity on ASPP2 wild-type (wt) but not mutant (N986A) peptide. Peptides were incubated with 7.5 µM FIH-1 at a concentration of 50 µM in the presence of co-factors and the indicated concentration of the competitive inhibitor NOG at 37°C for 2 h. Enzyme activity was monitored via release of $^{14}CO_2$ by scintillation counting. Triplicate values for each sample normalised to control samples lacking the enzyme are plotted.

3.3 FIH-1 dependent hydroxylation of ASPP2 in cells

To directly verify hydroxylation in cells, ASPP2 purified from HEK293T cells was analysed by LC-MS/MS. To this purpose, full length ASPP2 was transiently overexpressed in the cells for 24 h and purified from cell lysates by immunoprecipitation. The purified proteins were separated by SDS-PAGE. To generate peptides containing N986, protein bands displaying the correct molecular weight were excised and subjected to digestion by proteases.

Using chymotrypsin a peptide comprising the potential hydroxylation site N986 (GVNV**N**AADSDGWTPL, $[M+2H]^{2+}$=758.36) could reproducibly be detected. In addition to the signal at m/z 758.36, a signal with a mass difference of +16 ($[M+2H]^{2+}$=766.36) corresponding to the hydroxylated peptide was observed at a slightly earlier retention time. The signal intensity in the MS survey scan for both peptides at the respective peak in the elution profile (Fig. 19 A) shows, that in HEK293T cells with endogenous FIH-1 expression, the protein was detected in the hydroxylated and in the unmodified form, with a higher intensity for the hydroxylated species.

In order to show that the modification is indeed introduced by FIH-1, ASPP2 purified from cells containing different amounts of the active enzyme was analysed (Fig. 19 A and B). FIH-1 overexpression increased the relative amount of hydroxylation significantly, with the unmodified form close to the detection limit. In contrast, treatment with the hydroxylase inhibitor DMOG led to an increase of the unmodified variant with the hydroxylated species being barely detectable. Similarly, suppression of endogenous FIH-1 expression through lentiviral transduction of shRNA (shFIH-1) reduced the relative amount of hydroxylated protein. Although the FIH-1 knockdown was found to decrease hydroxylation less effectively as compared to the hydroxylase inhibitor, the reduction clearly demonstrated that ASPP2 hydroxylation is mediated by FIH-1. Residual hydroxylation probably results from an incomplete knockdown. The efficiency was nearly 90%, with still 10% of the active enzyme present in the cells used for the analysis (Fig. 19 B).

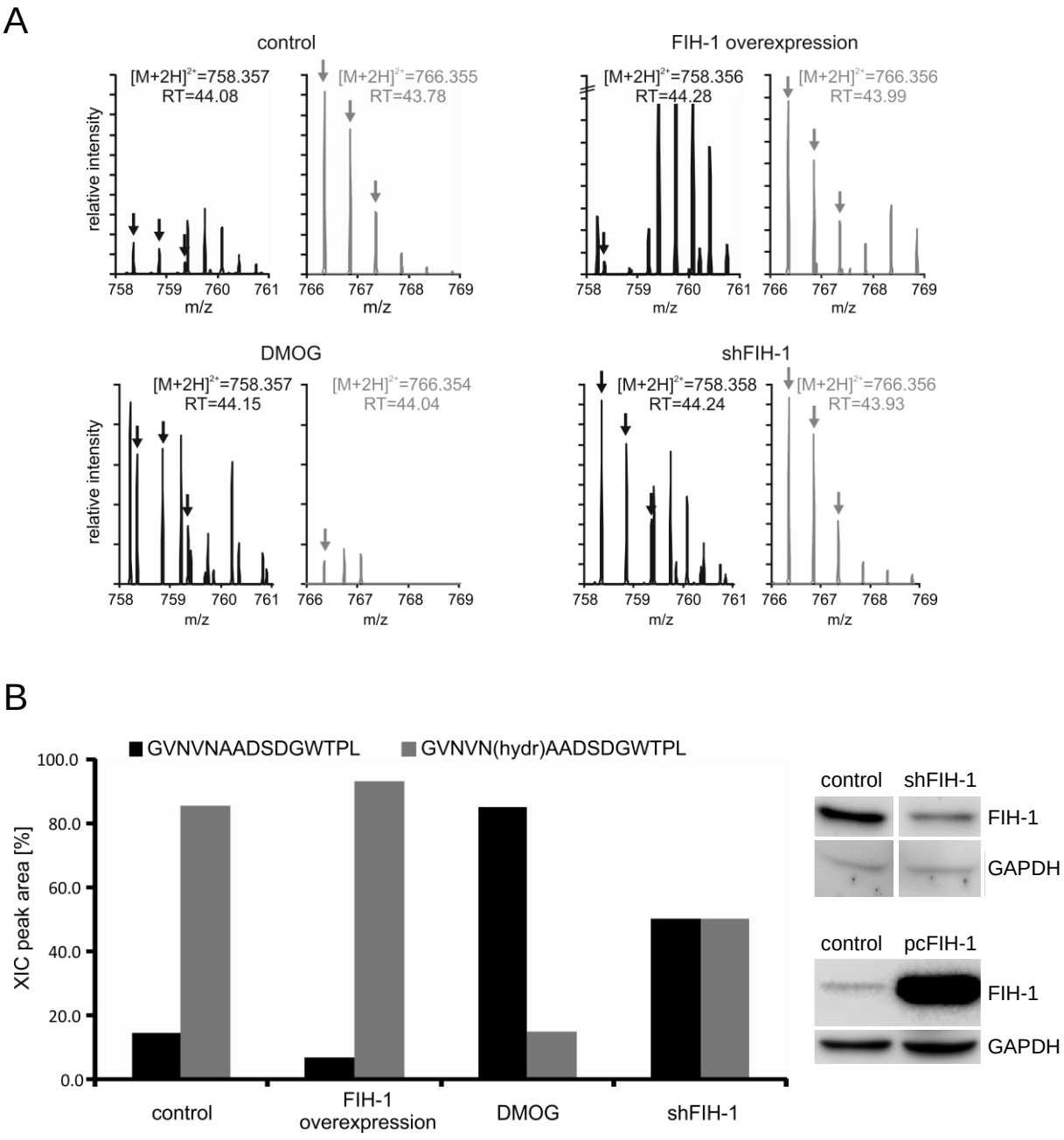

Fig. 19: ASPP2 hydroxylation is detectable in cells and depends on FIH-1 activity and abundance. Chymotrypsin cleavage yielded the ASPP2 peptide GVNVNAADSDGWTPL which was detectable in a hydroxylated and a non-modified variant by LC-MS/MS analysis using overexpressed ASPP2 purified from HEK293T cells expressing endogenous FIH-1, cells transduced with shRNA against FIH-1 (shFIH-1), FIH-1 overexpressing cells or cells treated with the hydroxylase inhibitor DMOG. (**A**) MS spectra from an LC-MS/MS analysis of ASPP2 purified from cells with different amounts or activity of FIH-1. The spectra are shown for the respective peak in the extracted ion chromatograms of the peptide variants (unmodified: $[M+2H]^{2+}$=758.36, hydroxylated: $[M+2H]^{2+}$=766.36). (**B**) Relative amounts of unmodified peptide in comparison to the hydroxylated peptide. Peak areas from extracted ion chromatograms (XIC) for the respective masses are shown. As control for overexpression and suppression of FIH-1 equal amounts of total cell lysates were subjected to SDS-PAGE and subsequent Western blotting (right panel). GAPDH was used as a loading control.

In addition, MS/MS analysis was performed to confirm the identity of the peptides detected (Fig. 20). The results showed a positive identification by the Mascot search engine with a false discovery rate of 1% and a Mascot score above 40. The b-ions which define N986 as the site of FIH-1-dependent hydroxylation are visible in the MS/MS spectrum. In summary, the results demonstrated that hydroxylation of ASPP2 at N986 occurs in cells and the amount of hydroxylation is correlated to FIH-1 activity and abundance.

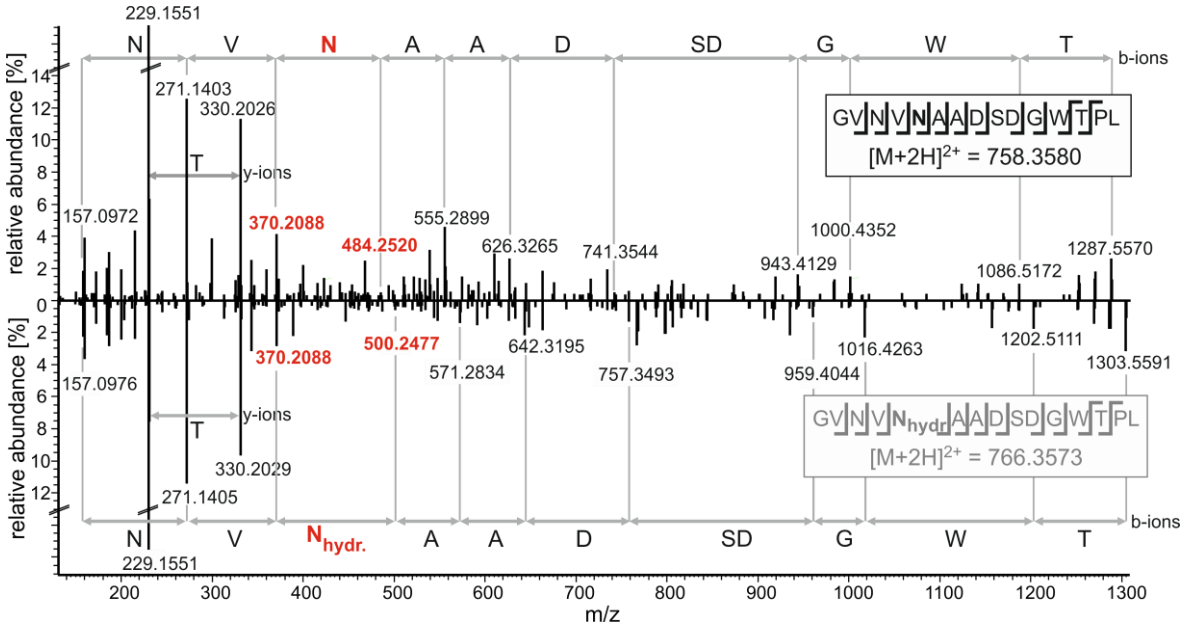

Fig. 20: N986 is the FIH-1 hydroxylation site in the ARD of ASPP2. Chymotrypsin cleavage yielded the ASPP2 peptide GVNVNAADSDGWTPL which was detectable in a non-modified (upper spectrum) and a hydroxylated (lower spectrum) variant by LC-MS/MS analysis using overexpressed ASPP2 purified from HEK293T cells. MS/MS spectra confirm the peptide identity demonstrating N986 as the site of modification. The mass shift of +16 Da and the hydroxylation site are highlighted in red.

3.4 FIH-1-ASPP2 interaction *in vitro*

As hydroxylation of ASPP2 by FIH-1 also occurs in cells we wanted to further characterise the enzyme-substrate interaction in an *in vitro* approach. To perform pull-down assays we generated the same substrate proteins used for the hydroxylation studies with an N-terminal GST-tag (chapter 3.2.1, Fig. 10) as these were expected to interact with the enzyme. The substrates were expressed in BL21 (DE3) *E. coli* and purified from lysates by glutathione affinity purification. As assessed on Coomassie-stained SDS-PAGE gels purity of the proteins was approximately 98% for the GST control and 90% for GST-HIF-1α wild-type and the N803A mutant (Fig. 21 A and B).

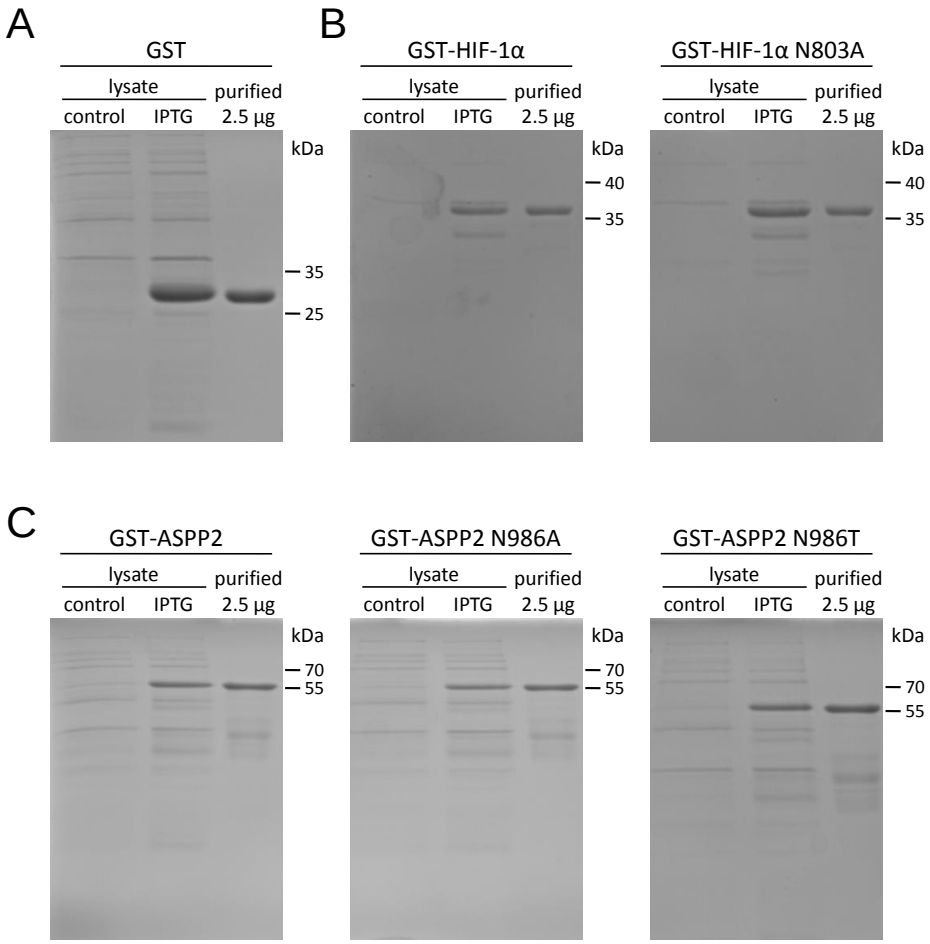

Fig. 21: Expression and purification of GST, GST-HIF-1α and GST-ASPP2. Expression of GST alone (**A**) and the indicated GST-tagged proteins (GST-HIF-1α aa 737-826 (**B**), GST-ASPP2 aa 852-1091 (**C**)) was induced by IPTG in BL21 (DE3) *E. coli* grown in LB medium. The recombinant proteins were purified from lysates by glutathione affinity purification. Lysates of the non-induced (control) and induced (IPTG) cultures were separated by SDS-PAGE and visualised by Coomassie staining together with 2.5 µg of the purified protein.

For GST-ASPP2 proteins including wild-type and the two hydroxylation site mutants, N986A and N986T, purification was less efficient with about 60% purity achieved (Fig. 21 C). To test interaction with the enzyme the GST fusion proteins or GST alone were incubated with radioactively labelled FIH-1 with the substitution of 2-OG and Fe(II) by NOG and zinc to prevent hydroxylation and release of the substrates which generates trapped enzyme-substrate complexes (Elkins *et al.*, 2003).

Upon GST pull-down of the substrates, a substantially higher amount of FIH-1 co-precipitated with GST-ASPP2 as compared to GST-HIF-1α while GST alone did not produce any signal (Fig. 22). Mutation of the GST-ASPP2 hydroxylation site N986 to alanine or threonine reduced interaction between enzyme and substrate substantially to the same extent. A similar effect could be observed for GST-HIF-1α following mutation of the hydroxylation site N803 to alanine. As less FIH-1 co-precipitated with GST-HIF-1α the mutation almost completely abrogated interaction while both GST-ASPP2 mutants were still able to bind a relatively high amount of the enzyme. Taken together these results demonstrate a strong interaction between ASPP2 and FIH-1 *in vitro*.

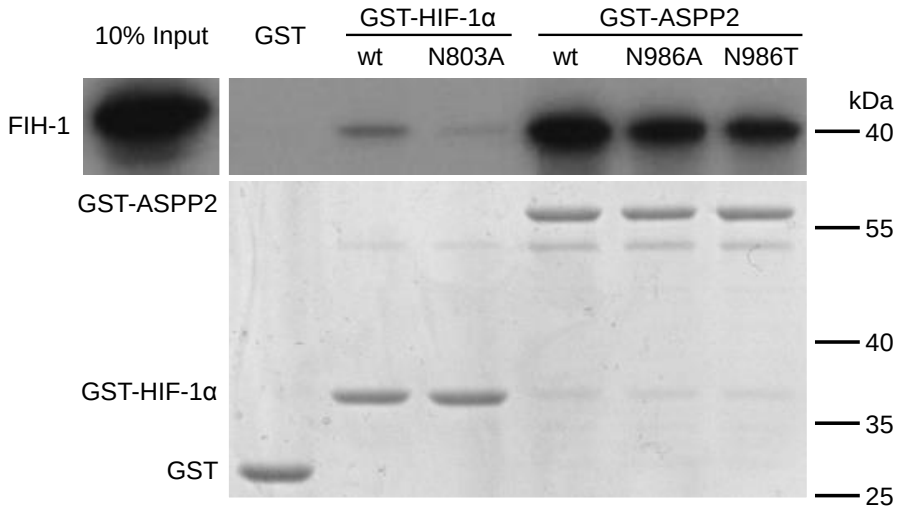

Fig. 22: Interaction of FIH-1 and ASPP2 *in vitro*. Recombinant GST fusion proteins in wild-type (wt) and mutant forms as indicated were incubated at a concentration of 5 µM with equal amounts of ^{35}S-methionine-labelled FIH-1 generated by *in vitro* transcription and translation. To prevent hydroxylation and release of the substrate, 2-OG and Fe(II) were substituted by NOG and zinc producing a trapped enzyme-substrate complex. Following incubation the reactions were subjected to GST pull-down, bound proteins separated by SDS-PAGE and visualised by autoradiography to detect FIH-1 (upper panel) or by Coomassie staining for GST fusion proteins (lower panel).

3.5 Impact of FIH-1-dependent hydroxylation of ASPP2

3.5.1 FIH-1 and ASPP2 co-localise in cells

Next, we wanted to explore the physiologic consequences of this interaction and the hydroxylation of ASPP2 by FIH-1. As a prerequisite for studies on the consequences of FIH-1-dependent hydroxylation of ASPP2, the intracellular localisation of both proteins was analysed by immunofluorescence staining. ASPP2 was almost exclusively located to the cell-cell contacts and cytoplasm of all human cancer cell lines examined. FIH-1 was shown to co-localise with ASPP2 in the cytoplasm of HCT116 colon cancer cells (Fig. 23). As ASPP2 was shown to modulate p53-dependent signalling pathways, this p53 wild-type cell line, which was also available in an isogenic p53-deficient form, was found most suitable to study the impact of hydroxylation on ASPP2-mediated modulation of p53 activity.

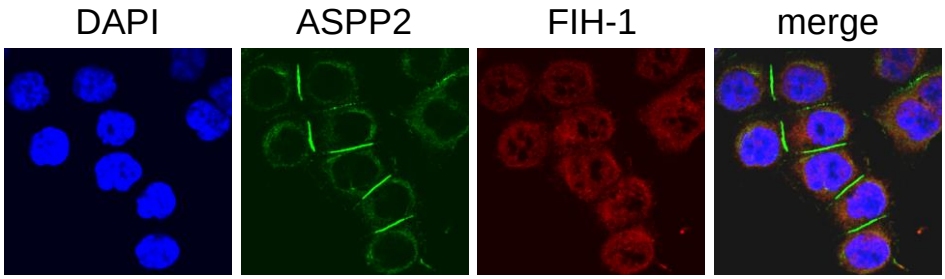

Fig. 23: Localisation of endogenous ASPP2 and FIH-1. Double immunofluorescence staining for endogenous ASPP2 (green) and FIH-1 (red) in untreated HCT116 cells. Nuclei were counterstained with DAPI.

3.5.2 ASPP2 protein stability

For further analysis of physiologic effects of ASPP2 hydroxylation by FIH-1 shFIH-1 cell lines were compared to control cells either transduced with an unspecific shRNA (shscrambled) or the empty vector pLKO.1. The knockdown efficiency for FIH-1 was found to be constantly higher than 80% (Fig. 24) for at least three weeks on the protein level. ASPP2 protein levels were examined using HCT116 cells following suppression of FIH-1 through shRNA transduction or exposure to hypoxic or anoxic conditions. In HCT116 cells (Fig. 24) as well as in other cell lines (e.g. MCF-7, H441) we found no changes in ASPP2 protein levels following depletion of FIH-1.

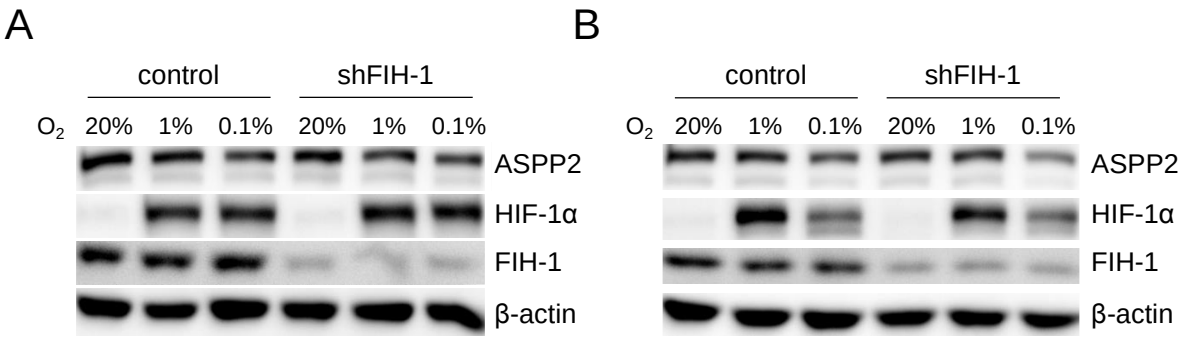

Fig. 24: ASPP2 protein levels are not affected by silencing of FIH-1. HCT116 cells were transduced with shRNA against FIH-1 (shFIH-1) or empty vector (control) and exposed to normoxic (20% O_2), hypoxic (1% O_2) and anoxic (0.1% O_2) conditions. Total cell lysates were produced after 4 h (**A**) or 24 h (**B**), equal protein amounts subjected to SDS-PAGE and subsequent Western blotting. β-actin served as a loading control.

In addition, we detected similar amounts of the protein under hypoxic and anoxic conditions in control and shFIH-1 cells at different time points, indicating that ASPP2 is not regulated by FIH-1-dependent hydroxylation on the protein level. Similar results were obtained for the well-characterised FIH-1 substrate HIF-1α which was induced by hypoxic or anoxic conditions to the same extent, irrespective of the FIH-1 status of the cells. Although these results argue against a regulation of protein stability by enzymatic hydroxylation, ASPP2 has previously been reported to be regulated on the protein level by the 26S proteasome with a half-life of 60 to 80 minutes and almost complete degradation following 3 h of treatment with the translation inhibitor cycloheximide (Zhu *et al.*, 2005). As alterations in the half-life of a protein are not necessarily associated with a change in overall protein levels (Kuhar, 2010), it is still possible that FIH-1-dependent hydroxylation of ASPP2 affects protein turnover. Therefore, we tried to determine the half-life of ASPP2 in HCT116 cells by two different methods. First, the translation inhibitor cycloheximide was applied in the absence and presence of the 26S proteasome inhibitor MG132 to monitor the proteasomal degradation of endogenous (Fig. 25 A) or exogenously expressed ASPP2 (Fig. 25 B). In the second approach, the pulse-chase technique was used to assess the degradation of overexpressed ASPP2 (Fig. 25 C).

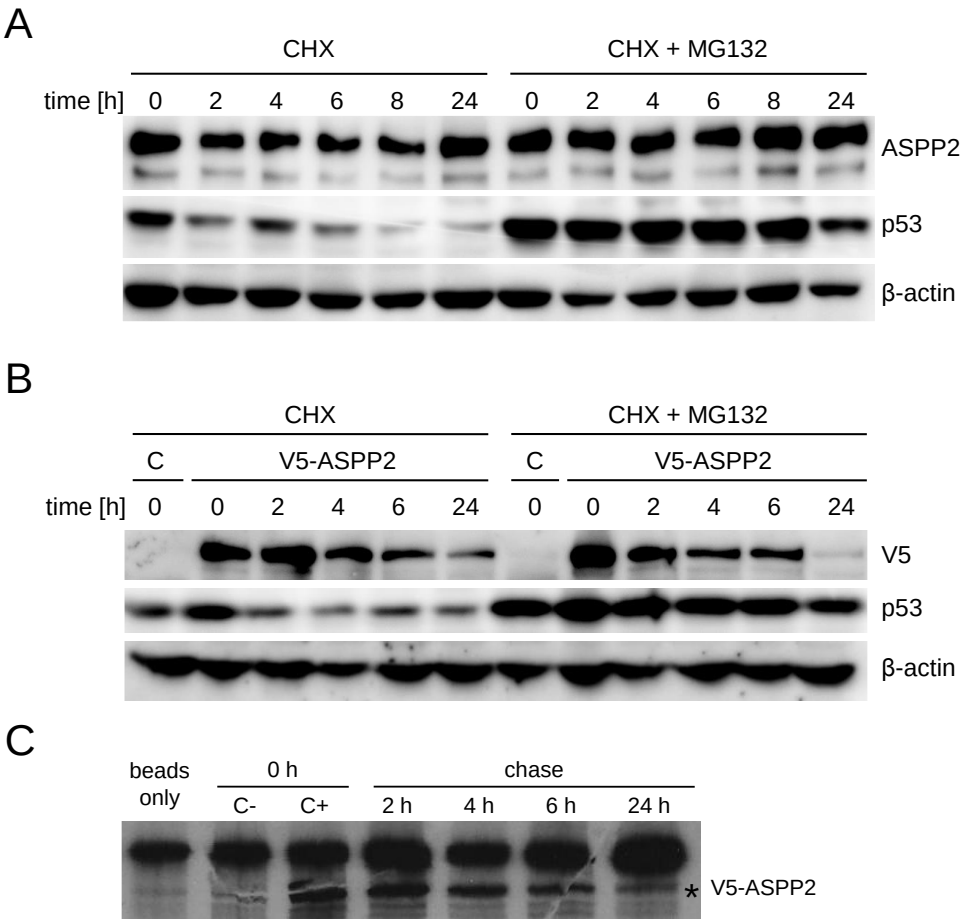

Fig. 25: ASPP2 is not regulated by proteasomal degradation in HCT116 cells. (**A**, **B**) HCT116 cells expressing endogenous ASPP2 (**A**) or transiently transfected with V5-ASPP2 for 18 h (**B**) were incubated with 100 µg/ml cycloheximide (CHX) with and without pretreatment with the proteasome inhibitor MG132 for 2 h at 25 µM. Total cell lysates were produced at the indicated time points and equal protein amounts subjected to SDS-PAGE and subsequent Western blotting. As control for treatments the proteasomal regulation of p53 was monitored. β-actin served as a loading control. (**C**) HCT116 cells transiently transfected with V5-ASPP2 for 18 h were starved in methionine-free medium for 15 min. Subsequently, cells were incubated with ^{35}S-labelled methionine for 40 min. The medium was exchanged to normal growth medium. Cells lysates were produced at the indicated time points and subjected to immunoprecipitation of V5-ASPP2 with 6 µg V5 antibody. Immunoprecipitates were separated by SDS-PAGE and visualised by subsequent autoradiography. The specific band for V5-ASPP2 is indicated by an asterisk.

For this purpose, following starvation in medium lacking methionine, transfected cells were incubated with ^{35}S-methionine for 40 min to achieve a defined pool of labelled protein. Subsequently, degradation of the protein pool was allowed for different periods in normal growth medium. Both approaches did not lead to consistent results. First, we did not detect proteasomal regulation of ASPP2 in HCT116 cells as similar protein levels were detected in the absence and presence of the 26S proteasome inhibitor MG132 while the control protein, p53, was potently induced by the treatment. Although a decrease could be observed at 2 h to 8 h after treatment with cycloheximide alone, the protein levels for endogenous ASPP2 were found to be comparable before (0 h) and 24 h after treatment while the control protein was

almost completely degraded confirming the efficacy of the treatment (Fig. 25 A). Similarly, proteasomal regulation could not be detected for exogenous ASPP2 expressed in HCT116 cells transiently transfected with V5-ASPP2. Half of the protein was degraded irrespective of the addition of MG132 4 h to 6 h after treatment with cycloheximide (Fig. 25 B). These results were confirmed by pulse-chase experiments (Fig. 25 C).

However, exogenous expression of V5-ASPP2 was found to induce apoptosis in HCT116 cells as early as 24 h after transfection and the additional treatments necessary for half-life determination, i.e. cycloheximide addition or starvation and labelling increased the apoptotic response even further. Therefore, the decrease in protein levels could not directly be attributed to proteasomal degradation which precludes a clear statement on the half-life of ASPP2 and the impact of FIH-1-dependent hydroxylation in this context.

3.5.3 Cell proliferation

As ASPP2 was reported to regulate p53, protein levels of the tumor suppressor and proapoptotic as well as antiapoptotic targets of p53 were examined. This revealed an induction of p53 and the cell cycle inhibitor p21 upon suppression of FIH-1 in HCT116 cells (Fig. 26) while expression of proapoptotic targets was not affected. Because this increase in p53 and p21 was expected to affect proliferation and apoptosis of the cancer cells we examined if these processes were altered in shFIH-1 cells. Proliferation of the cells was not altered upon suppression of FIH-1 as quantified by MTT measurements in HCT116 (Fig. 27 A) and H441 (Fig. 27 B) cells. These results were confirmed by cell counting experiments (data not shown).

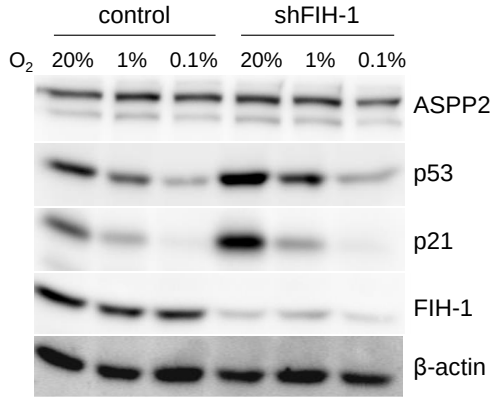

Fig. 26: FIH-1 silencing induces p53 and p21. HCT116 cells were transduced with shRNA against FIH-1 (shFIH-1) or empty vector (control) and exposed to normoxic (20% O_2), hypoxic (1% O_2) and anoxic (0.1% O_2) conditions. Total cell lysates were produced after 24 h, equal protein amounts subjected to SDS-PAGE and subsequent Western blotting. β-actin served as a loading control.

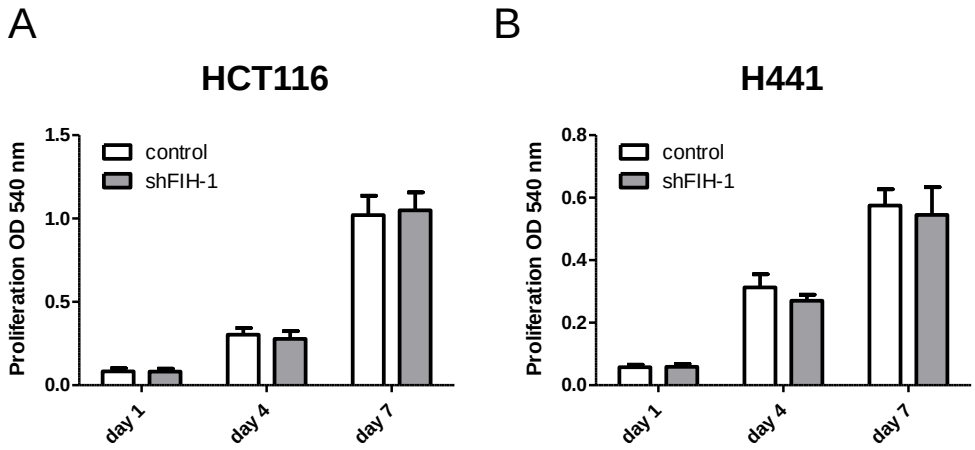

Fig. 27: FIH-1 depletion does not influence cellular proliferation in HCT116 and H441 cells. HCT116 (**A**) and H441 (**B**) cells were transduced with shRNA against FIH-1 (shFIH-1) or empty vector (control), seeded at low density and grown for the indicated periods. Following incubation with MTT, cells were lysed and proliferation was quantified by absorbance measurements at 540 nm.

3.5.4 Apoptosis

Apoptosis was induced by stimulation of HCT116 cells with chemotherapeutic drugs (etoposide or doxorubicin) for 48 h. Alternatively, apoptosis was analysed 72 h after ionizing radiation. The apoptotic response was quantified via the activity of the effector caspase-3 using a substrate which becomes fluorescent upon cleavage. FIH-1-dependent differences in the apoptotic response to chemotherapy or irradiation were not detected although all treatments increased caspase-3 activity significantly, from 1.5 fold for irradiation with 5 Gray to 4.5 fold for doxorubicin treatment (Fig. 28 A and B).

p53 was significantly induced following stimulation with doxorubicin and etoposide while p21 protein levels were decreased especially in response to doxorubicin treatment. Remarkably, we found an induction of ASPP2 on the protein level following doxorubicin treatment suggesting that ASPP2 shifts p53-dependent transactivation function from p21 to proapoptotic promoters.

However, this was not dependent on the presence of FIH-1 as no differences in apoptosis induction were detectable in control and shFIH-1 cells upon chemotherapy (Fig. 28). In line with this result, the increase in p53 and p21 protein levels upon suppression of FIH-1 disappeared following treatment with the chemotherapeutic drugs (Fig. 29), which implies that the mechanism leading to the induction in unstimulated cells is superimposed by the response to treatment.

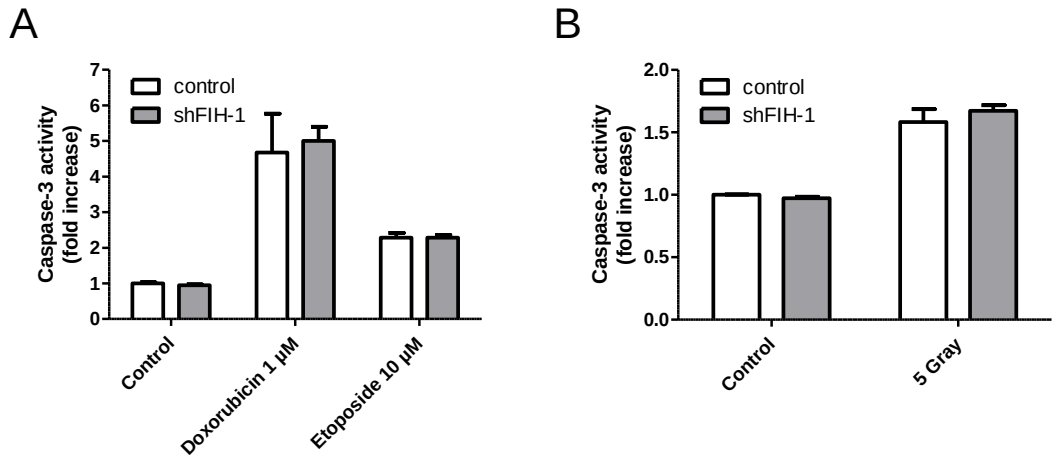

Fig. 28: Silencing of FIH-1 does not alter apoptosis in HCT116 cells. HCT116 cells were transduced with shRNA against FIH-1 (shFIH-1) or empty vector (control) and treated with the indicated concentration of chemotherapeutic agents (**A**) or irradiated with 5 Gray (**B**) to induce an apoptotic response. Total cell lysates were produced after 48 h (**A**) or 72 h (**B**). Equal protein amounts were subjected to caspase-3 activity measurements using a fluorescent substrate. Values are shown relative to the untreated empty vector control. Means and SD of three samples from the linear range of the substrate cleavage reaction are plotted.

Taken together these results imply that FIH-1-dependent hydroxylation of ASPP2 does not have gross effects on the apoptosis of cancer cells. As the induction of p53 may nevertheless be connected to ASPP2 we further characterised the connections between the two proteins.

A double immunofluorescence staining for the endogenous proteins revealed that ASPP2 localises predominantly to cell-cell contacts and cytoplasm while p53 is mainly located in the nucleus of HCT116 cells. This different localisation was also sustained under overexpression of ASPP2 until a very high expression level was achieved (Fig. 30). Up to this point, under moderate overexpression only very little ASPP2 was located in the nucleus. The absence of co-localisation of endogenous ASPP2 and p53 led to the question how efficiently the endogenous proteins can interact in HCT116 cells.

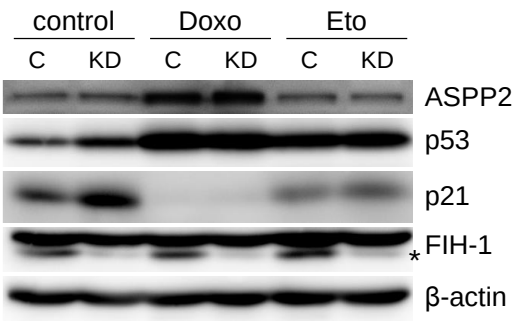

Fig. 29: Protein levels of ASPP2, p53 and p21 upon treatment with chemotherapeutic agents. HCT116 cells were transduced with shRNA against FIH-1 (KD) or empty vector (C) and treated with 1 µM doxorubicin (Doxo) or 10 µM etoposide (Eto). Total cell lysates of untreated (control) and treated samples were produced after 48 h, equal protein amounts subjected to SDS-PAGE and subsequent Western blotting. β-actin served as a loading control. The specific band for FIH-1 is indicated by an asterisk.

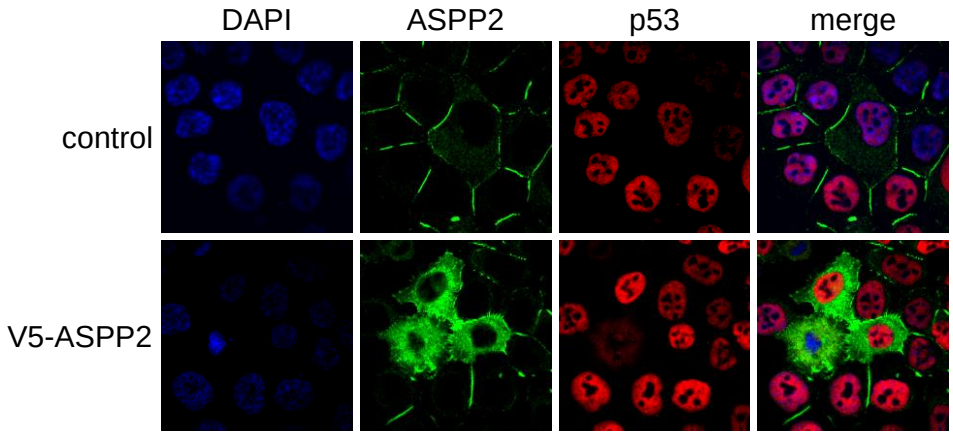

Fig. 30: Discrepant intracellular localisation of ASPP2 and p53. Double immunofluorescence staining for ASPP2 (green) and p53 (red) in HCT116 cells left untreated (control) or transiently transfected with V5-ASPP2 (V5-ASPP2) for 18 h. Nuclei were counterstained with DAPI.

To examine this further, the endogenous proteins were recovered from whole cell lysates by immunoprecipitation using specific antibodies. First, an interaction of the proteins could only be detected when the cells had been treated with a crosslinking agent prior to lysis and immunoprecipitation suggesting either a minor or a transient interaction. Furthermore, even under addition of a crosslinker, very little ASPP2 was co-precipitated with p53 (Fig. 31) confirming a weak interaction of the proteins in HCT116 cells. In addition, the degree of interaction was independent of FIH-1 as the same amount of ASPP2 co-precipitated with p53 in the presence or absence of the enzyme. In contrast to p53, the co-localisation of ASPP2 was found to be obvious for other interaction partners like Bcl-2 and Par-3 (Fig. 32).

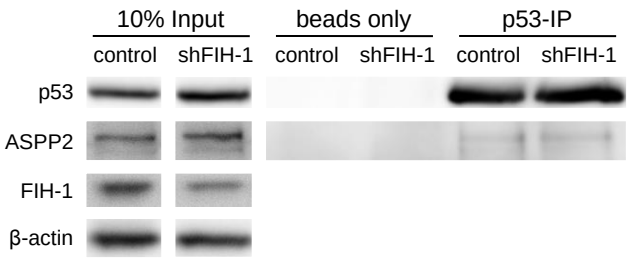

Fig. 31: Interaction between ASPP2 and p53. HCT116 cells were transduced with shRNA against FIH-1 (shFIH-1) or empty vector (control). Before preparation of total cell lysates, cells were incubated with 2 mM of the crosslinking agent DSP for 30 min. 250 µg cell lysate were subjected to immunoprecipitation using 0.7 µg p53 (Ab-6) antibody. Immunoprecipitates were subjected to SDS-PAGE and subsequent Western blotting. As negative control immunoprecipitations were performed in the absence of the specific antibody (beads only). For p53 detection a rabbit polyclonal antibody was used. In parallel 25 µg of the total cell lysate (10% input) was subjected to SDS-PAGE and subsequent Western blotting. β-actin served as a loading control.

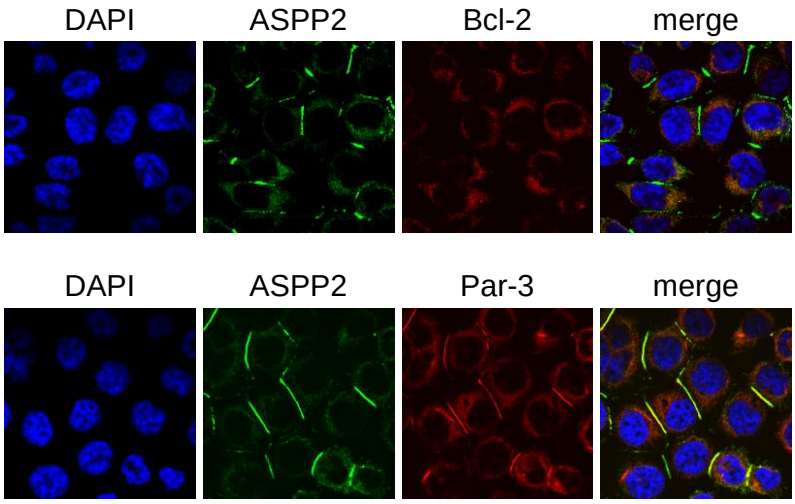

Fig. 32: Co-localisation of ASPP2 and the interaction partners Bcl-2 and Par-3. Double immunofluorescence staining for endogenous ASPP2 (green) and Bcl-2 or Par-3 (red) in untreated HCT116 cells. Nuclei were counterstained with DAPI.

For Bcl-2, which is also located in the cytoplasm, co-immunoprecipitation with ASPP2 was not detectable but Par-3 has previously been shown to be interdependently located to cell-cell contacts together with ASPP2 in several cancer cell lines (Cong *et al.*, 2010; Sottocornola *et al.*, 2010). In HCT116 cells a similar co-localisation was observed. Therefore we tested whether the localisation was also interdependent in HCT116 cells and generated stable ASPP2 and Par-3 knockdown cells through lentiviral transduction of shRNA, termed shASPP2 and shPar-3 cells, respectively. Using these cell lines, the localisation of both proteins was monitored by double immunofluorescence staining (Fig. 33). Again co-localisation of the proteins was observed in the control cells. Knockdown of each of the interaction partners abrogated the cell-cell contact localisation of the other protein confirming the interdependency. The ASPP2 antibody was found to react with high specificity in the immunofluorescence staining because the signal was almost completely abrogated upon suppression of ASPP2. In contrast, the Par-3 antibody produced a high background signal in the cytoplasm of the cells. However, the specific staining at cell-cell contacts disappeared upon depletion of ASPP2. Suppression of Par-3 had a similar effect on the localisation of ASPP2. In addition, the nuclear localisation of ASPP2 was increased in the absence of Par-3. This result suggested that the interaction with the tight junction protein may prevent a regulatory function of ASPP2 on p53-dependent signalling via modulation of the intracellular localisation in HCT116 cells. Thus, we tested whether the apoptotic response of the cells was altered upon disruption of the interaction between ASPP2 and Par-3.

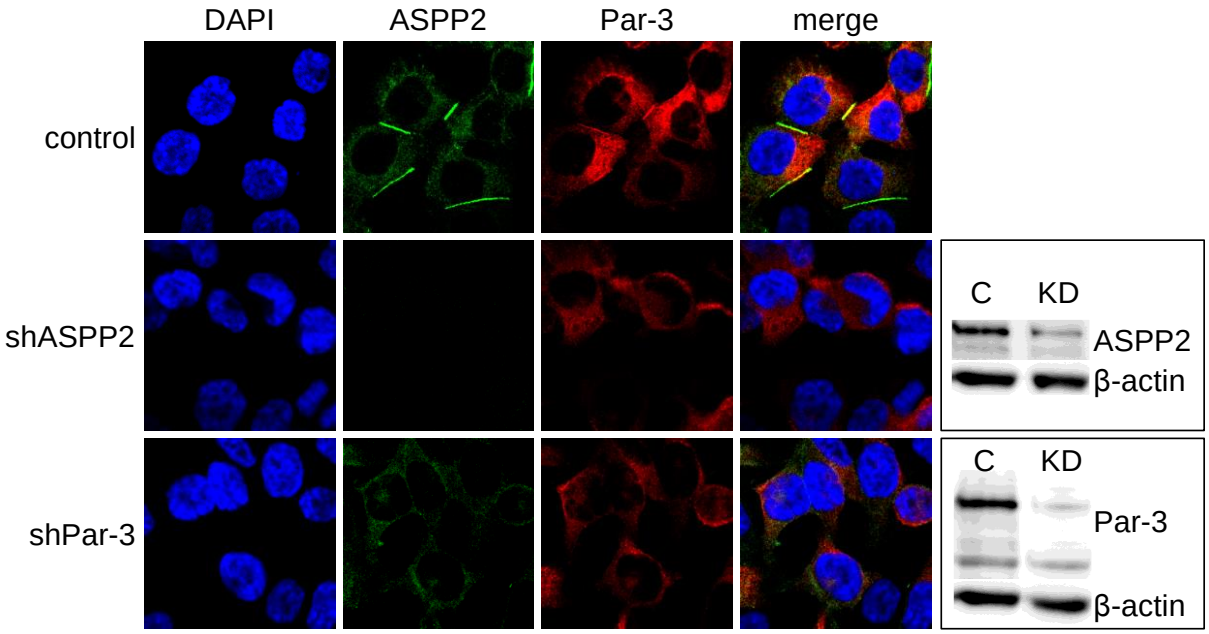

Fig. 33: Interdependent localisation of ASPP2 and Par-3 in HCT116 cells. HCT116 cells were transduced with shRNA against ASPP2 (shASPP2), Par-3 (shPar-3) or empty vector (control) and stained for endogenous ASPP2 (green) and Par-3 (red) by double immunofluorescence. Nuclei were counterstained with DAPI. In parallel, suppression of the respective protein (KD) was monitored in comparison to control cells (C) by SDS-PAGE and subsequent Western blotting of equal protein amounts from total cell lysates (right panel). β-actin served as a loading control.

To this end, we induced an apoptotic response using doxorubicin and etoposide. Indeed, an even more pronounced increase in nuclear localisation of ASPP2 could be observed in shPar-3 cells treated with the chemotherapeutic agents for 16 h (Fig. 34 A and B) as compared to untreated shPar-3 cells (Fig. 33). In contrast, control cells showed only little amounts of nuclear ASPP2 in the immunofluorescence staining upon treatment. However, the apoptotic response of HCT116 cells was not affected by the altered localisation of the protein (Fig. 34 C). In addition, apoptosis induction was found to be completely independent of the protein as shASPP2 cells showed no differences in caspase-3 activity upon treatment. Again, an increase in ASPP2 protein levels was detected following doxorubicin stimulation (Fig 34 D). Although this increase was partly inhibited in shASPP2 cells, no effect on apoptosis was observed demonstrating, that ASPP2, while induced, is not involved in the regulation of the response to doxorubicin. In summary, the results do not confirm a central role for ASPP2 in the regulation of apoptosis as reported previously. Depletion or altered localisation of the protein was not found to affect p53-dependent apoptosis and if at all, a minor interaction between ASPP2 and p53 was observed in HCT116 cells which was confirmed in another p53 wild-type cell line, MCF-7 (data not shown).

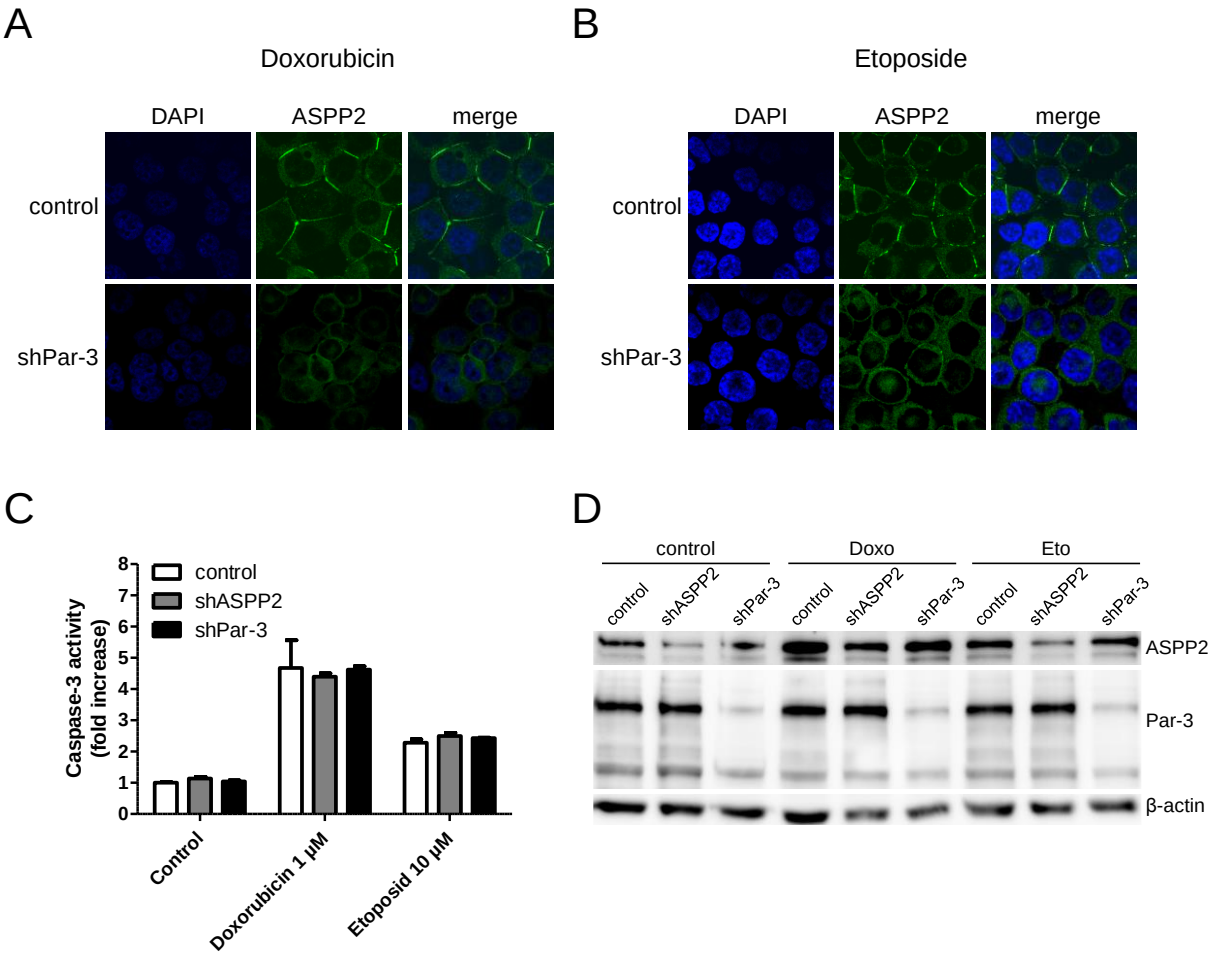

Fig. 34: Apoptosis in response to chemotherapeutic treatments is independent of ASPP2 in HCT116 cells. (**A**, **B**) HCT116 cells were transduced with shRNA against Par-3, treated with 1 µM doxorubicin (**A**) and 10 µM etoposide (**B**) for 16 h and stained for endogenous ASPP2 (green) by immunofluorescence. Nuclei were counterstained with DAPI. (**C**, **D**) HCT116 cells were transduced with shRNA against ASPP2 (shASPP2), Par-3 (shPar-3) or empty vector (control) and treated with 1 µM doxorubicin (Doxo) or 10 µM etoposide (Eto). Total cell lysates of untreated (control) and treated samples were produced after 48 h. (**C**) Equal protein amounts were subjected to caspase-3 activity measurements using a fluorescent substrate. Values are shown relative to the untreated empty vector control. Means and SD of three samples from the linear range of the substrate cleavage reaction are plotted. (**D**) Equal protein amounts were subjected to SDS-PAGE and subsequent Western blotting. β-actin served as a loading control.

This implies that ASPP2 predominantly binds other interaction partners instead of p53, particularly the tight junction protein Par-3, as ASPP2 showed a junctional localisation in all cancer cell lines examined including the p53 wild-type cell lines MCF-7 and U2OS (data not shown).

3.5.5 Protein interaction

Therefore, we further studied protein interactions of ASPP2 in the presence and absence of the enzyme. To screen for differences in protein interactions we performed ASPP2 pull-down assays using metabolically labelled HCT116 cells. Following a 15 min starvation period the cells were incubated with ^{35}S-methionine for radioactive labelling of all cellular proteins. Subsequently, ASPP2 was recovered from whole cell lysates by immunoprecipitation using a specific antibody, bound proteins were separated by SDS-PAGE using different gel percentages and visualised by autoradiography. This technique was expected to reveal differences in the interaction profile of cells transduced with shRNA against FIH-1 and control cells over a wide molecular weight range. Although initial experiments indicated differences in the interaction profile, e.g. for two proteins at approximately 45 kDa and 200 kDa, high variations in the background signal precluded a clear statement on effects of FIH-1 over several experiments (data not shown).

To circumvent the problems associated with this screening method, chosen candidates were directly tested for changes in protein interaction. As described before, interaction with p53 was not altered upon FIH-1 depletion and interaction with Bcl-2 was not detectable in HCT116 cells. The interdependent co-localisation with Par-3 pointed towards a preference of ASPP2 binding to this interaction partner in HCT116 cells. Thus, we monitored the localisation of both proteins upon suppression of FIH-1.

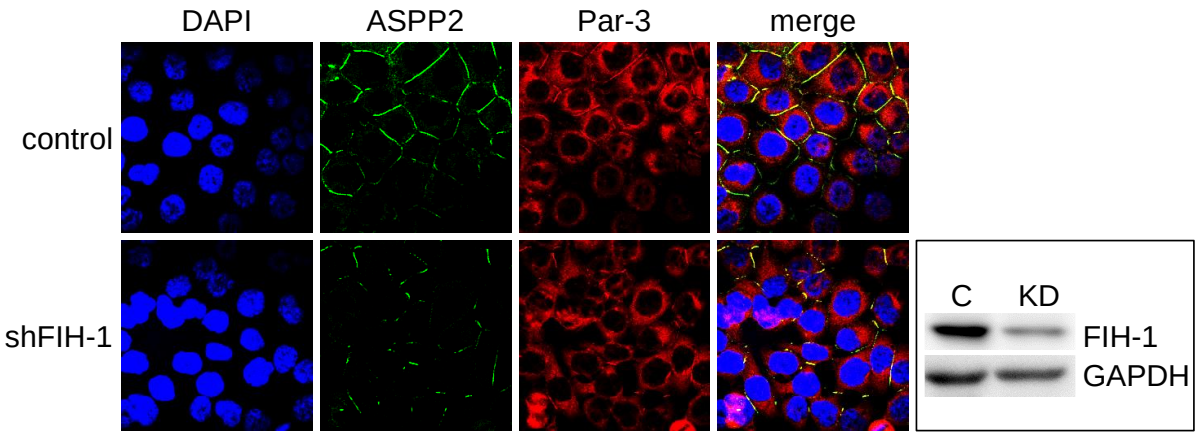

Fig. 35: Impact of FIH-1 on the localisation of ASPP2 and Par-3 in HCT116 cells. HCT116 cells were transduced with shRNA against FIH-1 (shFIH-1) or empty vector (control) and stained for endogenous ASPP2 (green) and Par-3 (red) by double immunofluorescence. Nuclei were counterstained with DAPI. In parallel, suppression of FIH-1 (KD) was monitored in comparison to control cells (C) by SDS-PAGE and subsequent Western blotting of equal protein amounts from total cell lysates (right panel). GAPDH served as a loading control.

The double immunofluorescence staining of HCT116 shFIH-1 cells showed substantially impaired junctional localisation of ASPP2 and Par-3 as compared to control cells (Fig. 35). Both proteins were partly redistributed into the cytoplasm of shFIH-1 cells while control cells showed a localisation pattern which was clearly dominated by cell-cell contacts, suggesting an effect of FIH-1 on the localisation. We further examined whether this was also reflected by an altered interaction between ASPP2 and Par-3 via reciprocal co-immunoprecipitation of the proteins from whole cell lysates.

Indeed, the comparison of control and shFIH-1 HCT116 cells revealed impaired interaction upon depletion of the enzyme while total protein levels of ASPP2 and Par-3 were not affected (Fig. 36). The interaction was not completely disrupted by silencing of FIH-1 but observed to be significantly reduced by 30% in comparison to control cells in several experiments regardless of which interaction partner was precipitated.

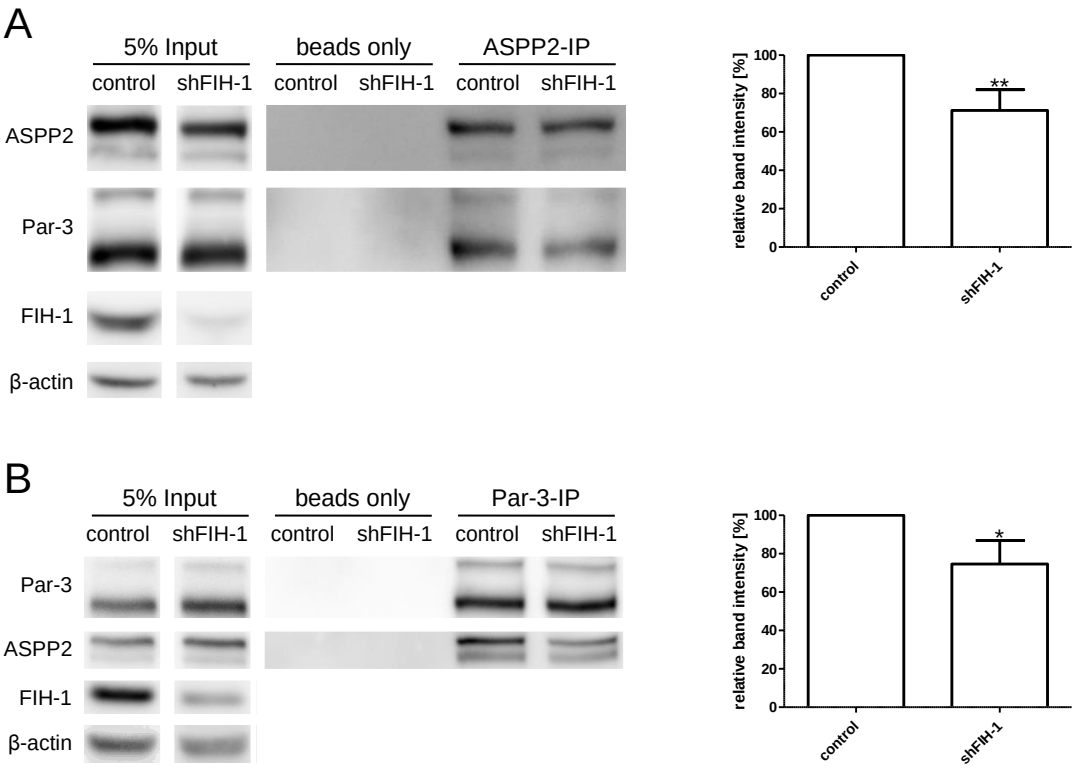

Fig. 36: Impact of FIH-1 on the interaction of ASPP2 and Par-3. HCT116 cells were transduced with shRNA against FIH-1 (shFIH-1) or empty vector (control). (**A**) 500 µg cell lysate were subjected to immunoprecipitation using 5 µg ASPP2 antibody. (**B**) 500 µg cell lysate were subjected to immunoprecipitation using 5 µg Par-3 antibody. As negative control immunoprecipitations were performed in the absence of the specific antibody (beads only). Immunoprecipitates were subjected to SDS-PAGE and subsequent Western blotting. In parallel 25 µg of the total cell lysate (5% input) were subjected to SDS-PAGE and subsequent Western blotting. β-actin served as a loading control for input samples. Significance of the reduction in protein interaction was tested over 5 (**A**) and 4 (**B**) independent experiments where band intensities were quantified relative to control cells. Statistical significance was tested by Student's t-test where * indicates $p < 0.05$ and ** indicates $p < 0.01$.

To assess whether the impact of FIH-1 on the interaction between ASPP2 and Par-3 is a general phenomenon, other cancer cell types were examined following suppression of FIH-1. H441 lung carcinoma cells which possess a more epithelial phenotype with more junctional contacts throughout the monolayer in comparison to HCT116 cells also showed an altered localisation of ASPP2 and Par-3 in the double immunofluorescence staining upon transduction with shRNA against FIH-1. In this case the proteins were not completely redistributed into the cytoplasm but the localisation of residual ASPP2 remaining at the cell-cell contacts was found to be highly disorganised in comparison to control cells (Fig. 37 A). In addition, two different colon cancer cell lines, CaCo-2 and DLD-1, were examined. Because these cell lines formed very thick monolayers, it was difficult to monitor all cell contacts present on one image section by confocal microscopy as the junctions were distributed over different levels of the samples. However, changes in the intracellular localisation of ASPP2 and Par-3 were not observed in shFIH-1 cells in comparison to the controls in these two cell lines (Fig. 37 B and C).

We further examined the interdependent localisation of ASPP2 and Par-3 in these cell lines. In H441 cells the junctional localisation was disrupted upon depletion of each of the interaction partners by lentiviral transduction of the respective shRNA (Fig. 38 A). In contrast, CaCo-2 cells did not show changes in ASPP2 localisation upon suppression of Par-3 (Fig. 38 B). These results imply that suppression of FIH-1 only affects the localisation of ASPP2 and Par-3 in cells where the localisation of the proteins depends on the presence of the interaction partner. Interestingly, the interdependent localisation of the proteins was not correlated to the p53 status of the cells as HCT116 cells harbour wild-type p53 while the tumor suppressor is mutated in H441 cells.

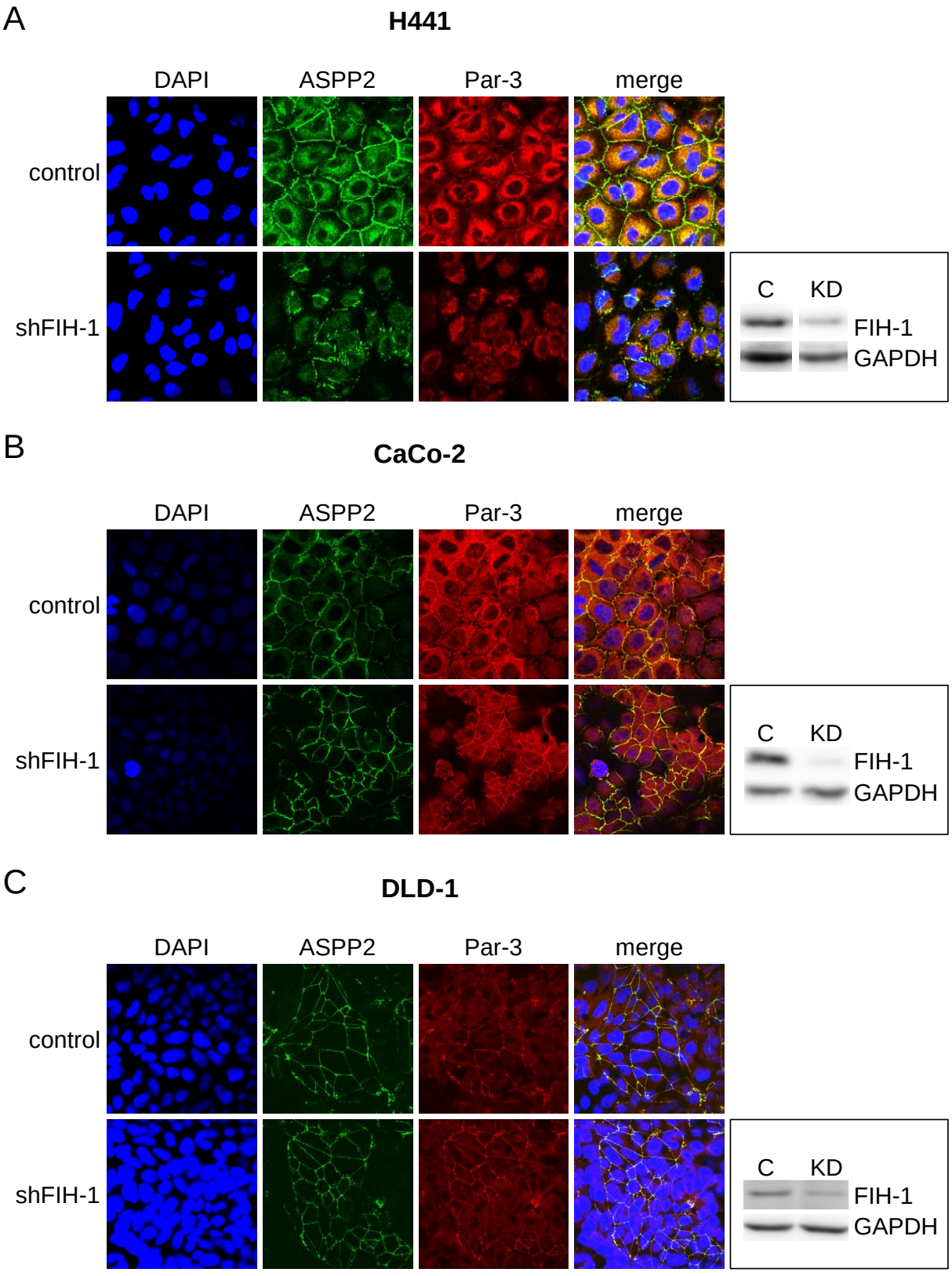

Fig. 37: Impact of FIH-1 on the localisation of ASPP2 and Par-3 in various cancer cell lines. H441 (**A**), CaCo-2 (**B**) and DLD-1 (**C**) cells were transduced with shRNA against FIH-1 (shFIH-1) or empty vector (control) and stained for endogenous ASPP2 (green) and Par-3 (red) by double immunofluorescence. Nuclei were counterstained with DAPI. In parallel, suppression of FIH-1 (KD) was monitored in comparison to control cells (C) by SDS-PAGE and subsequent Western blotting of equal protein amounts from total cell lysates. GAPDH served as a loading control.

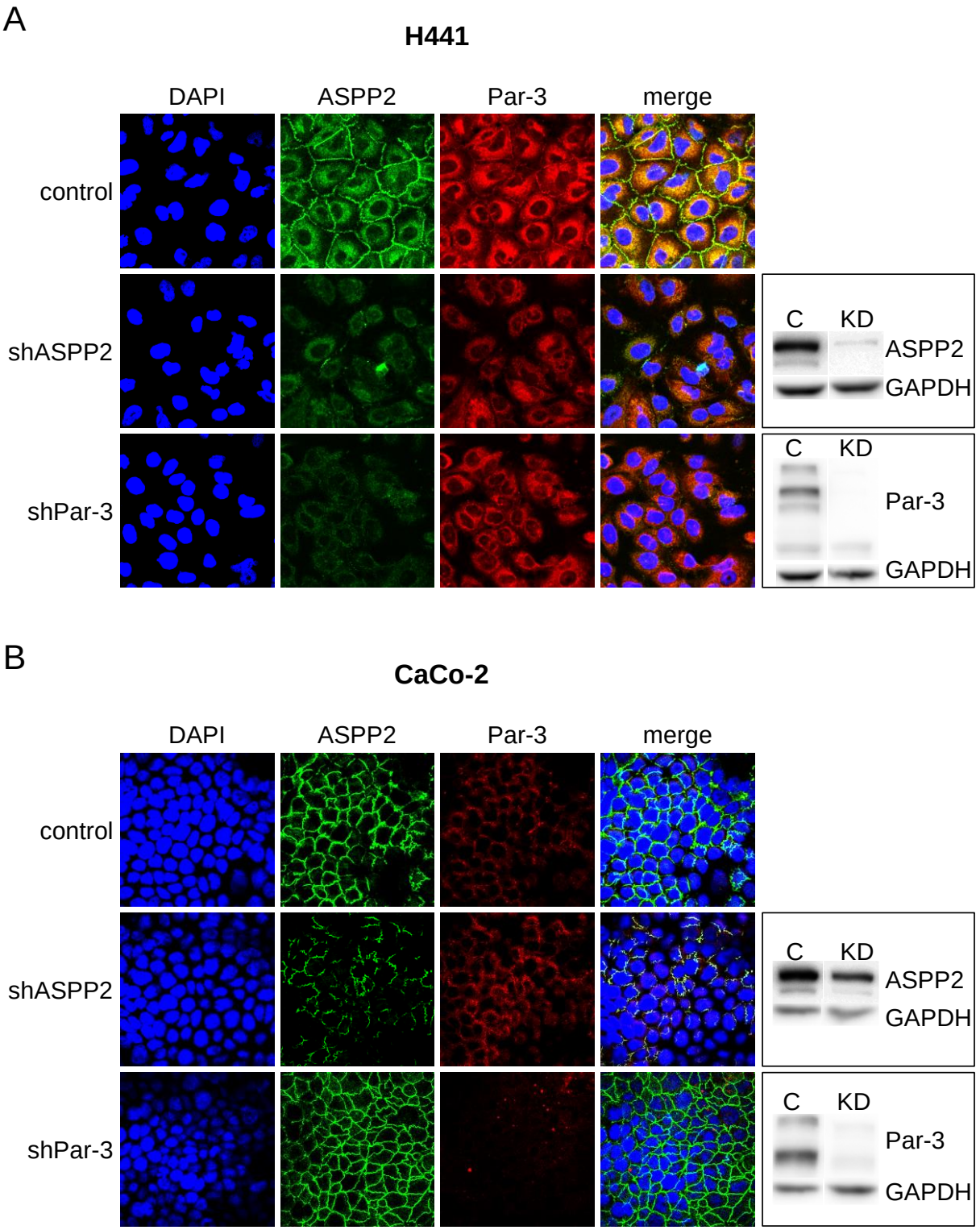

Fig. 38: Interdependent localisation of ASPP2 and Par-3 is cell type dependent. H441 (**A**) and CaCo-2 (**B**) cells were transduced with shRNA against ASPP2 (shASPP2), Par-3 (shPar-3) or empty vector (control) and stained for endogenous ASPP2 (green) and Par-3 (red) by double immunofluorescence. Nuclei were counterstained with DAPI. In parallel, suppression of the respective protein (KD) was monitored in comparison to control cells (C) by SDS-PAGE and subsequent Western blotting of equal protein amounts from total cell lysates. GAPDH served as a loading control.

To show that the effect of FIH-1 on the localisation of ASPP2 and Par-3 was dependent on hydroxylation of ASPP2 by FIH-1, cell lines showing the altered localisation upon FIH-1 suppression were treated with the hydroxylase inhibitor DMOG. Indeed, inhibition of FIH-1 activity had a similar effect on ASPP2 localisation like depletion of the enzyme in HCT116 and H441 cells as monitored by immunofluorescence staining (Fig. 39). The junctional localisation was even decreased further upon DMOG treatment of shFIH-1 cells demonstrating that inhibition of residual FIH-1 potentiated the effect.

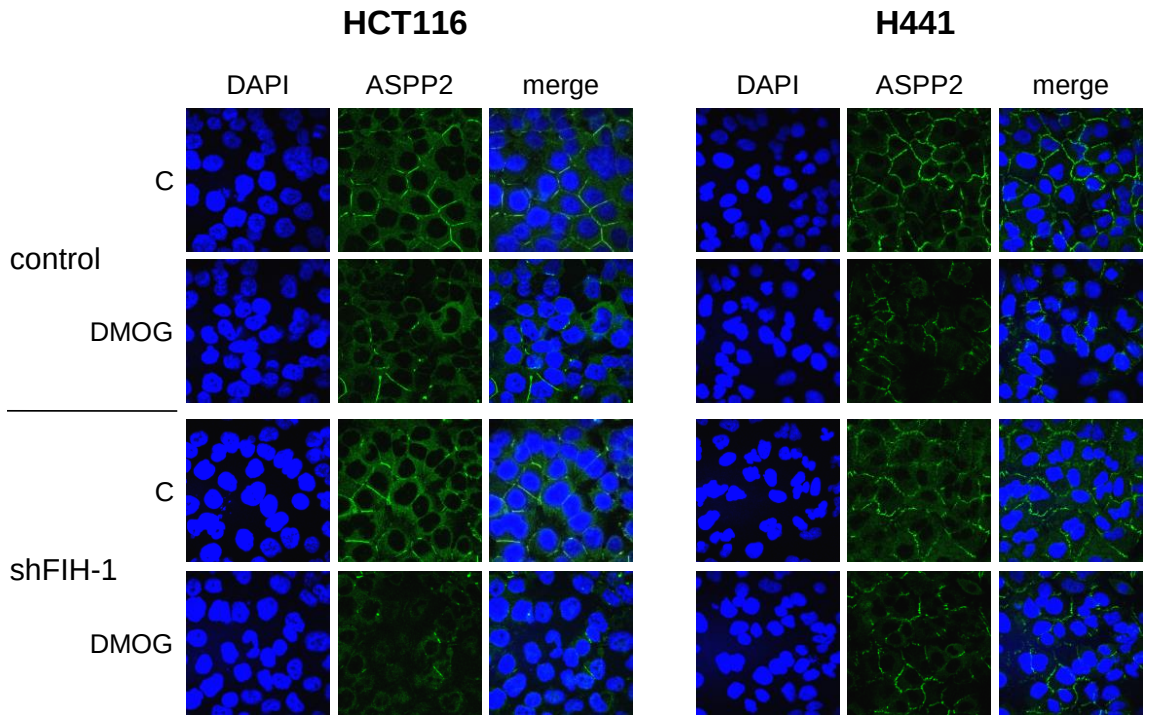

Fig. 39: Impact of FIH-1 on the localisation of ASPP2 depends on the activity of the enzyme. HCT116 (left panel) and H441 (right panel) cells were transduced with shRNA against FIH-1 (shFIH-1) or scrambled shRNA (control) and treated with 1 mM (HCT116) and 500 µM (H441) DMOG for 16 h. Subsequently, cells were stained for endogenous ASPP2 (green) by immunofluorescence. Nuclei were counterstained with DAPI.

3.5.6 Adhesion and migration

In the last part of the study, we assessed the physiologic consequences of the altered interaction and localisation of ASPP2 triggered by FIH-1-dependent hydroxylation. As an impaired integrity of tight junctions is expected to lead to the separation of the cells in the monolayer, adhesive as well as migratory capacities of the cells were investigated.

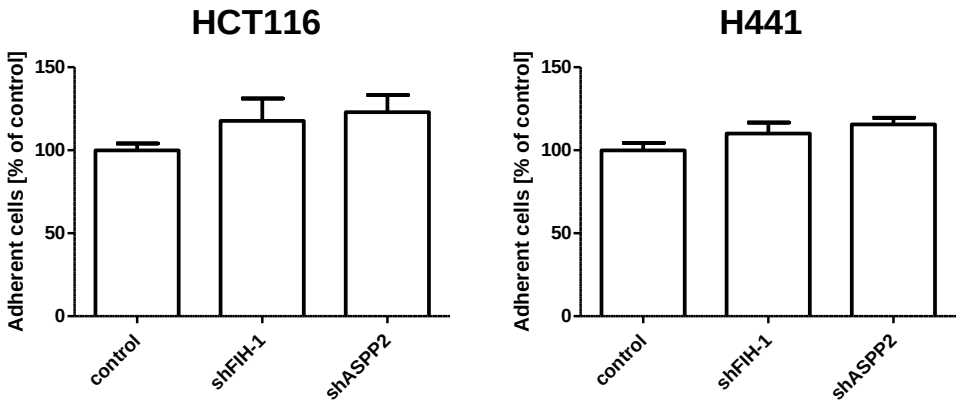

Fig. 40: Adhesion of cancer cells is slightly increased upon suppression of FIH-1 or ASPP2. HCT116 (left panel) and H441 (right panel) cells were transduced with shRNA against FIH-1 (shFIH-1), ASPP2 (shASPP2) or scrambled shRNA (control) and tested for adhesion capacity. Following 2 h on collagen-coated culture vessels, adherent cells were quantified by fluorescent labelling using calcein-AM. Values are shown relative to control cells. Combined values of two independent experiments with ten independent samples are plotted.

We analysed adhesion and migration in HCT116 and H441 cells depleted for FIH-1 by lentiviral transduction. As control for the implication of ASPP2 in these processes, shASPP2 cells were examined as well. Adhesion of the cells was significantly increased approximately 10% upon suppression of FIH-1 and ASPP2 in both cell lines (Fig. 40) suggesting a change potentially mediated by FIH-1-dependent hydroxylation of ASPP2.

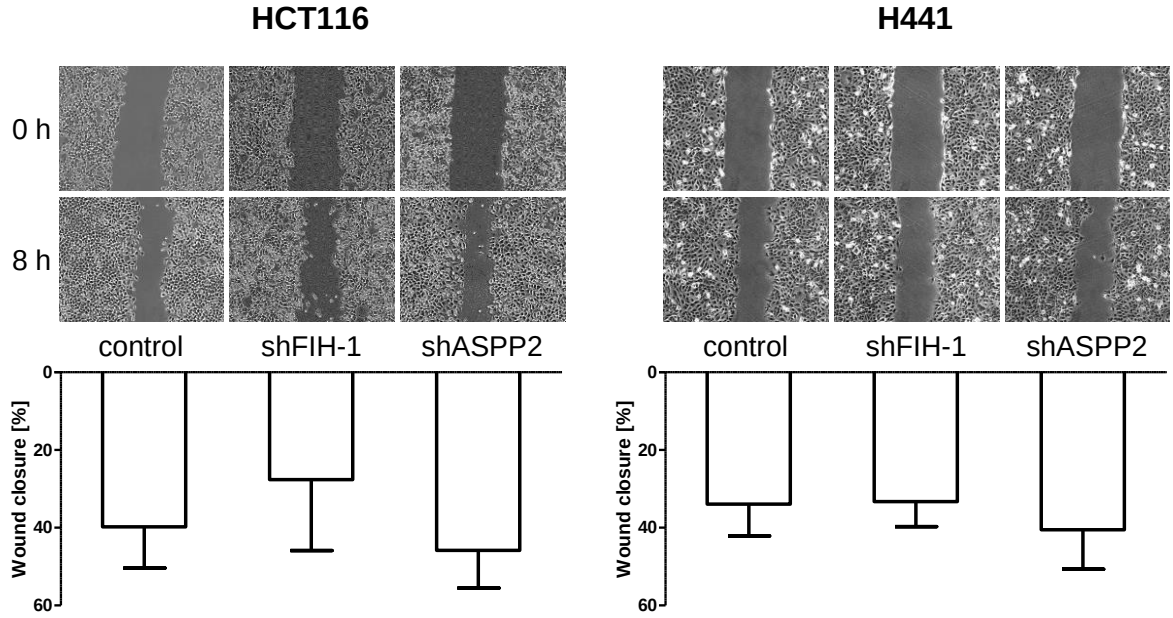

Fig. 41: Migration is reduced upon silencing of FIH-1 while ASPP2 depletion increases cancer cell motility. HCT116 (left panel) and H441 (right panel) cells were transduced with shRNA against FIH-1 (shFIH-1), ASPP2 (shASPP2) or scrambled shRNA (control), grown to confluence on collagen-coated culture dishes and subjected to scratch assays. Wound closure was quantified as reduced distance between the scratch ends after 8 h in comparison to the initial scratch at eleven different points of each scratch.

Migration of the cells was slightly decreased following silencing of FIH-1 but this effect was independent of ASPP2 as depletion of the protein triggered the migratory potential of the cells (Fig. 41). Moreover, the effects on migration were not significant due to high variation of the scratch ends. Taken together, adhesion and migration assays did not reveal a substantial effect of hydroxylation of ASPP2.

4 Discussion

Although hydroxylation was previously thought to be rather uncommon, it is more and more recognized as an important posttranslational modification mediating substantial effects on the interaction profile of proteins. One well-documented example is collagen where prolyl and lysyl hydroxylation mediate the stability of the peptide triple helices (Uitto and Lichtenstein, 1976). Another well-characterised example is the hydroxylation of α-subunits of the transcription factor HIF. In this case, prolyl hydroxylation triggers interaction with the recognition subunit of the E3 ubiquitin ligase responsible for ubiquitination and proteasomal degradation of HIF, the von Hippel-Lindau protein (Kaelin and Ratcliffe, 2008). In contrast, HIF asparaginyl hydroxylation blocks binding to the transcriptional co-activator p300/CBP (Lisy and Peet, 2008) thereby inhibiting HIF transcriptional activity. The hydroxylation of HIF-1α was the first reaction found to be catalysed by FIH-1. Over the last decade, it could be shown that some ARD-containing proteins are also hydroxylated by FIH-1. However, to date, no obvious physiologic effect or impact on protein interaction profiles of substrates could be revealed for ARD-hydroxylation (Cockman *et al.*, 2009b; Coleman and Ratcliffe, 2009). In our study we demonstrate that ARD-hydroxylation of ASPP2 by FIH-1 significantly alters the interaction profile as well as the subcellular localisation of ASPP2. In addition we report a new function of FIH-1-dependent hydroxylation in the modulation of protein interaction suggesting effects not only on ASPP2 but potentially also on other ARD-containing FIH-1 substrates. Alignments with currently known FIH-1 substrates demonstrated high sequence similarities to ASPPs. *In vitro* experiments directly identified ASPP2 as a new substrate for FIH-1. We detected a single hydroxylation site for FIH-1 in the ARD of ASPP2, N986, which was targeted by FIH-1 *in vitro* as well as in cells. In contrast to ASPP2, the conserved protein family member iASPP was not hydroxylated by FIH-1 at the corresponding potential target asparagine which proves the specificity of ARD-hydroxylation despite frequent occurrence.

4.1 ASPP2 is hydroxylated by FIH-1 at N986

The FIH-1 hydroxylation site N986, identified in this study, is situated within the ARD of ASPP2 in the loop region between two ankyrin repeats (Fig. 42). This position of the target amino acid is conserved among all ARD-containing substrates of the enzyme although the sequence of the hydroxylation site and even the hydroxylated residue can vary.

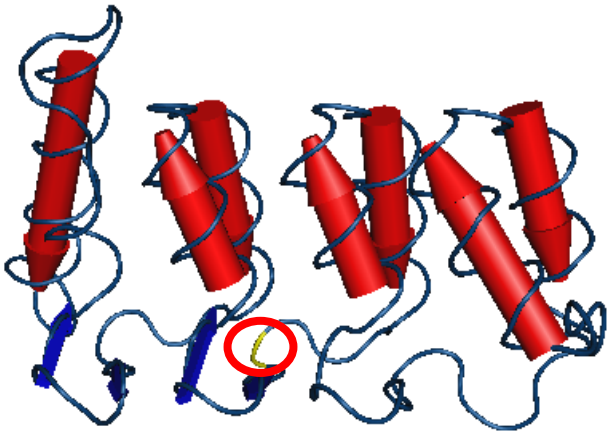

Fig. 42: Position of the FIH-1 hydroxylation site in the ARD of ASPP2. Schematic representations of the solution structure of the ARD and adjacent regions of ASPP2 (PDI entry 4A63_B) (Canning *et al.*, 2012). α-helices are shown as cylinders and β-sheet structures are indicated by arrows. The hydroxylation site N986 in the loop region between two ankyrin repeats is highlighted by a red circle. The structure was plotted using the Cn3D 4.3 macromolecular structure viewer (NCBI).

Our data on the hydroxylation of ASPP2 demonstrate that a second asparagine two amino acids upstream of N986 was neither targeted by FIH-1 *in vitro* nor in cultured cells. Thus, despite the high sequence variability of the hydroxylation site, the target amino acid has to be present in a certain structural context for FIH-1-dependent hydroxylation. As a high background signal was observed in hydroxylase activity assays on the whole ARD of ASPP2 upon mutation of N986 *in vitro*, we examined the presence of other FIH-1 hydroxylation sites in ASPP2. The background activity was not due to hydroxylation of N984 as shown by mutation studies using single and double mutants for N984 and N986. Furthermore, FIH-1 activity was almost completely abrogated using short ASPP2 peptides with a single mutation of N986. In addition, hydroxylation of N984 could not be detected in MS analyses on ASPP2 purified from cultured cells. As no additional potential FIH-1 hydroxylation site could be detected, the background activity on the long substrate proteins in the *in vitro* assays was most likely due to uncoupled activity of the enzyme which is also supported by variations in background activity observed for different substrate preparations. Taken together, we propose that N986 is a single hydroxylation site for FIH-1 present in ASPP2. Using short peptides *in vitro* we could demonstrate specificity of the hydroxylation reaction using the hydroxylase inhibitor NOG. Furthermore, the K_m value of 75 µM that we determined for hydroxylation of ASPP2 N986 in the context of a short peptide was comparable to those of substrates previously identified (Wilkins *et al.*, 2009). Importantly, efficient hydroxylation of ASPP2 N986 was also detected in cultured cells by MS analysis. Due to the high molecular weight and the amino acid sequence of ASPP2, digestion of the endogenous protein did not yield sufficient amounts of peptide for the analysis. Therefore, we purified overexpressed ASPP2 from HEK293T cells for the MS experiments. Remarkably, endogenous FIH-1 expressed in the cells was capable of hydroxylating the majority of overexpressed ASPP2 which indicates

a high affinity for the substrate. Co-transfection of the enzyme further triggered hydroxylation of N986. In addition, similar to the *in vitro* studies, application of the hydroxylase inhibitor DMOG almost completely blocked hydroxylation. Finally, suppression of FIH-1 expression through lentiviral transduction of shRNA clearly reduced but not completely abrogated hydroxylation of ASPP2 verifying the enzyme-substrate relation. The residual hydroxylation observed is likely to be catalysed by the remaining 10% of the enzyme amount in shFIH-1 cells because previous studies using a more efficient knockdown produced by siRNA transfection could completely block hydroxylation of other ARD-containing FIH-1 substrates (Webb *et al.*, 2009; Yang *et al.*, 2011a). All together these results clearly demonstrate that FIH-1 is the hydroxylase responsible for the modification and it is unlikely that another hydroxylase can compensate for depletion of FIH-1 in the case of ASPP2. The residual hydroxylation upon silencing of FIH-1 by shRNA transduction again points to a very high affinity of FIH-1 for ASPP2. Supporting this hypothesis, a strong interaction between enzyme and substrate could be observed in interaction studies *in vitro* with a higher binding affinity of FIH-1 for ASPP2 as compared to the well-characterised substrate HIF-1α.

4.2 Substrate recognition by FIH-1

4.2.1 Differences between HIF-1α and ASPP2

The stronger interaction observed between GST-ASPP2 protein fragments and FIH-1 as compared to GST-HIF-1α is in line with previous results on ARD-containing FIH-1 substrates suggesting a distinct substrate recognition mechanism which is different for ARD-containing substrates as compared to HIF-1α. For mouse Notch1 an increase in substrate length was found to improve binding to FIH-1 substantially while the interaction with HIF-1α substrates was not affected. In general, Notch substrate handling was shown to be very similar to ASPP2 because Notch substrates bound FIH-1 more efficiently than HIF-1α (Wilkins *et al.*, 2009) and we also observed a stronger binding affinity of FIH-1 to ASPP2 protein fragments as compared to HIF-1α. While the conformation of the ARD in solution was observed to be highly structured (Kohl *et al.*, 2003; Coleman *et al.*, 2007), the CTAD of HIF-1α has been reported to pre-exist in an unstructured form in solution and to adopt a structured conformation after binding to FIH-1 (Dames *et al.*, 2002). Despite these differences, both substrates were found to adopt a largely extended conformation in complex with FIH-1 with similar interaction interfaces (Elkins *et al.*, 2003; Coleman *et al.*, 2007).

Consequently, to enable accessibility of the target amino acid and to achieve the required extended conformation, ARD-containing FIH-1 substrates have to undergo a conformational change in terms of binding to the enzyme. These differences in the secondary structure may result in different hydroxylation efficiencies detected for ASPP2 and HIF-1α protein fragments. The HIF-1α wild-type CTAD was hydroxylated ten times more efficiently as compared to ASPP2 potentially because unfolding of the ARD is required for hydroxylation. In addition, hydroxylation of ASPP2 was augmented when short 20 amino acid peptides were tested for FIH-1 activity instead of longer 240 amino acids protein regions. These results support the hypothesis that the efficiency of the hydroxylation reaction is in part determined by the secondary and tertiary structure of the substrate. However, the *in vitro* data on hydroxylation efficiency may not apply to the *in vivo* situation as we still detected a large part of overexpressed ASPP2 hydroxylated in cells with substantially reduced FIH-1 protein levels. Together with the fact that the major proportion of overexpressed ASPP2 can be hydroxylated by endogenous FIH-1 this implies a higher hydroxylation rate for this substrate in cells. Of note, different hydroxylation levels have been reported for other ARD-containing substrates using quantitative MS analyses. For human Notch1 the endogenous protein was found to be almost 90% hydroxylated at N1956 in HEK293T cells (Coleman *et al.*, 2007) while overexpressed Rabankyrin-5 was found to be hydroxylated 20% to 55% depending on the hydroxylation site, under co-expression of the HIF-1α CTAD which may compete for hydroxylation (Singleton *et al.*, 2011). The latter report also compared the oxygen-dependency of HIF-1α CTAD and Rabankyrin-5 hydroxylation and revealed that ARD hydroxylation seems to be more sensitive to depletion of oxygen as compared to the transcription factor indicating a more efficient hydroxylation of HIF-1α. However, further quantitative studies on the hydroxylation levels of endogenous ARD-containing FIH-1 substrates in comparison to HIF-1α are required to determine the activity of FIH-1 *in vivo*. Particularly such analyses may help to answer the question whether HIF signalling is affected by ARD-hydroxylation as a recent study on overexpression of Gankyrin in mice suggested (Liu *et al.*, 2013). Although we could not perform such an analysis on endogenous ASPP2, our results imply that the enzyme activity on the protein is similar to Notch1 as even the overexpressed protein was hydroxylated to a great extent.

4.2.2 ASPP2 but not iASPP is hydroxylated by FIH-1

In contrast to ASPP2, we observed that the conserved protein family member iASPP was not modified by FIH-1 at the corresponding asparagine residue. Regarding the promiscuous character of the enzyme and the high conservation of the ARD, it was surprising that iASPP did not undergo hydroxylation in our *in vitro* study, although short peptides which were observed to produce the most reliable results were tested. In addition, the peptides are not expected to adopt a secondary structure precluding hydroxylation. Furthermore, although there are some differences in the primary sequence (Fig. 43 A), the C-termini of ASPP2 and iASPP, particularly the ARD, are highly conserved in the solution structure of the proteins (Fig. 43 B).

Our results indicate that the amino acid sequence, especially the residues in close proximity to the target asparagine, may also determine hydroxylation efficiency thereby precluding hydroxylation of iASPP while ASPP2 can be modified. A very recent report, which demonstrates that the primary sequence contributes to distinct characteristics of ARD substrates in contrast to HIF-1α, supports this hypothesis (Wilkins *et al.*, 2012). This study revealed that the kinetics of the hydroxylation reaction for ARD-containing substrates are affected by amino acids in close proximity of the hydroxylated residue. In addition, the authors suggest that single amino acid substitutions in this region disrupt the substrate conformation which is required for FIH-1-dependent hydroxylation. This might also apply to ASPP2 and iASPP which differ in the primary amino acid sequence at the -3, +1 and +2 position relative to the hydroxylation site. These differences potentially enable hydroxylation of ASPP2 while iASPP was not able to serve as substrate for FIH-1 *in vitro*. The +1 position is potentially crucial in this context because the majority of the FIH-1 substrates show hydrophobic residues at this position (alanine, valine or isoleucine). In contrast, iASPP shows a polar serine residue one amino acid downstream of the target asparagine which may interfere with hydroxylation as only one other hydroxylation site in Rabankyrin-5 also shows a serine at the same position. In summary, despite the low substrate specificity of FIH-1 distinct characteristics may be required in the case of ARD-containing proteins as well.

A

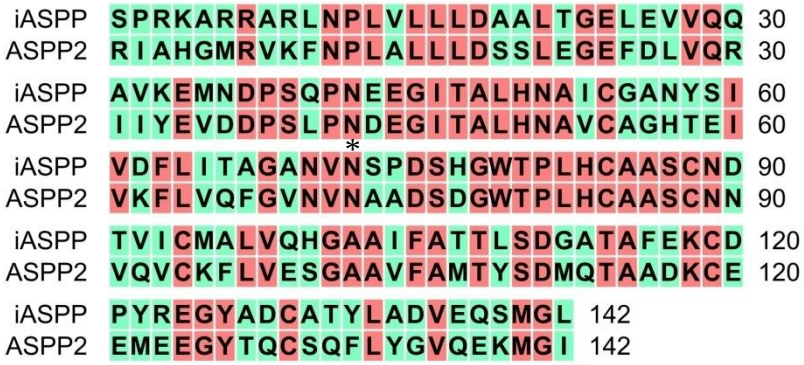

B

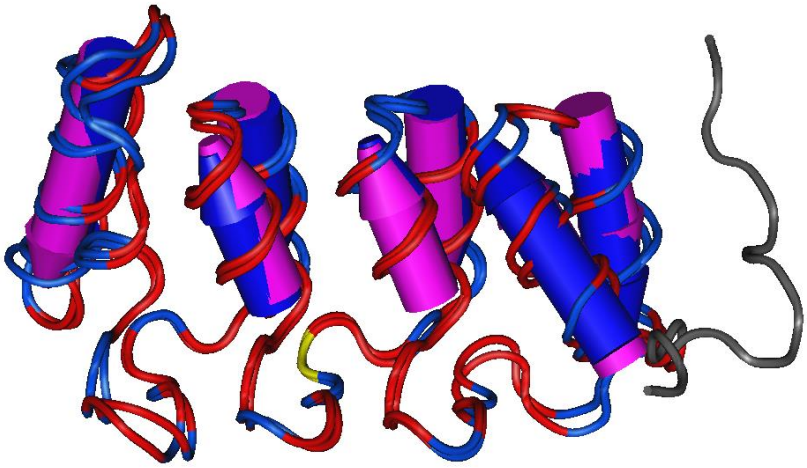

Fig. 43: Primary and secondary structure conservation of the ARD regions of ASPP2 and iASPP. Alignments of protein sequences of ASPP2 (aa 915-1056) and iASPP (aa 616-757) containing the whole ARD and adjacent regions. (**A**) Amino acid alignment. Identical residues are coloured in red and non-conserved amino acids are shown in green. Alignment was created using the CLC Bio sequence viewer 6. N986 and N687 are indicated by asterisk. (**B**) Alignment of the schematic representations of the solution structure of the ARD and adjacent regions of ASPP2 (PDI entry 4A63_B) (Canning *et al.*, 2012) and iASPP (PDI entry 2VGE_A) (Robinson *et al.*, 2008). Identical residues are shown in red and non-conserved amino acids are coloured in blue. α-helices are shown as cylinders in pink for ASPP2 and blue for iASPP. The hydroxylation site N986 in the loop region between two ankyrin repeats is shown in yellow. Non-aligned residues at the N-terminal region are shown in grey. Alignment was created using VAST similar structures (Gibrat *et al.*, 1996). Scheme was generated using the Cn3D 4.3 macromolecular structure viewer (NCBI).

4.2.3 Implications for the identification of new substrates

The fact that only one out of two highly conserved proteins is hydroxylated by FIH-1 may be beneficial for the prediction of additional new substrates and for the definition of a consensus FIH-1 hydroxylation motif. The low specificity of the enzyme makes it difficult to predict from the primary sequence of the protein whether an ARD can serve as FIH-1 hydroxylation site. A very recent study detected hydroxylation of serine and leucine residues catalysed by FIH-1 in the context of a consensus ankyrin repeat substrate peptide further emphasising the promiscuity of the enzyme (Yang *et al.*, 2013).

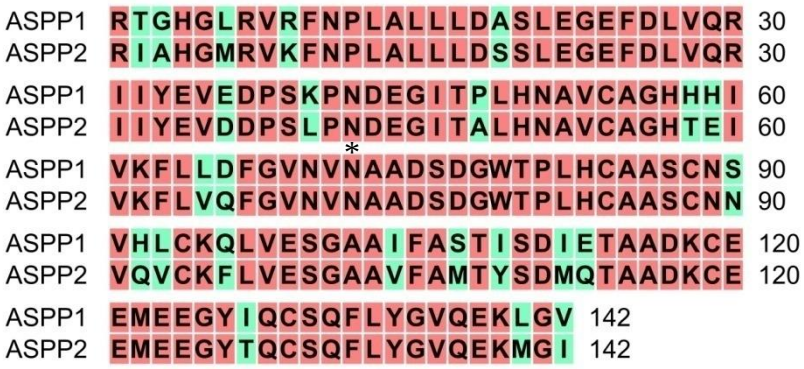

Fig. 44: Primary amino acid sequence conservation between ASPP1 and ASPP2. Alignment of protein sequences of ASPP2 (aa 915-1056) and ASPP1 (aa 877-1018) containing the whole ARD and adjacent regions. Identical residues are coloured in red and non-conserved amino acids are shown in green. Alignment was created using the CLC Bio sequence viewer 6. N986 and N948 are indicated by asterisk.

Nevertheless, our study highlights the importance of the amino acid sequence in the close proximity of the target asparagine. Especially the +1 position may be crucial for the identification of new substrates as this is the only position out of the amino acids conserved among 50% of all substrates differing between ASPP2 and iASPP. The 50% consensus sequence "AAXXXXXXXXXXLLXXGADVNAXDXXGXXPLHXAXXXXXX" did not change upon inclusion of ASPP2 but the importance of the downstream amino acid is emphasised by the comparative studies on iASPP and ASPP2. As the substrate requirements for FIH-1 are difficult to define, the identification of specific residues which may be crucial for hydroxylation is likely to facilitate identification of new FIH-1 substrates.

With respect to the third family member, ASPP1, hydroxylation by FIH-1 is very likely to occur as the C-termini of ASPP1 and ASPP2 are highly conserved. The primary amino acid sequence of the ARD and adjacent regions only slightly differs in ASPP1 (Fig. 44). Nonetheless, further studies on the putative FIH-1 target amino acid in ASPP1, N948, are required to demonstrate hydroxylation of the protein in cells. We anticipate that the physiologic effects of such a modification of ASPP1 are difficult to determine as the protein is mostly involved in the control of proliferation and apoptosis. In our studies we did not detect any effects of FIH-1 suppression on these processes suggesting that FIH-1-dependent hydroxylation of ASPP1 does not have an impact in this regard. However, similar to the situation we observed for ASPP2, other cellular functions, e.g. lymphatic vessel assembly where ASPP1 has been shown to be relevant (Hirashima *et al.*, 2008), may be affected by modulation of protein interaction.

4.3 Impact of FIH-1-dependent hydroxylation of ASPP2

4.3.1 ASPP2 protein stability is not regulated by FIH-1

Although the secondary structure of consensus ankyrin repeat proteins is stabilised by FIH-1-dependent hydroxylation (Hardy *et al.*, 2009; Kelly *et al.*, 2009) neither the half-life nor thermodynamic stability of a full length ARD-containing FIH-1 substrate were shown to be affected by hydroxylation to date (Devries *et al.*, 2010; Singleton *et al.*, 2011). Very recently, the thermal stability of a fragment of AnkyrinR (ankyrin repeats 13-24) was shown to be moderately increased upon hydroxylation by FIH-1 (Yang *et al.*, 2011b) indicating an impact of hydroxylation on secondary structure stability. However, this was not correlated to a difference in protein stability. In contrast, the interaction of this fragment with CDB3, a known interaction partner of this region of AnkyrinR was impaired.

Regarding ASPP2, we attempted to directly determine the half-life of the protein but two different methods did not lead to consistent results in this case. First, our results do not confirm the regulation of ASPP2 by the 26S proteasome which has been reported previously (Zhu *et al.*, 2005) because the proteasome inhibitor MG132 did not increase ASPP2 protein levels although functionality of the drug was proven by p53 induction. In addition, even 24 h of cycloheximide treatment were not sufficient to detect any degradation of the endogenous protein. Furthermore, we also examined exogenously expressed ASPP2 using the same approach and pulse chase experiments to obtain clearer results, but overexpression of the protein led to the induction of apoptosis and we were not able to differentiate between reduction due to apoptosis and degradation in these experimental settings. Taken together, for endogenous ASPP2, we demonstrated high protein stability. Therefore alterations of protein stability would be expected to affect the overall levels of the protein which was not the case upon silencing of FIH-1. As we did not detect any differences in total protein amounts of ASPP2 upon silencing of FIH-1 we propose that FIH-1-dependent hydroxylation does not substantially regulate stability or production of endogenous ASPP2.

4.3.2 Cell proliferation and apoptosis are not affected by FIH-1

Further comparisons between cells depleted of FIH-1 and control cells did not reveal differences in the proliferation of HCT116 cells, although p53 and p21 were induced on the protein level which has previously been reported to decrease proliferation in several wild-type p53 cell lines (Pelletier *et al.*, 2011). Moreover, we were not able to detect differences in the interaction of ASPP2 and p53 in the presence or absence of FIH-1. In line with this, we did not observe any changes in the mortality of the cells upon silencing of FIH-1 under control or stress conditions, as already reported by Pelletier *et al.* for wild-type p53 cancer cells. This is in contrast to another report which demonstrated that FIH-1 can trigger survival of renal cancer cells through suppression of apoptosis (Khan *et al.*, 2011). It has also been shown that osteosarcoma cells overexpressing FIH-1 display enhanced tumor growth in a xenograft mouse model while silencing of FIH-1 in these cells did not affect proliferation (Kuzmanov *et al.*, 2012). In summary, several studies on FIH-1 suggest that the physiologic effect of FIH-1 on survival decisions depends on the cell type examined.

In HCT116 cells bearing wild-type p53, we found that ASPP2 does not co-localise with p53 which may prevent an involvement in apoptotic signalling. Endogenous ASPP2 was mainly localised to cell-cell contacts due to the interaction with Par-3 while p53 was predominantly located in the nucleus. Even overexpression of ASPP2 did not lead to nuclear localisation of the protein until a certain level of expression was exceeded. In line with previous publications overexpression of ASPP2 led to the induction of apoptosis in HCT116 cells which is potentially due to an altered cytoplasmic localisation of the protein enabling regulation of p53 (Samuels-Lev *et al.*, 2001; Kobayashi *et al.*, 2005). In fact, few studies were able to confirm the role of ASPP2 in apoptosis regulation for the endogenous protein. A very recent report demonstrates that ASPP1 and ASPP2 trigger the apoptotic response of retinal ganglion cells to optic nerve damage *in vivo* in a p53-dependent manner (Wilson *et al.*, 2013). In line with this, studies on drosophila ASPP (dASPP), the homolog of mammalian ASPP1 and ASPP2, report an important role for dASPP in retinal development but this was not due to altered apoptosis but rather to modulation of cell-cell adhesion (Langton *et al.*, 2009). Similarly, in mice ASPP2 was shown to control polarity and proliferation of retinal precursor cells during CNS development (Sottocornola *et al.*, 2010) but it is not clear whether this function is related to p53 signalling. Two different studies on mice heterozygous for ASPP2 provide evidence that the observed tumor suppressive activity of the protein only partly depends on the presence of p53 suggesting a tumor type dependent regulation of p53 by ASPP2 (Vives *et al.*,

2006; Kampa *et al.*, 2009). In HCT116 cells we found very small amounts of ASPP2 interacting with p53 which indicates that the protein may prefer other interaction partners such as Par-3 which maybe prevents a regulation of p53 function. In order to examine whether the localisation of ASPP2 indeed precludes regulation of p53-dependent apoptosis, we disrupted the junctional localisation of the protein by depletion of the interaction partner Par-3. Indeed, this led to a redistribution of ASPP2 with small amounts of the endogenous protein also localising to the nucleus. However, we were still not able to detect differences in the apoptotic response of HCT116 cells. Neither depletion of ASPP2 nor the redistribution of the protein through silencing of Par-3 affected apoptosis induced by chemotherapeutic agents although one of the agents used, doxorubicin, induced ASPP2 on the protein level which initially suggested a role for ASPP2 in this apoptotic response. A very recent report provides a possible explanation for these results as it connects ASPP2 to Ras signalling (Wang *et al.*, 2013a). ASPP2 was shown to enhance Ras signalling thereby triggering p53-dependent apoptosis. This signalling axis might be disrupted by an activating KRas mutation in HCT116 cells potentially uncoupling Ras signalling from ASPP2.

Because, the stimulation of p53-dependent apoptosis by ASPP2 obviously depends on the cell type examined and the status of other cellular signalling factors particularly in cancer cells we investigated MCF-7 breast carcinoma cells bearing wild-type p53 in the absence of Ras mutations. However, we were not able to detect any interaction of endogenous p53 and ASPP2 confirming the results for HCT116 cells where a weak interaction of the proteins could be detected only following addition of a crosslinking agent. Nevertheless, the situation in untransformed primary cells may be completely different and ASPP2 may be able to stimulate p53-dependent apoptosis in these cells. The upregulation of ASPP2 following stimulation of an apoptotic response with doxorubicin supports this hypothesis. A similar upregulation of ASPP1 in response to treatment with the chemotherapeutic agent resveratrol has previously been reported to sensitise breast carcinoma cells to apoptosis induction (Shi *et al.*, 2011). In this case, the increase of ASPP1 was found to be mediated by E2F-1 on the transcriptional level. As ASPP2 was also shown to be a transcriptional target of E2F (Chen *et al.*, 2005) and doxorubicin treatment was found to lead to the induction of E2F transcription factors (Martinez *et al.*, 2010) a similar mechanism potentially leads to the increased ASPP2 protein levels in HCT116 cells following doxorubicin stimulation. Regarding the cell type specific effects of ASPP2 on apoptosis this regulatory mechanism may be important in other cell types, although an impact on apoptosis induction in HCT116 cells could not be observed.

In summary, the stimulatory function of ASPP2 on p53-dependent apoptosis does not seem to be a general phenomenon and further studies are required to fully elucidate the mechanism by which ASPP2 mediates the increase in p53 transactivating function on promoters of proapoptotic genes in some cell types. This may also contribute to an explanation why ASPP2 does not necessarily have the same impact on apoptotic signalling.

4.3.3 Protein interactions of ASPP2 are regulated by FIH-1

Even if neither the thermodynamic stability nor the half-life of an ARD-containing substrate is altered upon hydroxylation by FIH-1, the conformation of the protein can change due to hydroxylation and this may modulate the affinity to protein interaction partners. We confirmed this hypothesis, showing for the first time that protein interaction and localisation of an ARD-containing FIH-1 substrate are altered upon silencing of FIH-1 in two different cell lines. HCT116 shFIH-1 cells displayed reduced interaction of ASPP2 with Par-3 which led to an intracellular redistribution of ASPP2 from cell-cell contacts to the cytoplasm. The more epithelial-like H441 pulmonary adenocarcinoma cells demonstrated an obviously disorganized localization of ASPP2 at cell-cell contacts. In addition, these effects were found to depend on the hydroxylase activity of FIH-1 as the effect could be mimicked by the use of the hydroxylase inhibitor DMOG. In contrast, the interaction of ASPP2 with the tumor suppressor p53 was not affected by FIH-1-dependent hydroxylation. Taken together, these results suggest a distinct role for FIH-1 in formation and maintenance of cell-cell junctions through regulation of the ASPP2-Par-3 interaction which was previously shown to be relevant for these processes (Cong *et al.*, 2010; Sottocornola *et al.*, 2010).

The impact of FIH-1 on this interaction varied between different cancer cell lines, since CaCo-2 and DLD-1 colon cancer cells did not show an altered localisation of the proteins upon silencing of FIH-1. Further experiments on the function of ASPP2 and Par-3 in H441 and CaCo-2 cells revealed that the effect of FIH-1 required the interdependent localisation of both proteins. In HCT116 as well as in H441 cells we observed that the junctional localisation was disrupted upon silencing of one of the interaction partners while CaCo-2 cells showed a cell-cell contact localisation of ASPP2 irrespective of Par-3. This suggests another mechanism directing ASPP2 towards tight or adherens junctions which functions independently of Par-3.

Because tight and adherens junctions often display a cell-type specific composition with large complexes containing multiple proteins involved (Schneeberger and Lynch, 2004), it is possible that the lack of the scaffolding protein Par-3 can be compensated for in some cell types. Thus, the hydroxylation of ASPP2 by FIH-1 may only exert its effects in certain cell types through modulation of ASPP2-Par-3 interaction. Moreover, additional factors which stabilise the interaction may be present in some cell types and override more subtle effects of FIH-1-dependent hydroxylation on protein interaction. In addition, it is also possible that a trimeric complex of Par-3, ASPP2 and an unknown junctional protein is required for the cell-cell contact localisation of ASPP2 and Par-3, as the hydroxylation site is located in the C-terminus of ASPP2 while Par-3 interaction is mediated by the N-terminal part of ASPP2. A protein interacting with the C-terminal part of ASPP2 and Par-3 at the same time may be required to stabilise the protein interaction in some cell types. Importantly, the interaction between ASPP2 and Par-3 was not completely abrogated upon suppression of FIH-1, but only reduced, with, however, profound effects on the intracellular localisation of ASPP2 in HCT116 and H441 cells. The consequences on protein interaction may also depend on the quality of the FIH-1 knockdown on the protein level, as the MS analysis revealed that suppression of 90% of the enzyme in HEK293T cells was not sufficient to completely abolish hydroxylation of overexpressed ASPP2. The amount of FIH-1 necessary for hydroxylation of endogenous ASPP2 may vary, depending on the activity of the enzyme and the levels of other substrates present in the cell. Consequently, variations in FIH-1 activity potentially lead to different results depending on the cell line examined. Indeed, the effect for H441 cells was most prominent when a very high knockdown efficiency of more than 95% was achieved for FIH-1.

Taken together, the FIH-1 mediated effect on ASPP2-Par-3 interaction is probably a consequence of ASPP2 hydroxylation which directly triggers the interaction with Par-3 or indirectly improves binding through modulation of interaction with additional factors. However, our data propose a model, where FIH-1-dependent hydroxylation of ASPP2 triggers the interaction with Par-3 while neither binding of p53 nor p53-dependent signalling are affected (Fig. 45). Consequently, hydroxylation promotes the junctional localisation of ASPP2 and Par-3.

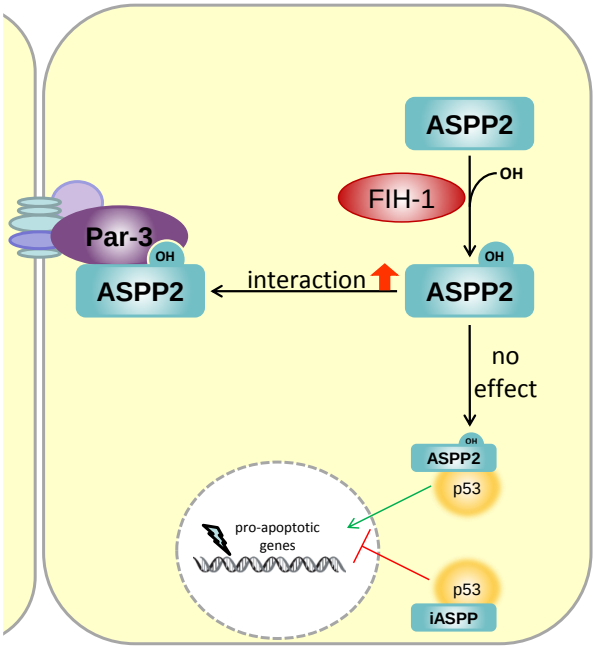

Fig. 45: Model for the regulation of ASPP2 by FIH-1-dependent hydroxylation. ASPP2 is modified by FIH-1 on the posttranslational level through hydroxylation of N986. In contrast, the conserved family member iASPP is not hydroxylated by FIH-1. The hydroxylation of ASPP2 does not modulate p53-dependent apoptosis but triggers the interaction between ASPP2 and Par-3 and the junctional localisation of this protein complex.

4.3.4 Physiological effects of altered protein interactions of ASPP2 – future perspectives

As ASPP2 and Par-3 are involved in the formation of tight junctions in epithelial cells, alterations in interaction and localisation of the proteins may affect the integrity and barrier function of epithelia. To examine theses processes experimentally, we tried to directly quantify junctional integrity in cooperation with H. Mairbäurl, University of Heidelberg, through measurement of monolayer permeability and transepithelial electrical resistance (TER) upon depletion of FIH-1 in cultured tumor cells. Despite considerable effort, we were not able to generate cells which exhibited stable suppression of FIH-1 following lentiviral transduction and show an interpretable TER simultaneously. In addition, the FIH-1-dependent effect on ASPP2 localisation was not present in all cell lines examined, e.g. CaCo-2 cells, which are often used as model system to study epithelial integrity and exhibit a high TER, did not show an altered localisation of ASPP2 upon silencing of FIH-1. Thus, we were not able to elucidate whether a reduced interaction between ASPP2 and Par-3 indeed affects tight junction integrity per se. Alternatively, an effect may only occur under distinct circumstances, e.g. pathophysiological conditions such as severe hypoxia. Interestingly, FIH-1-deficient mice do not display developmental defects but rather metabolic disorders (Zhang *et al.*, 2010). This rather suggests effects under pathophysiological conditions. In contrast, the mouse model for ASPP2 deficiency displays substantial defects in CNS development as a consequence of

deregulated polarity and expansion of neuronal progenitor cells (Sottocornola *et al.*, 2010) which may be due to defects in tight junction integrity.

To date, the interaction between ASPP2 and Par-3 and the physiologic effects have exclusively been characterized in epithelial cells. In these cells, the interaction was found to regulate particularly the early formation and the maintenance of cell-cell contacts (Cong *et al.*, 2010). Our data suggest an alternative mechanism which can direct ASPP2 to cell-cell contacts in the absence of Par-3 in CaCo-2 cells. Thus, ASPP2 probably interacts with other junctional proteins and further studies are required to elucidate the cell type dependent mechanisms which trigger the junctional localisation of ASPP2. It is now interesting to further explore the role of ASPP2 for tight junction formation or integrity in different cell types. The impact of FIH-1 on the localisation of ASPP2 is particularly interesting to study under pathophysiological conditions where hypoxic conditions are encountered. The ASPP2-Par-3 interaction in endothelial cells which has not been studied to date may be an interesting model to study the impact of FIH-1 as hypoxia increases e.g. the permeability of the blood brain barrier after ischemic injury (Natah *et al.*, 2009; Lochhead *et al.*, 2010). This increase in permeability has been shown to be triggered upon reoxygenation due to a mechanism involving the response to oxidative stress (Witt *et al.*, 2008). Interestingly, FIH-1 was found to be highly sensitive to oxidative stress, and peroxide treatment was shown to inhibit hydroxylation of HIF-1α and the ARD-containing FIH-1 substrate Rabankyrin-5 (Masson *et al.*, 2012). Furthermore, expression of FIH-1 was shown to be reduced after transient cerebral ischemia in mice (Shang *et al.*, 2011). In addition, FIH-1 overexpression has been reported to partially rescue barrier dysfunction in human pulmonary vein endothelial cells (Qi *et al.*, 2011). Although the authors suggest that suppression of HIF activity is responsible for the beneficial effect of FIH-1, the modulation of ASPP2 interaction may provide another mechanism for the protection against barrier dysfunction. Of note, the disruption of barrier function upon oxidative stress has also been reported for epithelial cells (Bailey *et al.*, 2004; Gonzalez *et al.*, 2009; Elamin *et al.*, 2013) where ASPP2 has already been demonstrated to be important for tight junction formation and maintenance (Cong *et al.*, 2010; Sottocornola *et al.*, 2010).

In vitro, we were not able to show substantial effects of FIH-1 on proliferation, apoptosis, migration and adhesion of cultured cancer cells. However, the restrictive function of epithelia or the blood brain barrier, as the interaction between ASPP2 and Par-3 was shown to affect CNS development, are difficult to reproduce *in vitro*. Despite the limitations of *in vitro*

models, our results may encourage further studies on *in vivo* disease models which are potentially more suitable to assess the physiological consequences of FIH-1-dependent hydroxylation of ASPP2 particularly on the integrity of cell-cell junctions.

Besides a possible impact on barrier function, the regulation of cell contact formation or maintenance by FIH-1-dependent hydroxylation of ASPP2 might also affect cancer progression *in vivo* because loss of cell-cell contacts as well as oxidative stress and hypoxia contribute to epithelial to mesenchymal transition of cancer cells (Cannito *et al.*, 2008; Tamiya *et al.*, 2010). Although the proliferation of cancer cells has previously been shown to decrease upon suppression of FIH-1 in some cell types (Pelletier *et al.*, 2011), a temporary decrease in FIH-1 activity is maybe sufficient to disrupt cell-cell contacts via impaired interaction of ASPP2 and Par-3. In this context it is interesting to further study the influence of FIH-1-dependent hydroxylation of ASPP2, and potentially ASPP1, on binding of further protein interaction partners. Both proteins were found to be implicated in the regulation of the Hippo signalling pathway which has also been shown to be involved in cell-cell contact dependent inhibition of proliferation (Zhao *et al.*, 2007; Ota and Sasaki, 2008; Liu *et al.*, 2010c). As the deregulation of Hippo signalling can also contribute to epithelial to mesenchymal transition, the protein interactions of ASPP2 with components of this pathway, PP1 and YAP, may also be regulated by hypoxia via FIH-1. In addition, the recently identified interaction of ASPP2 with Ras may potentially also be modulated by FIH-1. In fact, initial metabolic labelling experiments performed to identify affected protein interactions suggested additional alterations for ASPP2 binding to other proteins than Par-3, e.g. a protein of 45 kDa. Although these results were not reproducible, this may be a hint to further FIH-1-dependent variations in the interaction profile of ASPP2.

A regulation of multiple signalling pathways by FIH-1 through modulation of protein interactions might also provide an explanation for the cell type specific effects on cancer cell proliferation. Although the physiologic effects of FIH-1-dependent hydroxylation of ASPP2 remain to be explored our study suggests that hydroxylation may in general affect protein interactions of ARD-containing substrates of FIH-1. Thus quantitative interaction proteomic analyses (Trinkle-Mulcahy *et al.*, 2008; Wepf *et al.*, 2009) on the interaction profile of ARD-containing proteins in the presence and absence of FIH-1 may be a useful tool to further study the impact of hydroxylation on other protein interactions not only for ASPP2 but also for other ARD-containing FIH-1 substrates.

5 Summary

Hydroxylation by Fe(II)- and 2-oxoglutarate-dependent dioxygenases is increasingly recognised as an important protein modification. FIH-1-dependent hydroxylation of HIF-α subunits has previously been shown to influence the interaction of this protein with important transcriptional co-activators thereby modulating HIF transcriptional activity. Recently, another substrate group could be identified for FIH-1. All substrates of this new group are hydroxylated within a highly conserved protein interaction domain, the ankyrin repeat domain (ARD).

In our study, we identified a single hydroxylation site for FIH-1 within the ARD of apoptosis-stimulating p53 binding protein 2 (ASPP2), N986, *in vitro* and in cells. In contrast, the highly conserved family member inhibitory ASPP (iASPP) was not hydroxylated by FIH-1 at the corresponding asparagine *in vitro* revealing distinct characteristics required for the hydroxylation site despite rather low substrate specificity previously reported for FIH-1. Physiologic effects of ASPP2 hydroxylation were studied in cancer cells depleted of FIH-1 by lentiviral transduction. Interestingly, p53-dependent apoptosis which has previously been shown to be modulated by ASPP2 as well as the interaction between p53 and ASPP2 were not affected by silencing of FIH-1. In general, a role for endogenous ASPP2 in the induction of chemotherapy-induced apoptosis could not be confirmed using wild-type p53 cancer cells. In addition, neither proliferation nor adhesion or migration were affected substantially upon FIH-1 depletion. In contrast, the interaction of ASPP2 with the tight junction protein partitioning defective 3 homolog (Par-3) was impaired upon suppression of FIH-1. This interaction was previously found important for the regulation of polarity and proliferation of neuronal progenitor cells *in vivo* and for the formation and maintenance of tight junctions of epithelial cells *in vitro*. In our study, we observed that the interaction between ASPP2 and Par-3 is impaired following silencing of FIH-1which leads to changes in the intracellular localisation of the protein complex in a cell type dependent manner. These findings demonstrate for the first time an impact of FIH-1-dependent hydroxylation on ARD-containing FIH-1 substrates. In contrast to HIF-α where hydroxylation of N803 prevents the association with transcriptional co-activators, the interaction of ASPP2 and Par-3 and the junctional localisation of both proteins was triggered by FIH-1-dependent hydroxylation. Depletion of FIH-1 as well as incubation with the hydroxylase inhibitor dimethyloxalylglycine (DMOG) in part disrupted the interaction and the interdependent

junctional localisation of ASPP2 and Par-3. Although cancer cell adhesion and migration were not altered *in vitro*, FIH-1-dependent hydroxylation of ASPP2 may well affect the integrity of tight junctions and the barrier function of epithelia *in vivo*. Thus further *in vivo* studies are required to examine the physiologic effects of FIH-1-depletion. Furthermore, the role of the interaction between ASPP2 and Par-3 may be interesting to study in other cell types as to date all studies were performed in epithelial cells exclusively. Taken together, our results demonstrate that protein interactions of ARD-containing FIH-1 substrates can be modified by hydroxylation. This is likely to apply to other FIH-1 substrates indicating implications for FIH-1 in a broad range of cellular signalling pathways where ARD-containing proteins are involved.

6 Zusammenfassung

Die posttranslationale Hydroxylierung durch Fe(II)- und 2-Oxoglutarat-abhängige Dioxygenasen wird zunehmend als bedeutsame Protein-Modifikation anerkannt. Es wurde z.B. gezeigt, dass FIH-1-abhängige Hydroxylierung von HIF-α Untereinheiten die Interaktion mit Co-Aktivatoren beeinflusst und dadurch die transkriptionelle Aktivität von HIF reguliert. Drüber hinaus wurde kürzliche eine neue Gruppe von FIH-1-Substraten entdeckt, die alle in einer hochkonservierten Protein Interaktionsdomäne, der Ankyrin Repeat Domäne (ARD), hydroxyliert werden.

In dieser Arbeit wurde ein neues Substrat von FIH-1, Apoptose-stimulierendes p53-bindendes Protein 2 (ASPP2) identifiziert und charakterisiert. Es wurde gezeigt, dass N986 in der ARD von ASPP2 sowohl *in vitro* als auch in kultivierten Zelllinien durch FIH-1 hydroxyliert wird. Im Gegensatz dazu wurde ein hochkonserviertes Mitglied der gleichen Proteinfamilie, inhibitorisches ASPP (iASPP) *in vitro* nicht durch FIH-1 modifiziert. Dies belegt, dass, obwohl bereits einige ARD Proteine als Substrate identifiziert wurden und das Enzyme eine hohe Variabilität der Hydroxylierungsstelle toleriert, bestimmte Voraussetzungen für die Hydroxylierung durch FIH-1 gegeben sein müssen und die Reaktion mit einer gewissen Spezifität erfolgt.

Die physiologischen Effekte der FIH-1-abhängigen Hydroxylierung von ASPP2 wurden in Krebs-Zelllinien, in denen die Expression des Enzyms durch lentivirale Transduktion von shRNA supprimiert wurde, untersucht. Obwohl ASPP2 als Regulator der p53-abhängigen Apoptose identifiziert wurde, hatte die Suppression von FIH-1 keinen Einfluss auf diesen Signalweg und auch die Interaktion zwischen ASPP2 und p53 wurde durch Silencing von FIH-1 nicht beeinflusst. Generell hatte endogenes ASPP2 keinen Einfluss auf die Stressantwort von p53-profizienten Zellen nach Behandlung mit verschiedenen Chemotherapeutika. Darüber hinaus waren auch Proliferation, Adhäsion und Migration nach Suppression von FIH-1 im Wesentlichen unverändert. Im Gegensatz dazu war die Interaktion zwischen ASPP2 und dem Tight Junction Protein partitioning defective 3 Homolog (Par-3), welche sowohl für die Regulation der Zellpolarität und der Proliferation neuronaler Vorläuferzellen *in vivo* als auch für die Ausbildung und Aufrechterhaltung von Tight Junctions in Epithelzellen *in vitro* von Bedeutung ist, durch Suppression von FIH-1 beeinträchtigt. In dieser Arbeit konnten wir nachweisen, dass die reduzierte Interaktion von ASPP2 und Par-3 nach Depletion von FIH-1 zu einer Umverteilung beider Proteine innerhalb der Zelle führt, wobei ASPP2 und Par-3 nicht länger vorwiegend an Zell-Zell-Kontakten

lokalisiert sind. Somit konnten wir zum ersten Mal einen Nachweis für die Funktion der Hydroxylierung von ARD Proteinen erbringen. Wie im Falle von HIF beeinflusst FIH-1-abhängige Hydroxylierung die Assoziation von ASPP2 mit Interaktionspartnern. Im Gegensatz zu HIF-α Untereinheiten, deren Hydroxylierung durch FIH-1 die Interaktion mit transkriptionellen Co-Aktivatoren hemmt, fördert FIH-1-abhängige Hydroxylierung Zelltyp-spezifisch die Interaktion zwischen Par-3 und ASPP2. Der gleiche Effekt wurde auch durch den Hydroxylase-Inhibitor Dimethyloxalylglycin (DMOG) erzielt, was den Effekt eindeutig auf die Aktivität des Enzyms und somit die Modifikation zurückführt. Obwohl weder Adhäsion noch Migration der Zellen *in vitro* von der Suppression von FIH-1 beeinflusst waren, ist es möglich, dass beispielsweise die Integrität und Barriere-Funktion von Epithelien *in vivo* beeinträchtigt ist. Daher sind weiterführende *in vivo* Studien erforderlich, um den physiologischen Effekt der veränderten Lokalisation und Interaktion von ASPP2 und Par-3 aufzuklären. Außerdem wäre es interessant, die Interaktion von ASPP2 und Par-3, die bisher nur in Epithelzellen untersucht wurde, sowie den Einfluss von FIH-1 in anderen Zelltypen zu charakterisieren. Zusammenfassend konnten wir am Beispiel von ASPP2 zeigen, dass Proteininteraktionen von ARD-Proteinen durch FIH-1-abhängige Hydroxylierung reguliert werden können. Dies könnte nicht nur auf ASPP2 zutreffen, sondern auch auf andere ARD-Proteine. FIH-1-abhängige Hydroxylierung könnte somit eine Vielzahl zellulärer Signalwege, in denen ARD-Substrate involviert sind, durch Modulation von Proteininteraktionen regulieren.

7 References

Agirre X., Roman-Gomez J., Jimenez-Velasco A., Garate L., Montiel-Duarte C., Navarro G., Vazquez I., Zalacain M., Calasanz M. J., Heiniger A., Torres A., Minna J. D. and Prosper F. (2006). "ASPP1, a common activator of TP53, is inactivated by aberrant methylation of its promoter in acute lymphoblastic leukemia" Oncogene 25(13): 1862-1870

Ahn J., Byeon I. J., Byeon C. H. and Gronenborn A. M. (2009). "Insight into the structural basis of pro- and antiapoptotic p53 modulation by ASPP proteins" J Biol Chem 284(20): 13812-13822

Aylon Y., Ofir-Rosenfeld Y., Yabuta N., Lapi E., Nojima H., Lu X. and Oren M. (2010). "The Lats2 tumor suppressor augments p53-mediated apoptosis by promoting the nuclear proapoptotic function of ASPP1" Genes Dev 24(21): 2420-2429

Bailey T. A., Kanuga N., Romero I. A., Greenwood J., Luthert P. J. and Cheetham M. E. (2004). "Oxidative stress affects the junctional integrity of retinal pigment epithelial cells" Invest Ophthalmol Vis Sci 45(2): 675-684

Barrick D., Ferreiro D. U. and Komives E. A. (2008). "Folding landscapes of ankyrin repeat proteins: experiments meet theory" Curr Opin Struct Biol 18(1): 27-34

Bell H. S. and Ryan K. M. (2008). "iASPP inhibition: increased options in targeting the p53 family for cancer therapy" Cancer Res 68(13): 4959-4962

Benyamini H. and Friedler A. (2011). "The ASPP interaction network: electrostatic differentiation between pro- and anti-apoptotic proteins" J Mol Recognit 24(2): 266-274

Bergamaschi D., Samuels Y., Jin B., Duraisingham S., Crook T. and Lu X. (2004). "ASPP1 and ASPP2: common activators of p53 family members" Mol Cell Biol 24(3): 1341-1350

Bergamaschi D., Samuels Y., O'Neil N. J., Trigiante G., Crook T., Hsieh J. K., O'Connor D. J., Zhong S., Campargue I., Tomlinson M. L., Kuwabara P. E. and Lu X. (2003). "iASPP oncoprotein is a key inhibitor of p53 conserved from worm to human" Nat Genet 33(2): 162-167

Bergamaschi D., Samuels Y., Sullivan A., Zvelebil M., Breyssens H., Bisso A., Del Sal G., Syed N., Smith P., Gasco M., Crook T. and Lu X. (2006). "iASPP preferentially binds p53 proline-rich region and modulates apoptotic function of codon 72-polymorphic p53" Nat Genet 38(10): 1133-1141

Buti L., Spooner E., Van der Veen A. G., Rappuoli R., Covacci A. and Ploegh H. L. (2011). "Helicobacter pylori cytotoxin-associated gene A (CagA) subverts the apoptosis-stimulating protein of p53 (ASPP2) tumor suppressor pathway of the host" Proc Natl Acad Sci U S A 108(22): 9238-9243

Cai Y., Qiu S., Gao X., Gu S. Z. and Liu Z. J. (2012). "iASPP inhibits p53-independent apoptosis by inhibiting transcriptional activity of p63/p73 on promoters of proapoptotic genes" Apoptosis 17(8): 777-783

Canning P., von Delft F. and Bullock A. N. (2012). "Structural basis for ASPP2 recognition by the tumor suppressor p73" J Mol Biol 423(4): 515-527

Cannito S., Novo E., Compagnone A., Valfre di Bonzo L., Busletta C., Zamara E., Paternostro C., Povero D., Bandino A., Bozzo F., Cravanzola C., Bravoco V., Colombatto S. and Parola M. (2008). "Redox mechanisms switch on hypoxia-dependent epithelial-mesenchymal transition in cancer cells" Carcinogenesis 29(12): 2267-2278

Cao L., Huang Q., He J., Lu J. and Xiong Y. (2013). "Elevated expression of iASPP correlates with poor prognosis and chemoresistance/radioresistance in FIGO Ib1-IIa squamous cell cervical cancer" Cell Tissue Res

Cao Y., Hamada T., Matsui T., Date T. and Iwabuchi K. (2004). "Hepatitis C virus core protein interacts with p53-binding protein, 53BP2/Bbp/ASPP2, and inhibits p53-mediated apoptosis" Biochem Biophys Res Commun 315(4): 788-795

Chen D., Padiernos E., Ding F., Lossos I. S. and Lopez C. D. (2005). "Apoptosis-stimulating protein of p53-2 (ASPP2/53BP2L) is an E2F target gene" Cell Death Differ 12(4): 358-368

Chen J., Xie F., Zhang L. and Jiang W. G. (2010). "iASPP is over-expressed in human non-small cell lung cancer and regulates the proliferation of lung cancer cells through a p53 associated pathway" BMC Cancer 10(694

Chen Y., Liu W., Naumovski L. and Neve R. L. (2003). "ASPP2 inhibits APP-BP1-mediated NEDD8 conjugation to cullin-1 and decreases APP-BP1-induced cell proliferation and neuronal apoptosis" J Neurochem 85(3): 801-809

Chikh A., Matin R. N., Senatore V., Hufbauer M., Lavery D., Raimondi C., Ostano P., Mello-Grand M., Ghimenti C., Bahta A., Khalaf S., Akgul B., Braun K. M., Chiorino G., Philpott M. P., Harwood C. A. and Bergamaschi D. (2011). "iASPP/p63 autoregulatory feedback loop is required for the homeostasis of stratified epithelia" EMBO J 30(20): 4261-4273

Cockman M. E., Lancaster D. E., Stolze I. P., Hewitson K. S., McDonough M. A., Coleman M. L., Coles C. H., Yu X., Hay R. T., Ley S. C., Pugh C. W., Oldham N. J., Masson N., Schofield C. J. and Ratcliffe P. J. (2006). "Posttranslational hydroxylation of ankyrin repeats in IkappaB proteins by the hypoxia-inducible factor (HIF) asparaginyl hydroxylase, factor inhibiting HIF (FIH)" Proc Natl Acad Sci U S A 103(40): 14767-14772

Cockman M. E., Webb J. D., Kramer H. B., Kessler B. M. and Ratcliffe P. J. (2009a). "Proteomics-based identification of novel factor inhibiting hypoxia-inducible factor (FIH) substrates indicates widespread asparaginyl hydroxylation of ankyrin repeat domain-containing proteins" Mol Cell Proteomics 8(3): 535-546

Cockman M. E., Webb J. D. and Ratcliffe P. J. (2009b). "FIH-dependent asparaginyl hydroxylation of ankyrin repeat domain-containing proteins" Ann N Y Acad Sci 1177(9-18

Coleman M. L., McDonough M. A., Hewitson K. S., Coles C., Mecinovic J., Edelmann M., Cook K. M., Cockman M. E., Lancaster D. E., Kessler B. M., Oldham N. J., Ratcliffe P. J. and Schofield C. J. (2007). "Asparaginyl hydroxylation of the Notch ankyrin repeat domain by factor inhibiting hypoxia-inducible factor" J Biol Chem 282(33): 24027-24038

Coleman M. L. and Ratcliffe P. J. (2009). "Signalling cross talk of the HIF system: involvement of the FIH protein" Curr Pharm Des 15(33): 3904-3907

Cong W., Hirose T., Harita Y., Yamashita A., Mizuno K., Hirano H. and Ohno S. (2010). "ASPP2 regulates epithelial cell polarity through the PAR complex" Curr Biol 20(15): 1408-1414

Cummins E. P., Berra E., Comerford K. M., Ginouves A., Fitzgerald K. T., Seeballuck F., Godson C., Nielsen J. E., Moynagh P., Pouyssegur J. and Taylor C. T. (2006). "Prolyl hydroxylase-1 negatively regulates IkappaB kinase-beta, giving insight into hypoxia-induced NFkappaB activity" Proc Natl Acad Sci U S A 103(48): 18154-18159

Dames S. A., Martinez-Yamout M., De Guzman R. N., Dyson H. J. and Wright P. E. (2002). "Structural basis for Hif-1 alpha /CBP recognition in the cellular hypoxic response" Proc Natl Acad Sci U S A 99(8): 5271-5276

Dann C. E., 3rd and Bruick R. K. (2005). "Dioxygenases as O2-dependent regulators of the hypoxic response pathway" Biochem Biophys Res Commun 338(1): 639-647

Dayan F., Roux D., Brahimi-Horn M. C., Pouyssegur J. and Mazure N. M. (2006). "The oxygen sensor factor-inhibiting hypoxia-inducible factor-1 controls expression of distinct genes through the bifunctional transcriptional character of hypoxia-inducible factor-1alpha" Cancer Res 66(7): 3688-3698

Deng Q., Sheng L., Su D., Zhang L., Liu P., Lu K. and Ma S. (2010). "Genetic polymorphisms in ATM, ERCC1, APE1 and iASPP genes and lung cancer risk in a population of southeast China" Med Oncol 28(3): 667-672

Devries I. L., Hampton-Smith R. J., Mulvihill M. M., Alverdi V., Peet D. J. and Komives E. A. (2010). "Consequences of IkappaB alpha hydroxylation by the factor inhibiting HIF (FIH)" FEBS Lett 584(23): 4725-4730

Elamin E., Masclee A., Juuti-Uusitalo K., van Ijzendoorn S., Troost F., Pieters H. J., Dekker J. and Jonkers D. (2013). "Fatty Acid Ethyl Esters Induce Intestinal Epithelial Barrier Dysfunction via a Reactive Oxygen Species-Dependent Mechanism in a Three-Dimensional Cell Culture Model" PLoS One 8(3): e58561

Elkins J. M., Hewitson K. S., McNeill L. A., Seibel J. F., Schlemminger I., Pugh C. W., Ratcliffe P. J. and Schofield C. J. (2003). "Structure of factor-inhibiting hypoxia-inducible factor (HIF) reveals mechanism of oxidative modification of HIF-1 alpha" J Biol Chem 278(3): 1802-1806

Epstein A. C., Gleadle J. M., McNeill L. A., Hewitson K. S., O'Rourke J., Mole D. R., Mukherji M., Metzen E., Wilson M. I., Dhanda A., Tian Y. M., Masson N., Hamilton D. L., Jaakkola P., Barstead R., Hodgkin J., Maxwell P. H., Pugh C. W., Schofield C. J. and Ratcliffe P. J. (2001). "C. elegans EGL-9 and mammalian homologs define a family of dioxygenases that regulate HIF by prolyl hydroxylation" Cell 107(1): 43-54

Espanel X. and Sudol M. (2001). "Yes-associated protein and p53-binding protein-2 interact through their WW and SH3 domains" J Biol Chem 276(17): 14514-14523

Ferguson J. E., 3rd, Wu Y., Smith K., Charles P., Powers K., Wang H. and Patterson C. (2007). "ASB4 is a hydroxylation substrate of FIH and promotes vascular differentiation via an oxygen-dependent mechanism" Mol Cell Biol 27(18): 6407-6419

Fogal V., Kartasheva N. N., Trigiante G., Llanos S., Yap D., Vousden K. H. and Lu X. (2005). "ASPP1 and ASPP2 are new transcriptional targets of E2F" Cell Death Differ 12(4): 369-376

Gibrat J. F., Madej T. and Bryant S. H. (1996). "Surprising similarities in structure comparison" Curr Opin Struct Biol 6(3): 377-385

Gillotin S. and Lu X. (2011). "The ASPP proteins complex and cooperate with p300 to modulate the transcriptional activity of p53" FEBS Lett 585(12): 1778-1782

Gonzalez J. E., DiGeronimo R. J., Arthur D. E. and King J. M. (2009). "Remodeling of the tight junction during recovery from exposure to hydrogen peroxide in kidney epithelial cells" Free Radic Biol Med 47(11): 1561-1569

Gorina S. and Pavletich N. P. (1996). "Structure of the p53 tumor suppressor bound to the ankyrin and SH3 domains of 53BP2" Science 274(5289): 1001-1005

Gorres K. L. and Raines R. T. (2010). "Prolyl 4-hydroxylase" Crit Rev Biochem Mol Biol 45(2): 106-124

Hakuno F., Kurihara S., Watson R. T., Pessin J. E. and Takahashi S. (2007). "53BP2S, interacting with insulin receptor substrates, modulates insulin signaling" J Biol Chem 282(52): 37747-37758

Halder G. and Johnson R. L. (2011). "Hippo signaling: growth control and beyond" Development 138(1): 9-22

Hardy A. P., Prokes I., Kelly L., Campbell I. D. and Schofield C. J. (2009). "Asparaginyl beta-hydroxylation of proteins containing ankyrin repeat domains influences their stability and function" J Mol Biol 392(4): 994-1006

Helps N. R., Barker H. M., Elledge S. J. and Cohen P. T. (1995). "Protein phosphatase 1 interacts with p53BP2, a protein which binds to the tumour suppressor p53" FEBS Lett 377(3): 295-300

Hershko T., Chaussepied M., Oren M. and Ginsberg D. (2005). "Novel link between E2F and p53: proapoptotic cofactors of p53 are transcriptionally upregulated by E2F" Cell Death Differ 12(4): 377-383

Hewitson K. S., McNeill L. A., Riordan M. V., Tian Y. M., Bullock A. N., Welford R. W., Elkins J. M., Oldham N. J., Bhattacharya S., Gleadle J. M., Ratcliffe P. J., Pugh C. W. and Schofield C. J. (2002). "Hypoxia-inducible factor (HIF) asparagine hydroxylase is identical to factor inhibiting HIF (FIH) and is related to the cupin structural family" J Biol Chem 277(29): 26351-26355

Hirashima M., Sano K., Morisada T., Murakami K., Rossant J. and Suda T. (2008). "Lymphatic vessel assembly is impaired in Aspp1-deficient mouse embryos" Dev Biol 316(1): 149-159

Ho S. N., Hunt H. D., Horton R. M., Pullen J. K. and Pease L. R. (1989). "Site-directed mutagenesis by overlap extension using the polymerase chain reaction" Gene 77(1): 51-59

Iwabuchi K., Bartel P. L., Li B., Marraccino R. and Fields S. (1994). "Two cellular proteins that bind to wild-type but not mutant p53" Proc Natl Acad Sci U S A 91(13): 6098-6102

Jaakkola P., Mole D. R., Tian Y. M., Wilson M. I., Gielbert J., Gaskell S. J., von Kriegsheim A., Hebestreit H. F., Mukherji M., Schofield C. J., Maxwell P. H., Pugh C. W. and Ratcliffe P. J. (2001). "Targeting of HIF-alpha to the von Hippel-Lindau ubiquitylation complex by O2-regulated prolyl hydroxylation" Science 292(5516): 468-472

Janke K., Brockmeier U., Kuhlmann K., Eisenacher M., Nolde J., Meyer H. E., Mairbäurl H. and Metzen E. (2013). "Factor Inhibiting HIF-1 (FIH-1) modulates protein interactions of Apoptosis-Stimulating p53 binding Protein 2 (ASPP2)" J Cell Sci [Epub ahead of print] PMID: 23606740.

Jiang L., Siu M. K., Wong O. G., Tam K. F., Lu X., Lam E. W., Ngan H. Y., Le X. F., Wong E. S., Monteiro L. J., Chan H. Y. and Cheung A. N. (2011). "iASPP and chemoresistance in ovarian cancers: effects on paclitaxel-mediated mitotic catastrophe" Clin Cancer Res 17(21): 6924-6933

Kaelin W. G., Jr. and Ratcliffe P. J. (2008). "Oxygen sensing by metazoans: the central role of the HIF hydroxylase pathway" Mol Cell 30(4): 393-402

Kampa K. M., Acoba J. D., Chen D., Gay J., Lee H., Beemer K., Padiernos E., Boonmark N., Zhu Z., Fan A. C., Bailey A. S., Fleming W. H., Corless C., Felsher D. W., Naumovski L. and Lopez C. D. (2009). "Apoptosis-stimulating protein of p53 (ASPP2) heterozygous mice are tumor-prone and have attenuated cellular damage-response thresholds" Proc Natl Acad Sci U S A 106(11): 4390-4395

Katz C., Benyamini H., Rotem S., Lebendiker M., Danieli T., Iosub A., Refaely H., Dines M., Bronner V., Bravman T., Shalev D. E., Rudiger S. and Friedler A. (2008). "Molecular basis of the interaction between the antiapoptotic Bcl-2 family proteins and the proapoptotic protein ASPP2" Proc Natl Acad Sci U S A 105(34): 12277-12282

Kelly L., McDonough M. A., Coleman M. L., Ratcliffe P. J. and Schofield C. J. (2009). "Asparagine beta-hydroxylation stabilizes the ankyrin repeat domain fold" Mol Biosyst 5(1): 52-58

Khan M. N., Bhattacharyya T., Andrikopoulos P., Esteban M. A., Barod R., Connor T., Ashcroft M., Maxwell P. H. and Kiriakidis S. (2011). "Factor inhibiting HIF (FIH-1) promotes renal cancer cell survival by protecting cells from HIF-1alpha-mediated apoptosis" Br J Cancer 104(7): 1151-1159

Kobayashi S., Kajino S., Takahashi N., Kanazawa S., Imai K., Hibi Y., Ohara H., Itoh M. and Okamoto T. (2005). "53BP2 induces apoptosis through the mitochondrial death pathway" Genes Cells 10(3): 253-260

Koditz J., Nesper J., Wottawa M., Stiehl D. P., Camenisch G., Franke C., Myllyharju J., Wenger R. H. and Katschinski D. M. (2007). "Oxygen-dependent ATF-4 stability is mediated by the PHD3 oxygen sensor" Blood 110(10): 3610-3617

Kohl A., Binz H. K., Forrer P., Stumpp M. T., Pluckthun A. and Grutter M. G. (2003). "Designed to be stable: crystal structure of a consensus ankyrin repeat protein" Proc Natl Acad Sci U S A 100(4): 1700-1705

Koivunen P., Hirsila M., Gunzler V., Kivirikko K. I. and Myllyharju J. (2004). "Catalytic properties of the asparaginyl hydroxylase (FIH) in the oxygen sensing pathway are distinct from those of its prolyl 4-hydroxylases" J Biol Chem 279(11): 9899-9904

Kuhar M. J. (2010). "Measuring levels of proteins by various technologies: can we learn more by measuring turnover?" Biochem Pharmacol 79(5): 665-668

Kuzmanov A., Wielockx B., Rezaei M., Kettelhake A. and Breier G. (2012). "Overexpression of factor inhibiting HIF-1 enhances vessel maturation and tumor growth via platelet-derived growth factor-C" Int J Cancer 131(5): E603-613

Lando D., Peet D. J., Gorman J. J., Whelan D. A., Whitelaw M. L. and Bruick R. K. (2002a). "FIH-1 is an asparaginyl hydroxylase enzyme that regulates the transcriptional activity of hypoxia-inducible factor" Genes Dev 16(12): 1466-1471

Lando D., Peet D. J., Whelan D. A., Gorman J. J. and Whitelaw M. L. (2002b). "Asparagine hydroxylation of the HIF transactivation domain a hypoxic switch" Science 295(5556): 858-861

Langton P. F., Colombani J., Chan E. H., Wepf A., Gstaiger M. and Tapon N. (2009). "The dASPP-dRASSF8 complex regulates cell-cell adhesion during Drosophila retinal morphogenesis" Curr Biol 19(23): 1969-1978

Li G., Wang R., Gao J., Deng K., Wei J. and Wei Y. (2011). "RNA interference-mediated silencing of iASPP induces cell proliferation inhibition and G0/G1 cell cycle arrest in U251 human glioblastoma cells" Mol Cell Biochem 350(1-2): 193-200

Li J., Mahajan A. and Tsai M. D. (2006). "Ankyrin repeat: a unique motif mediating protein-protein interactions" Biochemistry 45(51): 15168-15178

Li S., Shi G., Yuan H., Zhou T., Zhang Q., Zhu H. and Wang X. (2012). "Abnormal expression pattern of the ASPP family of proteins in human non-small cell lung cancer and regulatory functions on apoptosis through p53 by iASPP" Oncol Rep 28(1): 133-140

Linke S., Hampton-Smith R. J. and Peet D. J. (2007). "Characterization of ankyrin repeat-containing proteins as substrates of the asparaginyl hydroxylase factor inhibiting hypoxia-inducible transcription factor" Methods Enzymol 435(61-85

Linke S., Stojkoski C., Kewley R. J., Booker G. W., Whitelaw M. L. and Peet D. J. (2004). "Substrate requirements of the oxygen-sensing asparaginyl hydroxylase factor-inhibiting hypoxia-inducible factor" J Biol Chem 279(14): 14391-14397

Lisy K. and Peet D. J. (2008). "Turn me on: regulating HIF transcriptional activity" Cell Death Differ 15(4): 642-649

Liu C. Y., Lv X., Li T., Xu Y., Zhou X., Zhao S., Xiong Y., Lei Q. Y. and Guan K. L. (2010a). "PP1 cooperates with ASPP2 to dephosphorylate and activate TAZ" J Biol Chem 286(7): 5558-5566

Liu H., Wang M., Diao S., Rao Q., Zhang X., Xing H. and Wang J. (2009). "siRNA-mediated down-regulation of iASPP promotes apoptosis induced by etoposide and daunorubicin in leukemia cells expressing wild-type p53" Leuk Res 33(9): 1243-1248

Liu T., Li L., Yang W., Jia H., Xu M., Bi J., Li Z., Liu X., Jing H. and Kong C. (2011). "iASPP is important for bladder cancer cell proliferation" Oncol Res 19(3-4): 125-130

Liu W. K., Jiang X. Y., Ren J. K. and Zhang Z. X. (2010b). "Expression pattern of the ASPP family members in endometrial endometrioid adenocarcinoma" Onkologie 33(10): 500-503

Liu Y., Higashitsuji H., Itoh K., Sakurai T., Koike K., Hirota K., Fukumoto M. and Fujita J. (2013). "Overexpression of gankyrin in mouse hepatocytes induces hemangioma by suppressing factor inhibiting hypoxia-inducible factor-1 (FIH-1) and activating hypoxia-inducible factor-1" Biochem Biophys Res Commun 432(1): 22-27

Liu Y., Xin Y., Ye F., Wang W., Lu Q., Kaplan H. J. and Dean D. C. (2010c). "Taz-tead1 links cell-cell contact to zeb1 expression, proliferation, and dedifferentiation in retinal pigment epithelial cells" Invest Ophthalmol Vis Sci 51(7): 3372-3378

Liu Z., Zhang X., Huang D., Liu Y., Liu L., Li G., Dai Y., Tan H., Xiao J. and Tian Y. (2012). "Elevated expression of iASPP in head and neck squamous cell carcinoma and its clinical significance" Med Oncol 29(5): 3381-3388

Liu Z. J., Lu X., Zhang Y., Zhong S., Gu S. Z., Zhang X. B., Yang X. and Xin H. M. (2005). "Downregulated mRNA expression of ASPP and the hypermethylation of the 5'-untranslated region in cancer cell lines retaining wild-type p53" FEBS Lett 579(7): 1587-1590

Liu Z. J., Zhang Y., Zhang X. B. and Yang X. (2004). "Abnormal mRNA expression of ASPP members in leukemia cell lines" Leukemia 18(4): 880

Llanos S., Royer C., Lu M., Bergamaschi D., Lee W. H. and Lu X. (2011). "Inhibitory member of the apoptosis-stimulating proteins of the p53 family (iASPP) interacts with protein phosphatase 1 via a noncanonical binding motif" J Biol Chem 286(50): 43039-43044

Lochhead J. J., McCaffrey G., Quigley C. E., Finch J., DeMarco K. M., Nametz N. and Davis T. P. (2010). "Oxidative stress increases blood-brain barrier permeability and induces alterations in occludin during hypoxia-reoxygenation" J Cereb Blood Flow Metab 30(9): 1625-1636

Loenarz C. and Schofield C. J. (2011). "Physiological and biochemical aspects of hydroxylations and demethylations catalyzed by human 2-oxoglutarate oxygenases" Trends Biochem Sci 36(1): 7-18

Lossos I. S., Natkunam Y., Levy R. and Lopez C. D. (2002). "Apoptosis stimulating protein of p53 (ASPP2) expression differs in diffuse large B-cell and follicular center lymphoma: correlation with clinical outcome" Leuk Lymphoma 43(12): 2309-2317

Lu B., Guo H., Zhao J., Wang C., Wu G., Pang M., Tong X., Bu F., Liang A., Hou S., Fan X., Dai J., Wang H. and Guo Y. (2010). "Increased expression of iASPP, regulated by hepatitis B virus X protein-mediated NF-kappaB activation, in hepatocellular carcinoma" Gastroenterology 139(6): 2183-2194 e2185

Mahon P. C., Hirota K. and Semenza G. L. (2001). "FIH-1: a novel protein that interacts with HIF-1alpha and VHL to mediate repression of HIF-1 transcriptional activity" Genes Dev 15(20): 2675-2686

Mak V. C., Lee L., Siu M. K., Wong O. G., Lu X., Ngan H. Y., Wong E. S. and Cheung A. N. (2011). "Downregulation of ASPP1 in gestational trophoblastic disease: correlation with hypermethylation, apoptotic activity and clinical outcome" Mod Pathol 24(4): 522-532

Martin-Belmonte F. and Perez-Moreno M. (2011). "Epithelial cell polarity, stem cells and cancer" Nat Rev Cancer 12(1): 23-38

Martinez L. A., Goluszko E., Chen H. Z., Leone G., Post S., Lozano G., Chen Z. and Chauchereau A. (2010). "E2F3 is a mediator of DNA damage-induced apoptosis" Mol Cell Biol 30(2): 524-536

Masson N. and Ratcliffe P. J. (2003). "HIF prolyl and asparaginyl hydroxylases in the biological response to intracellular O(2) levels" J Cell Sci 116(Pt 15): 3041-3049

Masson N., Singleton R. S., Sekirnik R., Trudgian D. C., Ambrose L. J., Miranda M. X., Tian Y. M., Kessler B. M., Schofield C. J. and Ratcliffe P. J. (2012). "The FIH hydroxylase is a cellular peroxide sensor that modulates HIF transcriptional activity" EMBO Rep 13(3): 251-257

Metzen E., Berchner-Pfannschmidt U., Stengel P., Marxsen J. H., Stolze I., Klinger M., Huang W. Q., Wotzlaw C., Hellwig-Burgel T., Jelkmann W., Acker H. and Fandrey J. (2003). "Intracellular localisation of human HIF-1 alpha hydroxylases: implications for oxygen sensing" J Cell Sci 116(Pt 7): 1319-1326

Mori T., Okamoto H., Takahashi N., Ueda R. and Okamoto T. (2000). "Aberrant overexpression of 53BP2 mRNA in lung cancer cell lines" FEBS Lett 465(2-3): 124-128

Mosavi L. K., Cammett T. J., Desrosiers D. C. and Peng Z. Y. (2004). "The ankyrin repeat as molecular architecture for protein recognition" Protein Sci 13(6): 1435-1448

Nakagawa H., Koyama K., Murata Y., Morito M., Akiyama T. and Nakamura Y. (2000). "APCL, a central nervous system-specific homologue of adenomatous polyposis coli tumor suppressor, binds to p53-binding protein 2 and translocates it to the perinucleus" Cancer Res 60(1): 101-105

Natah S. S., Srinivasan S., Pittman Q., Zhao Z. and Dunn J. F. (2009). "Effects of acute hypoxia and hyperthermia on the permeability of the blood-brain barrier in adult rats" J Appl Physiol 107(4): 1348-1356

Naumovski L. and Cleary M. L. (1996). "The p53-binding protein 53BP2 also interacts with Bc12 and impedes cell cycle progression at G2/M" Mol Cell Biol 16(7): 3884-3892

Notari M., Hu Y., Koch S., Lu M., Ratnayaka I., Zhong S., Baer C., Pagotto A., Goldin R., Salter V., Candi E., Melino G. and Lu X. (2011). "Inhibitor of apoptosis-stimulating protein of p53 (iASPP) prevents senescence and is required for epithelial stratification" Proc Natl Acad Sci U S A 108(40): 16645-16650

Ota M. and Sasaki H. (2008). "Mammalian Tead proteins regulate cell proliferation and contact inhibition as transcriptional mediators of Hippo signaling" Development 135(24): 4059-4069

Overmeyer J. H. and Maltese W. A. (2011). "Death pathways triggered by activated Ras in cancer cells" Front Biosci 16(1693-1713

Park S. W., An C. H., Kim S. S., Yoo N. J. and Lee S. H. (2010). "Mutational Analysis of ASPP1 and ASPP2 Genes, a p53-related Gene, in Gastric and Cololorectal Cancers with Microsatellite Instability" Gut Liver 4(2): 292-293

Patel S., George R., Autore F., Fraternali F., Ladbury J. E. and Nikolova P. V. (2008). "Molecular interactions of ASPP1 and ASPP2 with the p53 protein family and the apoptotic promoters PUMA and Bax" Nucleic Acids Res 36(16): 5139-5151

Pelletier J., Dayan F., Durivault J., Ilc K., Pecou E., Pouyssegur J. and Mazure N. M. (2011). "The asparaginyl hydroxylase factor-inhibiting HIF is essential for tumor growth through suppression of the p53-p21 axis" Oncogene 31(24): 2989-3001

Pugh C. W., O'Rourke J. F., Nagao M., Gleadle J. M. and Ratcliffe P. J. (1997). "Activation of hypoxia-inducible factor-1; definition of regulatory domains within the alpha subunit" J Biol Chem 272(17): 11205-11214

Pylayeva-Gupta Y., Grabocka E. and Bar-Sagi D. (2011). "RAS oncogenes: weaving a tumorigenic web" Nat Rev Cancer 11(11): 761-774

Qi H., Wang P., Liu C., Li M., Wang S., Huang Y. and Wang F. (2011). "Involvement of HIF-1alpha in MLCK-dependent endothelial barrier dysfunction in hypoxia" Cell Physiol Biochem 27(3-4): 251-262

Robinson R. A., Lu X., Jones E. Y. and Siebold C. (2008). "Biochemical and structural studies of ASPP proteins reveal differential binding to p53, p63, and p73" Structure 16(2): 259-268

Samuels-Lev Y., O'Connor D. J., Bergamaschi D., Trigiante G., Hsieh J. K., Zhong S., Campargue I., Naumovski L., Crook T. and Lu X. (2001). "ASPP proteins specifically stimulate the apoptotic function of p53" Mol Cell 8(4): 781-794

Schmierer B., Novak B. and Schofield C. J. (2010). "Hypoxia-dependent sequestration of an oxygen sensor by a widespread structural motif can shape the hypoxic response--a predictive kinetic model" BMC Syst Biol 4(139

Schneeberger E. E. and Lynch R. D. (2004). "The tight junction: a multifunctional complex" Am J Physiol Cell Physiol 286(6): C1213-1228

Schofield C. J. and Ratcliffe P. J. (2004). "Oxygen sensing by HIF hydroxylases" Nat Rev Mol Cell Biol 5(5): 343-354

Semenza G. L. (2012). "Hypoxia-inducible factors in physiology and medicine" Cell 148(3): 399-408

Shang J., Liu N., Tanaka N. and Abe K. (2011). "Expressions of hypoxic stress sensor proteins after transient cerebral ischemia in mice" J Neurosci Res 90(3): 648-655

Shi Y., Yang S., Troup S., Lu X., Callaghan S., Park D. S., Xing Y. and Yang X. (2011). "Resveratrol induces apoptosis in breast cancer cells by E2F1-mediated up-regulation of ASPP1" Oncol Rep 25(6): 1713-1719

Singleton R. S., Trudgian D. C., Fischer R., Kessler B. M., Ratcliffe P. J. and Cockman M. E. (2011). "Quantitative mass spectrometry reveals dynamics of factor-inhibiting hypoxia-inducible factor-catalyzed hydroxylation" J Biol Chem 286(39): 33784-33794

Slee E. A., Gillotin S., Bergamaschi D., Royer C., Llanos S., Ali S., Jin B., Trigiante G. and Lu X. (2004). "The N-terminus of a novel isoform of human iASPP is required for its cytoplasmic localization" Oncogene 23(56): 9007-9016

Sottocornola R., Royer C., Vives V., Tordella L., Zhong S., Wang Y., Ratnayaka I., Shipman M., Cheung A., Gaston-Massuet C., Ferretti P., Molnar Z. and Lu X. (2010). "ASPP2 binds Par-3 and controls the polarity and proliferation of neural progenitors during CNS development" Dev Cell 19(1): 126-137

Spandidos D. A., Sourvinos G., Tsatsanis C. and Zafiropoulos A. (2002). "Normal ras genes: their onco-suppressor and pro-apoptotic functions (review)" Int J Oncol 21(2): 237-241

Sun W. T., Hsieh P. C., Chiang M. L., Wang M. C. and Wang F. F. (2008). "p53 target DDA3 binds ASPP2 and inhibits its stimulation on p53-mediated BAX activation" Biochem Biophys Res Commun 376(2): 395-398

Takahashi N., Kobayashi S., Kajino S., Imai K., Tomoda K., Shimizu S. and Okamoto T. (2005). "Inhibition of the 53BP2S-mediated apoptosis by nuclear factor kappaB and Bcl-2 family proteins" Genes Cells 10(8): 803-811

Tamiya S., Liu L. and Kaplan H. J. (2010). "Epithelial-mesenchymal transition and proliferation of retinal pigment epithelial cells initiated upon loss of cell-cell contact" Invest Ophthalmol Vis Sci 51(5): 2755-2763

Tidow H., Andreeva A., Rutherford T. J. and Fersht A. R. (2007). "Solution structure of ASPP2 N-terminal domain (N-ASPP2) reveals a ubiquitin-like fold" J Mol Biol 371(4): 948-958

Tidow H., Veprintsev D. B., Freund S. M. and Fersht A. R. (2006). "Effects of oncogenic mutations and DNA response elements on the binding of p53 to p53-binding protein 2 (53BP2)" J Biol Chem 281(43): 32526-32533

Trinkle-Mulcahy L., Boulon S., Lam Y. W., Urcia R., Boisvert F. M., Vandermoere F., Morrice N. A., Swift S., Rothbauer U., Leonhardt H. and Lamond A. (2008). "Identifying specific protein interaction partners using quantitative mass spectrometry and bead proteomes" J Cell Biol 183(2): 223-239

Uhlmann-Schiffler H., Kiermayer S. and Stahl H. (2009). "The DEAD box protein Ddx42p modulates the function of ASPP2, a stimulator of apoptosis" Oncogene 28(20): 2065-2073

Uitto J. and Lichtenstein J. R. (1976). "Defects in the biochemistry of collagen in diseases of connective tissue" J Invest Dermatol 66(02): 59-79

Vigneron A. M., Ludwig R. L. and Vousden K. H. (2010). "Cytoplasmic ASPP1 inhibits apoptosis through the control of YAP" Genes Dev 24(21): 2430-2439

Vigneron A. M. and Vousden K. H. (2011). "An indirect role for ASPP1 in limiting p53-dependent p21 expression and cellular senescence" EMBO J 31(2): 471-480

Vives V., Su J., Zhong S., Ratnayaka I., Slee E., Goldin R. and Lu X. (2006). "ASPP2 is a haploinsufficient tumor suppressor that cooperates with p53 to suppress tumor growth" Genes Dev 20(10): 1262-1267

Wang X. D., Lapi E., Sullivan A., Ratnayaka I., Goldin R., Hay R. and Lu X. (2011). "SUMO-modified nuclear cyclin D1 bypasses Ras-induced senescence" Cell Death Differ 18(2): 304-314

Wang Y., Godin-Heymann N., Dan Wang X., Bergamaschi D., Llanos S. and Lu X. (2013a). "ASPP1 and ASPP2 bind active RAS, potentiate RAS signalling and enhance p53 activity in cancer cells" Cell Death Differ 20(4): 525-534

Wang Z., Liu Y., Takahashi M., Van Hook K., Kampa-Schittenhelm K. M., Sheppard B. C., Sears R. C., Stork P. J. and Lopez C. D. (2013b). "N terminus of ASPP2 binds to Ras and enhances Ras/Raf/MEK/ERK activation to promote oncogene-induced senescence" Proc Natl Acad Sci U S A 110(1): 312-317

Webb J. D., Muranyi A., Pugh C. W., Ratcliffe P. J. and Coleman M. L. (2009). "MYPT1, the targeting subunit of smooth-muscle myosin phosphatase, is a substrate for the asparaginyl hydroxylase factor inhibiting hypoxia-inducible factor (FIH)" Biochem J 420(2): 327-333

Wei W. L., Hu H. Y., Zhang L. J., Chen Y., Ye E. and Wang X. F. (2011). "[Promoter methylation of ASPP1 and ASPP2 genes in non-small cell lung cancers]" Zhonghua Bing Li Xue Za Zhi 40(8): 532-536

Wepf A., Glatter T., Schmidt A., Aebersold R. and Gstaiger M. (2009). "Quantitative interaction proteomics using mass spectrometry" Nat Methods 6(3): 203-205

Wilkins S. E., Hyvarinen J., Chicher J., Gorman J. J., Peet D. J., Bilton R. L. and Koivunen P. (2009). "Differences in hydroxylation and binding of Notch and HIF-1alpha demonstrate substrate selectivity for factor inhibiting HIF-1 (FIH-1)" Int J Biochem Cell Biol 41(7): 1563-1571

Wilkins S. E., Karttunen S., Hampton-Smith R. J., Murchland I., Chapman-Smith A. and Peet D. J. (2012). "Factor inhibiting HIF (FIH) recognizes distinct molecular features within hypoxia-inducible factor-alpha (HIF-alpha) versus ankyrin repeat substrates" J Biol Chem 287(12): 8769-8781

Wilson A. M., Morquette B., Abdouh M., Unsain N., Barker P. A., Feinstein E., Bernier G. and Di Polo A. (2013). "ASPP1/2 regulate p53-dependent death of retinal ganglion cells through PUMA and Fas/CD95 activation in vivo" J Neurosci 33(5): 2205-2216

Witt K. A., Mark K. S., Sandoval K. E. and Davis T. P. (2008). "Reoxygenation stress on blood-brain barrier paracellular permeability and edema in the rat" Microvasc Res 75(1): 91-96

Yang J. P., Hori M., Sanda T. and Okamoto T. (1999a). "Identification of a novel inhibitor of nuclear factor-kappaB, RelA-associated inhibitor" J Biol Chem 274(22): 15662-15670

Yang J. P., Hori M., Takahashi N., Kawabe T., Kato H. and Okamoto T. (1999b). "NF-kappaB subunit p65 binds to 53BP2 and inhibits cell death induced by 53BP2" Oncogene 18(37): 5177-5186

Yang M., Chowdhury R., Ge W., Hamed R. B., McDonough M. A., Claridge T. D., Kessler B. M., Cockman M. E., Ratcliffe P. J. and Schofield C. J. (2011a). "Factor-inhibiting hypoxia-inducible factor (FIH) catalyses the post-translational hydroxylation of histidinyl residues within ankyrin repeat domains" FEBS J 278(7): 1086-1097

Yang M., Ge W., Chowdhury R., Claridge T. D., Kramer H. B., Schmierer B., McDonough M. A., Gong L., Kessler B. M., Ratcliffe P. J., Coleman M. L. and Schofield C. J. (2011b). "Asparagine and aspartate hydroxylation of the cytoskeletal ankyrin family is catalyzed by factor-inhibiting hypoxia-inducible factor" J Biol Chem 286(9): 7648-7660

Yang M., Hardy A. P., Chowdhury R., Loik N. D., Scotti J. S., McCullagh J. S., Claridge T. D., McDonough M. A., Ge W. and Schofield C. J. (2013). "Substrate selectivity analyses of factor inhibiting hypoxia-inducible factor" Angew Chem Int Ed Engl 52(6): 1700-1704

Zhang B., Xiao H. J., Chen J., Tao X. and Cai L. H. (2011). "Inhibitory member of the apoptosis-stimulating protein of p53 (ASPP) family promotes growth and tumorigenesis in human p53-deficient prostate cancer cells" Prostate Cancer Prostatic Dis 14(3): 219-224

Zhang N., Fu Z., Linke S., Chicher J., Gorman J. J., Visk D., Haddad G. G., Poellinger L., Peet D. J., Powell F. and Johnson R. S. (2010). "The asparaginyl hydroxylase factor inhibiting HIF-1alpha is an essential regulator of metabolism" Cell Metab 11(5): 364-378

Zhang X., Wang M., Zhou C., Chen S. and Wang J. (2005). "The expression of iASPP in acute leukemias" Leuk Res 29(2): 179-183

Zhao B., Wei X., Li W., Udan R. S., Yang Q., Kim J., Xie J., Ikenoue T., Yu J., Li L., Zheng P., Ye K., Chinnaiyan A., Halder G., Lai Z. C. and Guan K. L. (2007). "Inactivation of YAP oncoprotein by the Hippo pathway is involved in cell contact inhibition and tissue growth control" Genes Dev 21(21): 2747-2761

Zhao J., Wu G., Bu F., Lu B., Liang A., Cao L., Tong X., Lu X., Wu M. and Guo Y. (2010). "Epigenetic silence of ankyrin-repeat-containing, SH3-domain-containing, and proline-rich-region- containing protein 1 (ASPP1) and ASPP2 genes promotes tumor growth in hepatitis B virus-positive hepatocellular carcinoma" Hepatology 51(1): 142-153

Zheng X., Linke S., Dias J. M., Gradin K., Wallis T. P., Hamilton B. R., Gustafsson M., Ruas J. L., Wilkins S., Bilton R. L., Brismar K., Whitelaw M. L., Pereira T., Gorman J. J., Ericson J., Peet D. J., Lendahl U. and Poellinger L. (2008). "Interaction with factor inhibiting HIF-1 defines an additional mode of cross-coupling between the Notch and hypoxia signaling pathways" Proc Natl Acad Sci U S A 105(9): 3368-3373

Zhu Z., Ramos J., Kampa K., Adimoolam S., Sirisawad M., Yu Z., Chen D., Naumovski L. and Lopez C. D. (2005). "Control of ASPP2/(53BP2L) protein levels by proteasomal degradation modulates p53 apoptotic function" J Biol Chem 280(41): 34473-34480

8 Appendix

8.1 Abbreviations

2-OG	2-oxoglutarate
53BP2	p53 binding protein 2
aa	amino acids
ACN	acetonitrile
AGC	automatic gain control
AJC	apical junctional complex
AM	acetoxymethyl ester
Amc	7-amino-4-methylcoumarin
AnkyrinR	erythrocyte ankyrin
ANOVA	analysis of variance
APCL	adenomatous polyposis coli protein 2
ape-1	apoptotic enhancer 1 protein
aPKC	atypical protein kinase C
APP-BP1	amyloid β precursor protein-binding protein 1
APS	ammonium persulfate
ARD	ankyrin repeat domain
ASB4	ankyrin repeat and SOCS box protein 4
ASPP	apoptosis-stimulating p53 binding protein
ATP	adenosine triphosphate
Bbp	Bcl-2 binding protein
BCA	bicinchoninic acid
Bcl-2	B-cell lymphoma 2
Bcl-W	Bcl-2-like protein 2
Bcl-X_L	B-cell lymphoma-extra large
bHLH	basic helix-loop-helix domain
Bnip3	Bcl-2/adenovirus E1B 19kDa interacting protein 3
bp	base pairs
BSA	bovine serum albumin
Ca-9	carbonic anhydrase 9
CagA	cytotoxin-associated gene A
CBP	CREB binding protein
CDB3	cytoplasmic domain of band 3
CHAPS	3-[(3-cholamidopropyl)dimethylammonio]-1-propanesulfonate hydrate
CHX	cycloheximide
CNS	central nervous system
cpm	counts per minute
CREB	cAMP responsive element-binding
CTAD	C-terminal transactivation domain
Cu	Curie

DAPI	4',6-diamidino-2-phenylindole
DDA3	proline serine-rich coiled-coil protein 1
DDX42	DEAD (Asp-Glu-Ala-Asp) box polypeptide 42
Dlg1	drosophila disc large tumor suppressor
DMEM	dulbecco´s modified eagle medium
DMOG	dimethyloxalylglycine
DMSO	dimethylsulfoxid
DNA	deoxyribonucleic acid
dNTP	deoxynucleotide triphosphate
Doxo	doxorubicin
DSMZ	Deutsche Sammlung von Mikroorganismen und Zellkulturen
DSP	dithiobis[succinimidylpropionate]
DTT	dithiothreitol
ECL	enhanced chemiluminescence
EDTA	ethylenediaminetetraacetic acid
EMT	epithelial to mesenchymal transition
Eto	etoposide
FBS	fetal bovine serum
FEM1β	fem-1 homolog B
FGIF	fibroblast growth inhibitory factor
Fig.	figure
FIH-1	factor inhibiting HIF-1
GABP	GA-binding protein
GAPDH	glyceraldehyde 3-phosphate dehydrogenase
Glut-1	glucose transporter 1
GST	glutathione S-transferase
GTAR	gene trap ankyrin repeat
GTP	guanosine triphosphate
Gy	Gray
HCD	higher-energy collisional dissociation
HCV	hepatitis-C-virus
HEPES	4-(2-hydroxyethyl)-1-piperazineethanesulfonic acid
HIF	hypoxia-inducible factor
hMASK	human mammalian STE20-like protein kinase 4
HPLC	high-performance liquid chromatography
HRas	Harvey rat sarcoma
HRE	hypoxia-responsive element
HRP	horseradish peroxidase
iASPP	inhibitory ASPP
ILK-1	integrin-linked kinase 1
INK	inhibitor of cyclin-dependent kinase
IPTG	isopropyl β-D-1-thiogalactopyranoside
IRS-1	insulin receptor substrate 1
IκBα	NF-κB inhibitor α

kDa	kilodalton
L	linker region
LATS	large tumor suppressor
LB	Luria Broth
LC	liquid chromatography
mmu	milli mass units
mRNA	messenger RNA
MS	mass spectrometry
MTT	3-(4,5-dimethylthiazol-2-yl)-2,5-diphenyltetrazolium bromide
MW	molecular weight
MYPT1	myosin phosphatase target subunit 1
NF-κB	nuclear factor kappa-light-chain-enhancer of activated B-cells
NOG	N-oxalylglycine
NP-40	Nonidet P-40 (octylphenoxypolyethoxyethanol)
NTAD	N-terminal transactivation domain
OD	optical density
ODD	oxygen-dependent degradation domain
p.a.	pro analysis
PAGE	polyacrylamide gel electrophoresis
Par-3	partitioning defective 3 homolog
Par-6	partitioning defective 6 homolog
PAS	Per-Arnt-Sim domain
PBS	phosphate buffered saline
PCR	polymerase chain reaction
PDZ	PSD95, Dlg1, ZO-1 motif
Pfu	*Pyrococcus furiosus*
PGK1	phosphoglycerate kinase 1
PHD	prolyl hydroxylase domain containing protein
PMSF	phenylmethylsulfonyl fluoride
PP1	serine/threonine-protein phosphatase 1
ppm	parts per million
Pro	proline-rich region
PSD95	post synaptic density protein
PUMA	p53 upregulated modulator of apoptosis
PVDF	polyvinylidene fluoride
RAD	Ras-associated domain
RAI	RelA-associated inhibitor
Ras	rat sarcoma
REG	regulatory domain
RelA	NF-κB subunit p65
RNA	ribonucleic acid
RNaseL	ribonuclease L
rpm	rounds per minute
RPMI	Roswell Park Memorial Institute

SDS	sodium dodecyl sulphate
SH3	Src-homology 3
shRNA	small hairpin RNA
siRNA	small interfering RNA
SOCS	suppressor of cytokine signalling
Src	sarcoma
SV40	simian virus 40
TAD	transactivation domain
TAE	Tris-acetate-EDTA buffer
Taq	*Thermus aquaticus*
TAZ	transcriptional co-activator with PDZ-binding motif
TBS	Tris buffered saline
TCA	trichloroacetic acid
TEAD	TEA domain
TEMED	tetramethylethylenediamine
TER	transepithelial electrical resistance
TET	tetramerisation domain
TFA	trifluoroacetic acid
TRPV4	transient receptor potential cation channel subfamily V member 4
U	units
Ub	ubiquitin
Ubl	ubiquitin-like fold
VHL	von Hippel-Lindau
XIC	extracted ion chromatogram
YAP	Yes-associated protein
Yes	tyrosine-protein kinase
ZO-1	zonula occludens-1

8.2 List of Figures

8.3 List of Tables

8.4 Acknowledgement

An dieser Stelle möchte ich mich bei allen bedanken, die zur Entstehung dieser Arbeit beigetragen haben. Bei Prof. Dr. Joachim Fandrey möchte ich mich für die Möglichkeit bedanken, die Arbeit am Institut für Physiologie anzufertigen.

Außerdem danke ich Prof. Dr. Eric Metzen für die interessante Fragestellung und die engagierte Betreuung während meiner Promotion. Darüber hinaus danke ich ihm für die Gelegenheit, mein Projekt selbst auf Kongressen zu präsentieren.

Ganz besonders danke ich Dr. Ulf Brockmeier für die stetige Unterstützung, sowohl methodisch als auch theoretisch, stets konstruktive Kritik und viele nette Gespräche.

Außerdem möchte ich mich bei Frau Dr. Katja Kuhlmann für die erfolgreiche, reibungslose Zusammenarbeit und die Durchführung der Massenspektrometrie bedanken.

Darüber hinaus danke ich allen Kollegen des Instituts für Physiologie, insbesondere allen ehemaligen und derzeitigen Mitarbeitern der Arbeitsgruppe Metzen für die große Hilfsbereitschaft und die tolle Arbeitsatmosphäre. Frau Kirsten Göpelt, Frau Melanie Baumann und Herrn Frank Splettstoesser möchte ich für die exzellente technische Assistenz und die gute Stimmung im Labor danken. Meiner Bachelor-Studentin, Frau Natascha Gerads danke ich für ihre Motivation und ihre Begeisterung für das Projekt.

Besonderer Dank gilt außerdem meiner Familie und meinen Freunden für die persönliche Unterstützung während meiner Promotion. Ganz besonders herzlich danke ich meinem Mann für seine Geduld und dafür, dass er mich in jeder schwierigen Phase immer wieder zum Lachen gebracht hat.

8.5 Curriculum Vitae

Der Lebenslauf ist in der Online-Version aus Gründen des Datenschutzes nicht enthalten.

Der Lebenslauf ist in der Online-Version aus Gründen des Datenschutzes nicht enthalten.

8.6 Publication List

Publikationen:

Janke K, Brockmeier U, Kuhlmann K, Eisenacher M, Nolde J, Meyer H E, Mairbäurl H, Metzen E. 2012. Factor Inhibiting HIF-1 (FIH-1) modulates protein interactions of Apoptosis-Stimulating p53 binding Protein 2 (ASPP2). J Cell Sci. 2013 Apr 19. [Epub ahead of print] PMID: 23606740.

Brockmeier U, Platzek C, **Schneider K,** Patak P, Bernardini A, Fandrey J, Metzen E. 2011. The function of hypoxia-inducible factor (HIF) is independent of the endoplasmic reticulum protein OS-9. PLoS One. 2011 Apr 29;6(4):e19151.

Metzen E, **Schneider K.** 2010. How to manipulate cellular O2 sensing. Chem Biol. 2010 Apr 23;17(4):314-5.

Vorträge:

Janke K., Brockmeier U., Kuhlmann K. und Metzen E. 2013. *Factor Inhibiting HIF-1 Modulates Protein Interactions of Apoptosis-Stimulating p53-binding Protein 2*. 92nd Annual Meeting, Deutsche Physiologische Gesellschaft, 02.-05.03.2013, Heidelberg, Germany

Schneider K., Brockmeier U. und Metzen E. 2012. *Factor Inhibiting HIF-1 modulates protein interactions of ASPP2*. Keystone Symposium: Advances in Hypoxic Signaling: From Bench to Bedside (Q4) 12.-17.02.2012, Banff, Alberta, Canada.

Schneider K., Brockmeier U. und Metzen E. 2011. *Hydroxylation of p53-regulating proteins*. GRK 1431 und BIOME "Cell Biology and Genetics" Core Joint Meeting 03-04.05.2011, Dormagen/Zons, Germany.

Posterpräsentationen:

Schneider K., Brockmeier U. und Metzen E. 2012. *Factor Inhibiting HIF-1 modulates protein interactions of ASPP2*. Keystone Symposium: Advances in Hypoxic Signaling: From Bench to Bedside (Q4) 12.-17.02.2012, Banff, Alberta, Canada.

Schneider K., Brockmeier U. und Metzen E. 2011. *Regulation of protein interaction by FIH-1-dependent hydroxylation.* 10. Forschungstag der Medizinischen Fakultät 25.11.2011, Universitätsklinikum Essen, Germany.

Schneider K., Brockmeier U. und Metzen E. 2010. *The Endoplasmic Retidulum Protein OS-9 is not involved in the regulation of Hypoxia-inducible Factor (HIF).* HypoxiaNet EU COST TD0901 Meeting: Therapeutic Aspects of Hypoxia-Inducible Pathways 07.-08.10.2012, Dublin, Ireland.

Schneider K., Brockmeier U. und Metzen E. 2010. *Effekte von Sauerstoffmangel auf den Tumor-Suppressor p53: Eine neue Verbindung zwischen alten Wegen?* 9. Forschungstag der Medizinischen Fakultät 12.11.2010, Universitätsklinikum Essen, Germany.

8.7 Declarations

Erklärung:

Hiermit erkläre ich, gem. § 6 Abs. 2, f der Promotionsordnung der Math.-Nat. Fakultäten zur Erlangung der Dr. rer. nat., dass ich das Arbeitsgebiet, dem das Thema „Characterisation of apoptosis-stimulating p53 binding protein 2 (ASPP2) as a new substrate for asparaginyl hydroxylation“ zuzuordnen ist, in Forschung und Lehre vertrete und den Antrag von Kirsten Janke befürworte.

Essen, den _____ _____

Eric Metzen

Erklärung:

Hiermit erkläre ich, gem. § 7 Abs. 2, c und e der Promotionsordnung der Math.-Nat. Fakultäten zur Erlangung des Dr. rer. nat., dass ich die vorliegende Dissertation selbständig verfasst und mich keiner anderen als der angegebenen Hilfsmittel bedient habe und alle wörtlich oder inhaltlich übernommenen Stellen als solche gekennzeichnet habe.

Essen, den _____ _____

Kirsten Janke

Erklärung:

Hiermit erkläre ich, gem. § 7 Abs. 2, d und f der Promotionsordnung der Math.-Nat. Fakultäten zur Erlangung des Dr. rer. nat., dass ich keine anderen Promotionen bzw. Promotionsversuche in der Vergangenheit durchgeführt habe, dass diese Arbeit von keiner anderen Fakultät abgelehnt worden ist, und dass ich die Dissertation nur in diesem Verfahren einreiche.

Essen, den _____ _____

Kirsten Janke